Quantitative Analysis of the T cell Receptor Signaling Network in Response to Altered Peptide Ligands

By

Lucia Wille

B.S., Biology
College of William and Mary, 2000

SUBMITTED TO THE DEPARTMENT OF BIOLOGY IN PARTIAL FULFILLMENT OF THE REQUIREMENTS FOR THE DEGREEE OF

DOCTOR OF PHILOSOPHY IN BIOLOGY

AT THE
MASSACHUSETTS INSTITUTE OF TECHNOLOGY

JUNE 2006

Signature of Author: _____
Biology Department
May 26, 2006

Certified by: _____
Douglas A. Lauffenburger
Whitaker Professor of Biological Engineering, Chemical Engineering, and Biology
Thesis Supervisor

Certified by: _____
Frank Solomon
Professors of Biology
Chairman, Thesis Committee

Approved by: _____
Stephen P. Bell
Professor of Biology
Chair, Graduate Committee

Quantitative Analysis of the T cell Receptor Signaling Network in Response to Altered Peptide Ligands

By

Lucia Wille

Submitted to the Department of Biology
on May 26, 2006 in Partial Fulfillment of the
Requirements for the Degree of Doctor of Philosophy in
Biology

ABSTRACT

Understanding the adaptive immune system poses a great conceptual challenge. It has evolved to respond to foreign invaders with exquisite sensitivity and selectivity. In particular, the T cell branch of the immune system is trained to distinguish between self and non-self. This requires that a single receptor, the T cell receptor, bind to multiple ligands resulting in different cell fates, based in part on the avidity of the ligand.

To address the question of ligand affinity discrimination in T cells, several T cell lines, both mouse and human, were screened for their ability to exhibit multiple cell fates in response to stimulation through the T cell receptor. A hybridoma system was identified that exhibits different levels of both apoptosis and cytokine production in response to three altered peptide ligands.

We investigated how the consequent downstream signaling networks integrate to ultimately govern avidity-appropriate T cell responses in this hybridoma system. Here, we hypothesized that a quantitative combination of key downstream network signals can effectively represent the information processing generated by TCR ligation, providing a model capable of interpreting and predicting T cell functional responses. We generated a multivariate regression model from over 1100 signaling measurements that could predict IL-2 production in response, to a new ligand condition, implying that peptide avidity information is encoded in the magnitudes of downstream signals. Our model predicted *a priori* that IL-2 production is quantitatively related to both known and novel modulators, Erk and Akt, with verification by subsequent inhibitor studies. Furthermore, the model could predict the non-additive effect of inhibiting both molecules simultaneously. These findings demonstrate the power of our quantitative systems modeling approach for numerical prediction of T cell responses from a key set of dynamic signals, and conceptual understanding of how complex signaling networks integrate information to translate pMHC stimuli into functional responses.

To further analyze the relationship between Erk levels and IL-2 production in T cells, an epi-allelic series of stable Erk1 and Erk2 knockdowns was generated. We show that both total and phospho Erk levels are correlated with IL-2 production and provide a framework for interpreting the phenotypes of partial knockdowns in other systems.

Thesis Supervisor: Douglas A. Lauffenburger
Title: Whitaker Professor of Biologcial Engineering, Chemical Engineering, and Biology

BIOGRAPHICAL NOTE

Lucia Wille received a bachelor of science in Biology from the College of William and Mary in 2000. While at William and Mary, Lucia worked in the laboratory of Dr. Diane Shakes studying meiotic progression in *C. elegans* using a reverse genetic approach. Her published work is entitled "Multiple subunits of the Caenorhabditis elegans anaphase-promoting complex are required for chromosome segregation during meiosis I."

Lucia started her graduate thesis in 2000 with the Department of Biology at Massachusetts Institute of Technology. In 2005 she joined the Lab of Dr. Douglas Lauffenburger were she analyzed the T cell receptor signaling network. Her thesis is entitled "Quantitative Analysis of the T cell Receptor Signaling Network in Response to Altered Peptide Ligands."

After graduation, Lucia will join the pharmaceutical company Merrimack, located in Cambridge, Massachusetts.

ACKNOWLEDGMENTS

I would like to thank two people without whom this thesis would not have been possible: my advisor, Douglas Lauffenburger for his support, advice and encouragement; and Dr. Melissa Kemp a post-doctoral fellow in the Lauffenburger Lab and my collaborator and co-author on the work presented in this thesis.
I would also like to thank my committee members Frank Gertler, Jianzhu Chen, Lindsay Nicholson and Frank Solomon.
In addition, I have received advice, feedback and suggestions from Dr. Fei Hua, Megan Palmer, Dr. John Burke, and Dr. Chris Dillon.

Dr. Melissa Kemp contributed to Chapters 3 and 4 by generating the kinase activity assay data as well as the NFAT western blots. In addition, she was mainly responsible for technical aspects of the modeling efforts described in that chapter. In Chapter 4, Melissa generated the Erk kinases activity assay data. Both Chapters are co-written by Lucia and Melissa.
I would also like to thank Christina Lewis for her contributions to experimentally testing the model presented in Chapter 3 by generating inhibitor dose response curves and determining IL-2 production in response to Erk and Akt inhibition.
A former colleague of mine, Dr. Peter Sandy contributed to Chapter 4 by generating the lentiviral constructs of Erk shRNAs.

Lastly, I would like to thank my family and friends for their encouragement and support.

TABLE OF CONTENTS

LIST OF FIGURES AND TABLES

1. Introduction

The immune system responds to and eliminates challenges from foreign invaders such as bacteria, viruses, and parasites. It consists of two branches: the innate immune system, which is nonspecific for any one pathogen; and the adaptive immune system, which exhibits pathogen specificity (Goldsby et al., 2000). Two major cell types are represented in the adaptive immune system: B cells comprise the humoral branch of the immune system and are capable of recognizing soluble antigen; T cells are part of the cell-mediated branch and generally recognize antigen in the context of self-cell presentation. T cells can be further divided into two classes based on the co-receptor which they express, either CD4 or CD8. The role of CD8 T cells is to recognize intracellular pathogens presented on self-cells, and therefore they often kill the self-cell presenting the antigen. CD4 cells recognize extra-cellular pathogen presented on self-cells. Their primary role is to activate other cell types of the immune system capable of clearing an infection. This thesis will focus on CD4 T cells (also called T helper cells).

In the event of an immune response, activated CD4 T helper cells proliferate and assume an effector role. In most cases, this effector role results in the secretion of cytokines that mediate the immune response (Fig. 1.1.). The nature of the immune response can vary, depending on the cytokine profile released by the CD4 T helper cells. This cytokine profile defines the class of CD4 T cells that is generated during the infection. CD4 effector T cells generally fall into two major classes, either T_H1 (T helper1) or T_H2 (T helper2). T_H1 cells secrete inflammatory cytokines such as INF-γ, IL-2, and TNF-β, capable of activating macrophages and cytotoxic T cells. A T_H1 immune response is most effective on intracellular pathogens such as viral

infections. T_H2 cells secrete IL-4, IL-5, IL-10 and IL-13; these cytokines activate B cells, resulting in an antibody dependent immune response that is most effective at clearing extracellular pathogens, such as some bacteria. However, in the initial stages of CD4 T cell activation, prior to the differentiation into either T_H1 or T_H2 effector cells, T cells produce the cytokine IL-2 which has been shown to be critical for the clonal expansion of T cells. Therefore, IL-2 is required at the very early stages of T cell expansion in addition to its role in T_H1 cell effector function. Because of its role in the initial stages of T cell proliferation, IL-2 is often used as a primary readout for T cell activation and will be used as such throughout this thesis.

CD4 T helper cells are activated by antigenic peptides bound to class II major histocompatibility complexes (p:MHC) expressed on antigen presenting cell (APC). Activation partially depends on the binding interaction of p:MHC and TCR. TCR binding to p:MHC can result in several possible cell fates correlated to the amount of TCR stimulation received: anergy (a state of unresponsiveness), activation and cell growth, proliferation or apoptosis. The idea that the T cell receptor was more than an on/off switch was first suggested in 1991 when investigators found that the replacement of a glutamic acid residue with an aspartic acid residue within an antigenic peptide was capable of qualitatively altering the response of T cells. T cell stimulation with the endogenous peptide resulted in rapid T cell proliferation, while stimulation with the altered peptide ligand (APL) resulted in IL-4 production (Evavold and Allen, 1991). Since then, great strides have been made in our physiological understanding of ligand discrimination behavior.

Evidence suggests that the strength of TCR signaling, determined by the affinity of the TCR for the MHC/peptide complex, plays an important role in T cell fate (Yun and Bevan, 2001). The TCR-peptide/MHC interactions exhibit a range of binding affinities, with K_d values ranging from 10^{-4} to 10^{-7} M. These are low values when compared to other biological ligand/receptor interactions, such as those between cytokines, growth factors, and their receptors. Therefore, the term avidity is often used to describe TCR interactions with peptide MHC complexes, since it takes into account both the cumulative number of interactions and the affinity of the interaction, which together can create a strong bond.

The roles of weak and strong avidity TCR ligands in developing thymocytes has been well established (Yun and Bevan, 2001). In the thymus, T cells are selected specifically such that they recognize self-peptides with weak affinities. This is accomplished by selecting developing thymocytes with an affinity for self-peptide MHC while simultaneously selecting against autoreactive thymocytes with a high affinity for self-peptide MHC. Our understanding of weak and strong TCR-ligand interactions in the peripheral immune system is less clear. The significance of weak affinity interactions in the periphery has not been well established and there exists controversy as to whether weak affinity interactions are necessary for peripheral CD4 T cell survival (Clarke and Rudensky, 2000; Ohashi, 2002). In addition, peripheral T cell activation is largely dependent on co-stimulatory signals provided by the CD28 receptor (Acuto and Michel, 2003). However, evidence from autoimmune disease models suggests that low affinity self-peptides may play a role in the capacity of T cells to tune their peptide-MHC responsiveness in the periphery (Illes et al., 2005).

A major unanswered question in T cell biology is the molecular mechanism by which a population of clonal T cells can distinguish between various peptide sequences. T cells are so finely tuned that one amino acid change in the peptide sequence can significantly alter their response. This mechanism requires that the TCR complex be capable of sending multiple distinct signals resulting in different cell fates depending on the nature of the ligand encountered. Determining the primary mechanisms responsible for accurate ligand discrimination is complicated by the multiple interconnected pathways that are activated downstream of TCR ligation.

To date, one of the challenges in addressing the ligand discrimination problem has been the lack of consistent data sets that take into account both multivariate and dynamic signaling information. Many studies have successfully focused on particular molecules or details of the signaling pathway to further our understanding of TCR ligand affinity discrimination. However, a systematic study of the TCR network activated under different TCR stimulation conditions has not been reported. Such a study is the goal of this thesis as it would provide insights into how multiple signaling pathways function in concert to regulate gene transcription of cytokines a critical function of CD4 effector T cells.

1.1. Signaling Network structure in T cells

Binding of the T cell receptor to a p:MHC molecule can result in multiple downstream signaling events including nuclear factor of activated T cells (NFAT), Akt, nuclear factor kappaB (NF-κB) and mitogen activated protein kinase (MAPK) activation (Fig. 1.2.) (Germain and Stefanova,

1999; Huang and Wange, 2004). These molecules in turn activate or are themselves transcription factors capable of binding to the IL-2 promoter region and effecting a T cell response. Engagement of the T cell receptor activates the Src-family kinase Lck, which phosphorylates the immunoreceptor-based tyrosine activation motive (ITAM) sites on the CD3 co-receptor. ITAM phosphorylation causes Zap-70 localization and activation resulting in the integral membrane protein Linker for Activation of T cells (LAT) being phosphorylated at multiple different tyrosines (Weber et al., 1998; Zhang et al., 1998; Zhang et al., 1999b). Phospho-LAT functions as a scaffold for various other signaling molecules including the adaptor protein growth factor receptor-binding protein-2(Grb-2), Grb2-related adaptor downstream of Shc (Gads), and phospholipase C γ 1 (PLCγ 1).

Grb-2 recruitment to phosphorylated LAT leads to activation of the MAPK Erk and phosphatidylinositol-3 kinase (PI3K), through Ras co-localization with the guanine nucleotide exchange factor (GEF), son-of-sevenless (Sos) (Buday and Downward, 1993). PLCγ1 cleavages phosphatidylinositol 4,5-bisphosphate into inositol triphosphate and diacylglycerol (DAG). Inositol triphosphate stimulates calcium release for subsequent Ca^{++}-dependent NFAT activation. DAG activates RasGRP (Ebinu et al., 2000) another Ras GEF, protein kinase C θ (PKCθ), the three MAPK (ERK, JNK, p38) pathways and Akt. Activation of the MAPKs results in activation of the transcription factor AP-1. PKC θ switches on the CARMA /Bcl10/IκB kinase (IKK) pathway leading to activation of the NF-κB transcription factor. Propagation of stimuli from the receptor results in eventual nuclear localization of AP-1, NFAT, NF-κB, and Oct-1 - transcription factors all of which are known to bind to the IL-2 promoter region (Jain et al., 1995).

1.2. Background on the known relevance of individual pathways in ligand affinity discrimination and IL-2 production

This section will largely focus on the role of Erk and its upstream activator Ras in ligand affinity discrimination, since its role has been the focus of much of the recent research into ligand affinity discrimination. However, other pathways are activated in response to TCR ligantion and have been shown to be important for IL-2 production and background information on these pathways will also be provided.

It is important to note that the ability of the TCR to interpret different affinity ligands could rely on either quantitative or qualitative differences in the activation state of the signaling network following TCR engagement and that these are not strictly independent. Quantitative difference can be thought of as changes in the magnitude of activation of downstream signaling molecules while qualitative changes would result in different signaling pathways being activated in response to different affinity ligands. Much of the evidence points towards quantitative differences in signaling resulting in different cell fate decisions (Mariathasan et al., 2001; Werlen et al., 2003; Werlen et al., 2000; Yun and Bevan, 2001). However, several groups have also reported unique requirements of individual signaling molecules for particular cell fate decisions. In support of qualitative differences resulting in particular cell fates, the individual MAPKs have been uniquely implicated in T cell selection fates. Erk has been shown to be essential for positive selection while not required for negative selection (Alberola-Ila et al., 1995). Conversely, p38 and Jnk are important for negative selection (Rincon et al., 1998b; Sugawara et al., 1998).

1.2.1. Regulation of Erk activation via Ras during TCR signaling

The MAPK pathway is required for T lymphocyte differentiation (Alberola-Ila et al., 1995) as well as T cell homeostasis in the periphery (Priatel et al., 2002). Studies in mammalian neuronal (PC 12) cells have shown that the strength and duration of Erk activation is sufficient for determining cell fate decisions in these cells (Marshall, 1995). Recent studies indicate that strength and duration of Erk activation may play a similar role in both T cell development and T cell activation in the periphery (Werlen et al., 2003; Yun and Bevan, 2001). Studies have shown that the relative levels and duration of Erk activity changed in response to peptides that either induce negative or positive thymic T cell selection, two distinct cell fates (Mariathasan et al., 2001; Werlen et al., 2000).

It is possible that the regulation of Erk-activation dynamics are the result of tightly regulated Ras activation, both temporally and spatially. Ras is activated by TCR engagement (Downward et al., 1990) and can turn on various signaling cascades in response to T cell stimulation (Genot and Cantrell, 2000), most importantly, the Erk and PI3K pathways. Due to its well-defined role in both development and differentiation, Ras is a good candidate for regulation of T cell fate decisions.

If Ras is to play a central role in Erk regulation and consequently T cell fate decisions, then Ras activation must either be quantitatively or qualitatively different when distinct ligands are encountered, and must result in the activation of different signaling pathways depending on ligand affinity. Recently, three specific mechanisms for modulating the effects of Ras signaling and consequently Erk activation in T lymphocytes have been described. Cells can use different

Ras GEFs to both modulate how Ras signals and to determine on which membrane Ras is activated. In addition, scaffold proteins have been identified that regulate Ras signaling in yeast and mammalian cells by creating multi-enzyme complexes.

Ras regulation by two GEFs

Evidence that TCR signaling could lead to a change in the activation state of Ras was provided by Downward and colleagues (Downward et al., 1990). It was then subsequently recognized that Ras could be activated by two independent mechanisms (Izquierdo et al., 1992) in T lymphocytes. One mechanism required tyrosine kinase activity, the other could be triggered by addition of diacylglycerol (DAG, a major secondary messenger for T cell activation), and its pharmacological analogs, such as phorbol ester (Downward et al., 1990). The tyrosine kinase-dependent pathway activates Ras via the adaptor protein Grb-2 and the GEF Sos (Buday and Downward, 1993) in response to TCR stimulation (Buday et al., 1994). The diacylglycerol dependent pathway has only recently been defined with the discovery of a novel Ras GEF. This GEF, RasGRP (Ebinu et al., 1998), contains a diacyl-glycerol binding motif (Tognon et al., 1998) and can be activated by DAG analogs. RasGRP is present at high levels in T lymphocytes (Ebinu et al., 2000), and is critical for T lymphocyte maturation and function (Dower et al., 2000; Priatel et al., 2002).

Evidence from knockout mice suggests the Ras GEFs, RasGRP1 and Sos1, are important in determining the nature of T cell signaling downstream of the TCR. RasGRP1 knockout mice have reduced numbers of CD4+ and CD8+ T cells. However, these cells show death rates similar to wild type T cells when challenged with self-peptides (Priatel et al., 2002), indicating that

negative selection is not impaired in these mutant mice and that the T cell maturation block at the double positive stage is due to a defect in positive selection. This suggests that RasGRP1 has a role in transducing signals from low affinity TCR ligands (Layer et al., 2003; Priatel et al., 2002). Sos knockout mice are embryonic lethal and so far no T cell-specific knockout exists. However, we can infer from Grb2 deficient heterozygous mice that Sos is also a key molecule in T cell signaling. These mice exhibit reduced numbers of CD4+ and CD8+ T cells. When Grb2+/- T cells are challenged with self-peptide, they fail to die as efficiently as wild type T cells (Gong et al., 2001), indicating that negative selection may be impaired in these mice. This evidence suggests Sos and RasGRP are not redundant in activating Ras but rather that each GEF is responsible for transmitting distinct types of signals from the T cell receptor. Activating Ras through different GEFs provides a possible mechanism by which its activation could be spatially controlled determining T cell fate.

Regulation of Ras signaling via selective activation at specific endomembranes

Another potential mechanism for controlling the specificity of a signaling molecule is by restricting its subcellular localization. Ras is targeted to various cellular compartments including the ER and golgi (Apolloni et al., 2000; Choy et al., 1999) where activation can occur (Chiu et al., 2002; Choy et al., 1999). The microenvironment of these different membranes appears to affect both quantitative and qualitative aspects of Ras signaling, potentially by favoring recruitment of unique collections of Ras regulators and effectors. Therefore, restricting the localization of active Ras could contribute to TCR/ligand affinity discrimination.

In T cells the two Ras GEFs that are activated downstream of the T cell receptor appear to activate Ras at different subcellular locations. Sos activates Ras at the plasma membrane (Holsinger et al., 1995), while RasGRP, a diffusible GEF, activates Ras preferentially on the Golgi and negatively regulates Ras at the plasma membrane in response to TCR engagement (Bivona et al., 2003).

Activating Ras on specific endomembranes will result in qualitative differences in downstream signaling pathways if different effector molecules are recruited to specific endomembranes. Chiu and colleagues (2002) have recently provided evidence for qualitative changes in Ras signaling as a result of subcellular localization. Constitutively active Ras targeted to the ER was found to be a potent stimulator of the JNK pathway but did not activate either Erk or Akt (an indicator of PI3K activation); constitutively active Ras enriched on the golgi activated Erk and Akt but not JNK. In addition, evidence that Ras localization results in quantitative changes in its activation is suggested by the work of Bivona et al., (2003). Stimulating COS-1 cells with epidermal growth factor results in early, transient Ras activation on the plasma membrane followed by persistent, RasGRP dependent Ras activation on the Golgi (Bivona et al., 2003). Evidence in neuronal PC 12 cells, suggests that activation of Ras on the golgi is sufficient for cell differentiation. In these same cells, strength and duration of Erk (a Ras effector molecule) activation can determine cell fate (Marshall, 1995), potentially a mechanism which has also been proposed for determining T lymphocyte fate (Werlen et al., 2003; Yun and Bevan, 2001), linking the quantitative changes in Ras activation via localization to cell fate regulation.

Ras regulation by tethering downstream effectors to Scaffold proteins

One possible mechanism for cells to regulate the specificity of downstream targets is by employing scaffolding proteins (Burack and Shaw, 2000). Ras activation leads to the sequential activation of three downstream kinases: Raf (MAPKKK), MEK (MAPKK), and Erk (MAPK), were complexity and diversity in signals is created because multiple isoforms of each of these kinases coexist in T cells. The best understood scaffold proteins for the Ras pathway are in yeast where tethering kinases to a scaffold is sufficient for eliciting a specific cellular response after receptor stimulation (Park et al., 2003).

A distinct scaffold protein, Kinase Suppressor of Ras (KSR) was identified in Drosophila and C. elegans as a protein necessary for Ras signaling (Kornfeld et al., 1995; Sundaram and Han, 1995; Therrien et al., 1995). KSR associates independently with both Raf and MEK (Roy et al., 2002) in immuno-precipitation experiments suggesting a scaffold function for the MAPK signaling pathway downstream of Ras.

A mammalian homolog of KSR was identified through a yeast two-hybrid screen (Yu et al., 1998), and mouse knockouts of the KSR gene have been generated (Lozano et al., 2003; Nguyen et al., 2002). These mice have no defects in T cell development (Lozano et al., 2003). Both the spleen and the lymph nodes show no detectable differences from wild type mice in CD4 and CD8 T cell populations. However, T cells from KSR-/- mice stimulated via the antigen receptor do not proliferate as much as wild-type T cells and fail to produce IL-2 in response to TCR stimulation. Raf activation is not affected in KSR-/- thymocytes while Erk activation shows normal kinetics of activation, but lower levels of activity. This study suggests that KSR is not

essential for T cell development. However, the proliferative defect in addition to lower Erk activity displayed by KSR-/- thymocytes does not rule out the possibility that KSR functions to catalytically enhance the MAPK pathway in T cells (Nguyen et al., 2002).

Integrating the effectors of the Ras pathway

Ras regulation via the Erk pathway may be key in distinguishing between quantitative ligand binding events in T cells that lead to distinct cellular responses. While evidence exists to support such a role for the Ras pathway in T cells, the mechanisms responsible for regulating Ras function in T cells remain incompletely defined, and evidence suggests that no single mechanisms is responsible for Ras acting as a branch point for signaling. Rather, T cells appear to use a combination of different mechanisms to control the activity of Ras and to define cellular fate in response to antigen stimulation.

One potential integrated model for regulating Ras is through the phosphorylation of LAT at different tyrosines following TCR engagement resulting in the activation of distinct GEFs. The degree to which LAT is phosphorylated may be determined by the strength of TCR binding to MHC/peptide, and this may affect which GEF is preferentially used. The GEFs in turn are capable of activating Ras at different endomembranes, which may differ in the types of downstream signaling molecules present, consequently altering the nature of the Ras signal. It is possible that scaffold proteins play a role in recruiting distinct collections of kinases to activate Ras and thus playing a potential role in modulating the outcome of Ras signaling in T cells.

1.2.2. The PI3K pathway

That TCR ligation could result in the activation of PI3K was recognized over a decade ago (Ward et al., 1996). PI3K in T cells is activated through Ras and indirectly through PLCγ. Active PI3K results in membrane translocation of Akt through its PH domain (Vanhaesebroeck and Alessi, 2000) and its subsequent activation in T cells (Reif et al., 1997). While Akt does not directly activate a transcription factor that binds the IL-2 promoter region, there are several reported mechanisms by which Akt might regulate IL-2 production via its regulation of other transcription factors including NF-κB and NFAT. A constitutively active form of Akt has been shown to accelerate degradation of IκBα, resulting in increased translocation of NF-κB into the nucleus (Jones et al., 2000). Once in the nucleus, NF-κB can then bind to the IL-2 promoter resulting in IL-2 transcription. Another Akt target is GSK3, a regulator of glycogen metabolism. GSK3 has also been shown to be a negative regulator of T cell activation through its regulation of the IL-2 transcription factor NFAT. Akt-dependent phosphorylation inactivates GSK3 (Neilson et al., 2001) resulting in nuclear translocation of NFAT.

The role of PI3K in T cells has been studied using genetic knockouts. PI3K is composed of a catalytic and regulatory subunit. In mammalian cells there are four genes encoding the catalytic subunit called p110α, p110β, p110γ, and p110δ. There are two isoforms of the regulatory subunit of PI3K p85, p85α or p85γ, which contain both the SH2 and SH3 protein binding domain. Another regulatory subunit, p101, has been identified which contains a GPCR interaction domain and interacts with p110γ.

Mice targeting the regulator p85α subunit and the catalytic p110γ and p110δ subunits have been studied in T lymphocytes. The double knockout of the p100γ/δ subunits has also been studied. Two groups have generated p85α knockout mice, showing that they do not have a T lymphocyte proliferation defect, but neither group has specifically examined IL-2 production in T cells from these mice (Fruman et al., 1999; Suzuki et al., 1999). In *ex-vivo* T cells from mice bearing an inactive form of p110δ antigen induced proliferation, Ca++ mobilization and IL-2 production is attenuated (Jou et al., 2002; Okkenhaug et al., 2002). T cells from a mouse lacking the p110γ gene also have T cell proliferation defects and reduced levels of IL-2 production in response to antigen stimulation (Sasaki et al., 2000). The p100γ/δ double knockout mouse exhibits defect in T cell development, however IL-2 production in stimulated T cells has not been examined (Webb et al., 2005).

Genetic knockouts have also been generated for the three known Akt isoforms. Of the three Akt isoforms, Akt1, Akt2, and Akt3, Akt1 is the most highly and ubiquitously expressed isoform. Akt2 is also expressed in most adult tissues although at lower levels than Akt1. Akt3 is expressed at the lowest level in adult tissue except for in the testis and brain. Akt1 and Akt2 knockout mice have been generated. Akt1 knockout mice do not appear to exhibit severe T cell phenotypes although the *ex-vivo* T cell phenotype has not been determined (Chen et al., 2001); yet this isoform has been observed to localize to lipid rafts upon T cell activation (Bauer et al., 2003) suggesting that it may function to transmit TCR signals. One potential interpretation of this data is that there is compensation of Akt1 by Akt2 and Akt3. The role of the other Akt isoforms, Akt2 and Akt3 has not been looked at formally in T cells and it will be interesting to see if the three isoforms are functionally redundant for some cell decision processes. Given the

complexity of the Akt pathway and the lack of T cell activation specific phenotypes in Akt knockout mice, the role of Akt in T cells is still not entirely clear. The lack of specific inhibitors to Akt has also complicated the interpretation of the role Akt has in transmitting TCR signals.

PI3K pathways appears to play a critical role in propagating TCR signals. However, PI3K has been shown to activate both PKC and Akt through PDK1. It remains to be seen whether Akt truly participates in regulating TCR signals, or whether the observations of its role in TCR signaling that have been obtained through the use of PI3K specific inhibitors reflect the role of PKC in activating downstream signals, since in addition to activating Akt, PI3K downstream effectors may also activate some isoforms of PKC independently of Akt activation (Chou et al., 1998; Le Good et al., 1998). However, another well established mechanism for activating PKCθ in T cells is through PLCγ {Nishikawa, 1997 #179}.

1.2.3. Calcium dependent signaling pathway

NFAT positively regulates IL-2 gene transcription by translating cytosolic calcium levels into a nuclear transcriptional response. NFAT was first identified in 1988 (Shaw et al., 1988), and its role in IL-2 transcription has been well established (Jain et al., 1995; Rao, 1994). The IL-2 promoter contains two NFAT binding sites which can individually sustain promoter activity (Leiden et al., 1992), and NFAT activity has been shown to be required for IL-2 production (Chow et al., 1999). T cell receptor ligation results in activation of PCLγ and subsequent release of calcium into the cytosol, which results in activation of calcineurin. Calcineurin is the phosphatase responsible for dephosphorylation and activation of cytoplasmic NFAT. Active

NFAT then translocates into the nucleus where it functions as a transcription factor (Crabtree, 2001). Our understanding of NFAT nuclear export is less well defined. GSK3 has been identified as a negative regulator of T cell activation and appears to be the kinase responsible for NFAT nuclear export.

However, in addition to NFAT functioning as a positive regulator of IL-2 gene transcription, there are a couple of pieces of experimental evidence suggesting that certain isoforms of NFAT may also function to negatively regulate gene transcription (Liu, 2005). Three different NFAT knockout mice have been generated that each do not express one of the three members of the NFAT family of transcription factors, NFATc, NFATp, and NFAT4. NFATc was knocked out by two independent groups and both show no IL-2 production defect in T cells from these knockout mice (Ranger et al., 1998; Yoshida et al., 1998). T cells in NFATp and NFAT4 knockout mice also do not have defects in IL-2 production. In addition these T cells have hyperproliferation and hyperactivation defects in response to TCR stimuli (Hodge et al., 1996; Oukka et al., 1998; Xanthoudakis et al., 1996). The lack of an IL-2 production phenotype in NFATc knockout mice suggests that there may be redundancy in the NFAT pathway. And indeed, a mouse deficient in both NFATc and NFAT4 exhibits decreased levels of IL-2 production (Peng et al., 2001). One possible explanation of the hyperproliferative phenotypes seen in NFATp and NFAT4 knockouts may be the allosteric effect of DNA binding. The authors in Giffin et al. (Giffin et al., 2003) speculate, that the DNA sequence to which NFAT is bound could potentially result in conformational changes in NFAT resulting in distinct protein-protein interactions which could lead to either activation or repression of the bound promoter region.

In conclusion, there is little doubt about NFAT's role as a transcription factor capable of inducing IL-2 production; however, the role of individual NFAT proteins in IL-2 production is at this point difficult to determine possibly due to redundancy and compensation. In addition, evidence suggests that different NFAT isoforms play the more complex role as both positive and negative regulators of transcription.

1.2.4. NF-κB

Studies of the IL-2 promoter have linked NF-κB to IL-2 production. The IL-2 promoter contains one NF-κB binding site and mutations in that region have been shown to negatively affect IL-2 production (Garrity et al., 1994). The NF-κB transcription factor has been shown to play a critical role in T cell activation through its induction of genes that induce proliferation and cytokine production (Ghosh et al., 1998; May and Ghosh, 1998); however, the molecular mechanism by which NF-κB is activated and its role in different TCR mediated signaling events continues to be a topic of intense research. Recent work by multiple groups suggests that NF-κB activation is the result of PKCθ recruitment to the immunological synapse followed by Carma1/Bcl10/Malt recruitment (Thome and Tschopp, 2003). The mechanism that potentially links PKCθ, Carma1, and Bcl10 was only recently proposed, with evidence that PKC phosphorylates the scaffold protein Carma1 resulting in the recruitment of Bcl10 and Malt to the membrane (Matsumoto et al., 2005). This in turn activates IKK resulting in the degradation of IκB and translocation of NF-κB into the nucleus (May and Ghosh, 1998).

In furthering our understanding of the role of NF-κB in T cells and particularly in IL-2 production, knockout studies have been very instructive. NF-κB in cells exists as a dimer of rel-family proteins. Of the five c-rel family of proteins that have been knocked out in the mouse model system, p50 and c-rel appear to have a role in mediating immune responses to pathogens (Ghosh et al., 1998). Knocking out the c-Rel gene, whose expression is limited to the hematopoetic lineage, resulted in T cells unresponsive to TCR stimuli (Kontgen et al., 1995). Two groups have generated p50 gene knockouts (Sha et al., 1995; Weih et al., 1995). Both report that T cell function in p50 knockout mice is not significantly impaired but neither group reports IL-2 production levels in response to T cell stimulation. Sha and colleagues do report a defect in T cell proliferation in response to T cell activation.

Additional complexity to understanding the role of NF-κB family proteins in IL-2 gene transcription comes from their reported dual function as both transcriptional activators and transcriptional repressors, depending on their dimerization state (Zhong et al., 2002). p50/p50 homodimers have been shown to inhibit transcription, while p65/p50 heterodimers have been shown to function as transcriptional activators. Therefore, evidence suggests that NF-κB family proteins can function as transcriptional activators of IL-2, but wether they do function as activators may depend more on cell context (Grundstrom et al., 2004).

1.2.5. p38 and Jnk pathways

The p38 and Jnk MAPK pathways are known stress response pathways that can mediate differentiation and cell death and have roles in T cell differentiation and development. Genetic studies have shown that p38 is important for at least two cell decision processes during

thymocyte maturation and differentiation. Mice with a dominant negative form of p38 expressed from the lck promoter have severe T cell immunodeficiency - likely due to a block in the early stages of DN differentiation (Diehl et al., 2000). The same group of researchers has found that p38 appears to be important for Th1 differentiation but not Th2 differentiation (Rincon et al., 1998a). The functional role of p38 in ligand discrimination is complicated by the observation that activation is associated with negative selection of thymocytes (Sugawara et al., 1998).

Not surprisingly, the role of p38 IL-2 production is also controversial. A couple of groups have suggested that p38 functions as a positive regulator of IL-2 production (Matsuda et al., 1998; Zhang et al., 1999a). There are also reports indicating that p38 may act as a negative regulator of IL-2 production following TCR stimulation (Kogkopoulou et al., 2006; Song et al., 2000; Veiopoulou et al., 2004). Finally, there are reports of p38 having little or no influence on IL-2 production (Koprak et al., 1999; Mori et al., 1999; Schafer et al., 1999). It is possible that some of these contradictory findings are the result of intrinsic differences in mouse vs. human T cells. Two of the reports mentioned above use human primary T cells to show that a p38 specific inhibitor, SB203580, does not affect IL-2 production (Mori et al., 1999; Schafer et al., 1999) while a similar set of experiments in mouse primary T cells resulted in reduced IL-2 production (Zhang et al., 1999a). It is unclear what difference in molecular mechanism could account for these species-specific effects. And it is also possible that differences in the time of measurement between studies are reflecting differences in transient activation dynamics.

Genetic studies have examined the role of Jnk in TCR mediated signaling including negative selection and Th1, Th2 differentiation (Dong et al., 1998; Rincon et al., 1998b; Yang et al.,

1998). Mice expressing a dominant negative Jnk1 from the lck promoter exhibit delayed negative selection (Rincon et al., 1998b). This same effect has not been observed in mice lacking the Jnk2 gene (Dong et al., 1998), indicating either that the two Jnk isoforms have different functions in negative selection or that Jnk1 may be able to compensate for the lack of Jnk2. Consistent with the idea that the two Jnk isoforms have unique functions, studies from Jnk knockout mice indicate that Th2 differentiation appears to be negatively regulated by Jnk1 (Dong et al., 1998), while Th1 differentiation appears to be positively regulated by Jnk2 (Yang et al., 1998).

Cell signaling studies indicate that Jnk may play several roles in TCR mediated signaling. These include phosphorylation of c-Jun increasing AP1 transcription activity, and maintaining active NFAT in the nucleus. However, the role of Jnk in IL-2 production is still controversial. Evidence from studies examining the transcriptional activity of the IL-2 promoter has linked Jnk and subsequent c-Jun activity to IL-2 production (Jain et al., 1995). On the contrary, mice lacking both Jnk1 and Jnk2 in peripheral T cells produced more cytokines, including IL-2 following activation (Dong et al., 2000).

1.3. Modeling the immune system

There have been several recent, successful modeling efforts in immunology. In particular, modeling efforts have focused on trying to understand how the immune system attains its exquisite sensitivity, while remaining broadly specific to a wide range of pathogens, and capable

of recognizing and tolerating itself (Goldstein et al., 2004). An antigen presenting cell displays on the order of 10^5 - 10^6 p:MHC molecules on its surface, only a small number of which will be pathogen derived. However, T cells are capable of recognizing as few as one antigenic peptide presented in the context of self-peptides (Irvine et al., 2002). In this case, two early modeling efforts suggested different mechanisms that could account for this sensitivity to agonist peptide: kinetic proofreading (McKeithan, 1995) and serial triggering (Chan et al., 2001). There was experimental evidence to support both models; however, neither model could explain all the experimental evidence. A new model combining kinetic proofreading and serial triggering was proposed. This model could closely approximate more experimental data, providing a potential physical basis for explaining the sensitivity displayed by T cells to agonist peptides (Li et al., 2004).

It has been recognized that tremendous insight can be gained from attempting to understand the immune system in terms of physical phenomena through modeling (Chakraborty et al., 2003; Yates et al., 2001). By building a model that attempts to explain experimentally observed behavior, we can begin to understand the intricacies of a functioning immune system as well as the limitations of our current knowledge. There is a wide range of potential modeling techniques, ranging from biochemical reactions modeled by differential equations to purely statistical models that do not contain mechanistic information (Ideker and Lauffenburger, 2003). Any well-constructed model, ranging from mechanistic to statistical, should be capable of generating testable predictions. By determining when these model predictions are reflected by experimental evidence, we begin to codify our biochemical or statistical understanding of the functioning immune system. There is also a gain from model predictions that are not

corroborated by experimental data; these indicate that the model can be improved and our biological understanding is incomplete.

Membrane proximal events in TCR signaling are associated with very short time scales, and current models (Altan-Bonnet and Germain, 2005; Li et al., 2004) simulate activation only for 5-10 minutes. Increasing modeling time scales would allow the advantages of being able to include additional descriptors such as turning-off mechanisms, additional signaling molecules that have slower activation, and transcriptional feedback in the system. This kind of model would suggest additional experiments that address gaps in our current molecular understanding of signal transduction pathways. It could also provide additional information about molecules, such as the phosphatases that deactivate kinases in signal transduction pathways, that have not been well-studied due to experimental hurdles. Modeling can provide guidelines as to kinetic parameters the various phosphatases must possess in order to accurately describe observed kinase dynamics. In addition, models could shed light on molecules that exhibit slower activation dynamics, such as stress response molecules like p38, or nuclear translocation, which can only be captured by extending models out to longer simulation lengths, and ultimately provide a better representation of cellular responses. Early gene transcription can influence the state of intracellular networks by changing the cues (through autocrine signaling, see (Janes et al., 2005)) or the signals by upregulating specific intracellular molecules. These complex regulatory mechanisms will need to be understood in order to fully understand the diverse responses T cells exhibit post-activation.

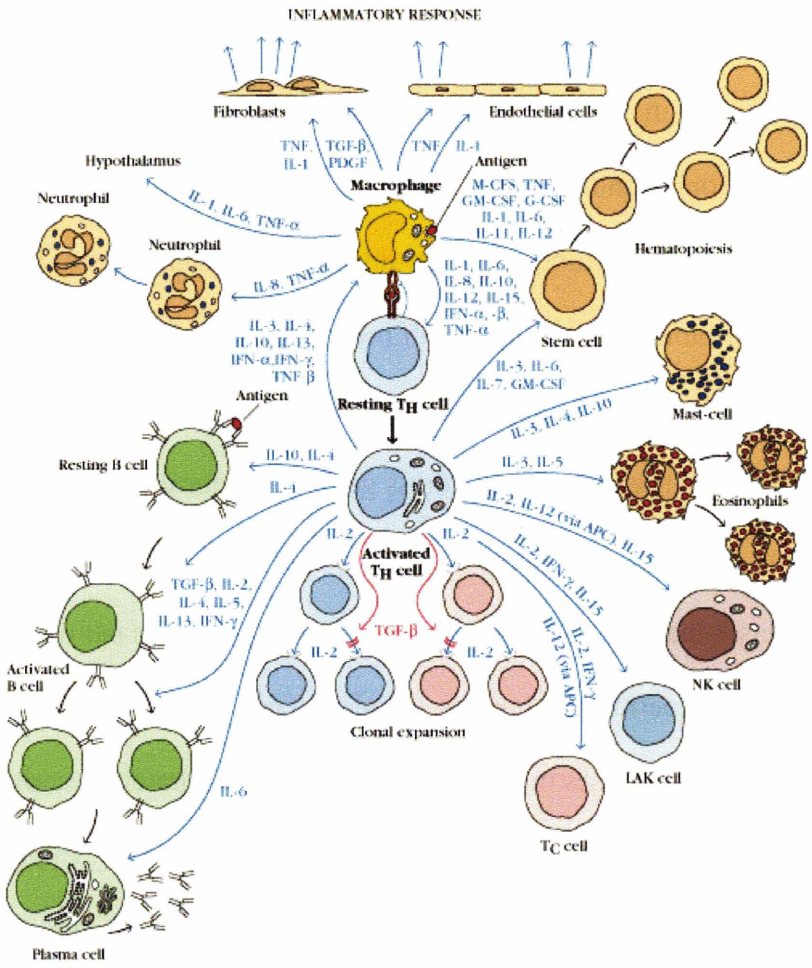

Figure 1.1. Cytokine secretion in T helper cells

Two classes of CD4 effector cells can produce a range of cytokines capable of modulating the outcome of an immune response by activating subsets of other immune effector cells. The left half of a diagram is representative of a T_H2 response, the right half is representative of a T_H1 response. **Figure Source:** (Goldsby et al., 2000)

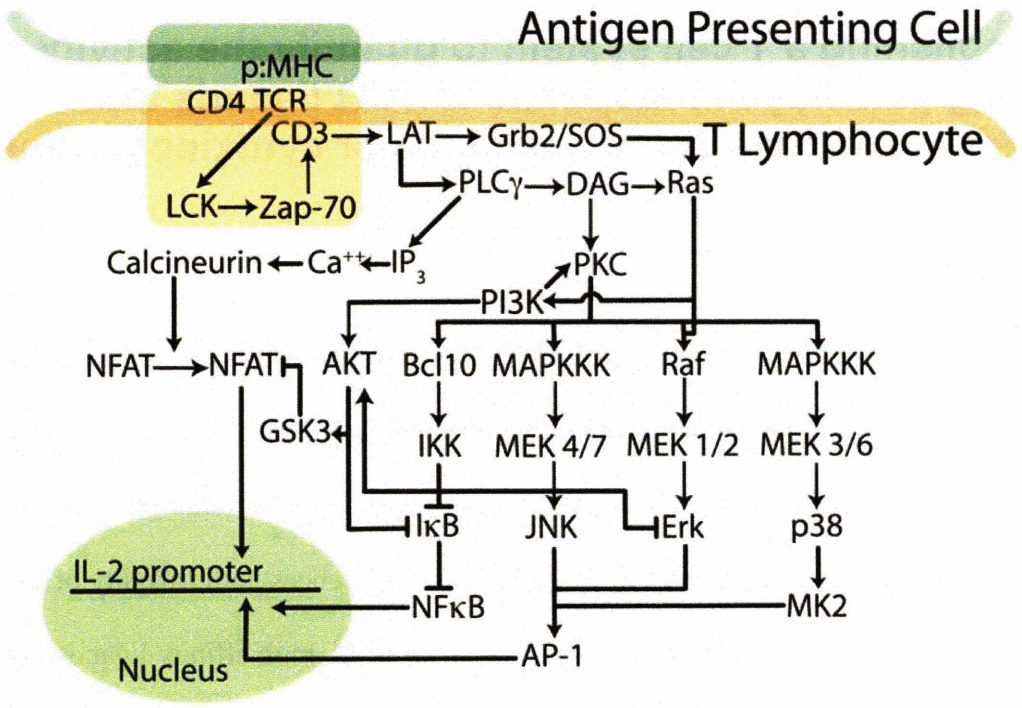

Figure 1.2. TCR signaling pathways

Schematic diagram showing the various signaling pathways activated downstream of TCR ligation resulting in IL-2 production.

2. Establishing a T cell system to quantify the activity of signaling pathways in response to TCR ligands that differentially induce either cell death or cytokine production.

2.1. Introduction

The engagement of the T cell receptor (TCR) by major histocompatibility molecules (MHC) and peptides can lead to multiple distinct cellular outcomes including proliferation, cytokine production, and cell death. How TCR engagement triggers distinct cellular responses is not completely understood. Current literature suggests that differences in the affinity of TCR ligands dictate the nature of induced TCR signals. At the cellular level, high affinity ligands in the periphery tend to induce proliferation, while low affinity ligands promote survival. An important question is: how does the TCR translate differences in the quality of ligands to the activation of distinct signaling pathways that result in different cellular responses? Addressing this question requires establishing an in vitro T cell system, capable of responding to different TCR stimuli. A key requirement for such an *in vitro* system is that different TCR stimuli elicit different cellular responses similar to T cell behavior seen *in vivo*.

TCR signals are propagated intracellularly through six TCR-associated CD3 transmembrane proteins resulting in the activation of TCR-associated signaling pathways. In vivo, T cells are stimulated through the TCR by ligation with an MHC containing a peptide displayed on the surface of an antigen presenting cell. This stimulation can be mimicked in vitro, using a co-culture system where two cell types, a T cell and a cell expressing MHC molecules are combined, resulting in the T cell being stimulated through its TCR. T cells in vitro can alternatively be stimulated using an anti-CD3 antibody that acts as a surrogate stimulus for the

TCR (Hara and Fu, 1985; Meuer et al., 1983; Oettgen et al., 1985; Weiss et al., 1984). In addition, pharmacological agents are available that mimic the release of downstream secondary messengers of T cell stimulation. This study focuses on using either anti-CD3 or peptide:MHC stimulation to differentiate between different cellular outcomes.

Anti-CD3 can be presented to T cells in one of two forms: surface-bound or soluble. Anti-CD3 can be surface-bound to either tissue culture wells or beads and may provide a unique signal to T cell for two potential reasons. First, surface-bound antigen can induce receptor aggregation and second, it can inhibit receptor internalization which has been shown to attenuate the signal (Valitutti et al., 1997). If stimulation with a different presentation of anti-CD3 leads to differences in cellular outcome, this would make a good system to answer the question of how a single receptor can induce different cellular phenotypes. Both human and mouse T cell lines are available that could potentially satisfy the requirements of the experimental system. I determined the feasibility of using two cell lines, one human T cell lymphoma cell line and one mouse T cell hybridoma.

The H9 human lymphoma cell line has been used extensively for HIV related research and was cloned based on its ability to sustain HIV virus replication (Chen, 1992; Mann et al., 1989; Popovic et al., 1984). The H9 cell line presented an attractive possibility as an experimental system since it responds to TCR stimuli by producing IL-2 and its TCR related signaling networks have been previously successfully studied. However, the specificity of its T cell receptor is not known. Therefore, the TCR of H9 cells is limited to stimulation by anti-CD3.

The mouse T cell hybridoma cell line expressing the 1B6 TCR has been widely studied in the autoimmune disease model experimental allergic encephalomyelitis (Kuchroo et al., 2002). One appealing aspect of this cell line is its known TCR specificity. In the 1B6 cell line, one can examine the cellular response to endogenous TCR ligands, peptides presented on MHC molecules. 1B6 T cells respond differently to altered peptides of myelin proteolipid protein 139-151. Three altered peptides have been shown to hierarchically affect proliferation, cytokine production and anergy in T cells containing the 1B6 TCR (Illes et al., 2005; Nicholson et al., 1998). The stimulating proteolipid protein peptides contain a single amino acid substitution at position 144 from tryptophan to glutamine, tyrosine or leucine and they all bind MHC class II with equivalent affinities (Nicholson et al., 1998).

In this work, we analyzed the signaling dynamics and consequent cellular response of both cell lines stimulated with plate-bound vs. soluble anti-CD3 and 1B6 cells stimulated with peptide ligand. These findings indicate that H9 T cells alter their signaling dynamics in response to plate-bound vs. soluble anti-CD3. However, changes in apoptosis could not be detected making this an unsuitable experimental system to analyze the cue-signal-response paradigm. 1B6 cells showed both altered signaling dynamics and cellular responses to plate-bound vs. soluble anti-CD3 as well as to altered peptide ligands. Due to the physiological relevance of peptide TCR stimulation, we determined that 1B6 cells stimulated with altered peptide ligands of PLP was the ideal experimental system to study how information about ligand avidity is transmitted to through the signaling network.

2.2. Materials and Methods

Cell Culture Conditions

H9 T lymphomas, DAS and 1B6 hybridomas were cultured in 1640 RPMI with Glutamine (VWR), 10% FBS (Hyclone, UT), Penicillin (100 units/ml) Streptomycin (100 μg/ml), Non-Essential Amino Acids (1x), HEPES (10 mM), and Sodium Pyruvate (1mM) (all Gibco)
For soluble anti-CD3 stimulation, anti-CD3 (BD Biosciences; mouse 2C11, human UCHT1) was diluted in cell culture media to the indicated concentration at the time of the experiment and added to 1B6 or H9 cells. For plate-bound anti-CD3 stimulation, anti-CD3 was diluted in PBS at the concentrations indicated and added to 24 well tissue culture plates. Plates were then incubated at 37 C for one hour up to overnight. PBS was removed and cell culture media containing 1B6 or H9 cells was added for time indicated.

Peptide Stimulation and Lysis

DAS cells (B7.1 positive fibroblasts transfected with I-As) (Munder et al., 2002) were grown to confluence in 6 or 24-well tissue culture plates (VWR). Q144 (HSLGKQLGHPDKF), Y144 (HSLGKYLGHPDKF), L144 (HSLGKLLGHPDKF) peptides (Anaspec) were added at concentrations indicated to DAS media 4-12 hours prior to addition of T cells. 1B6 hybridoma cells were added to DAS plates, which were centrifuged at 1000 rpm for 1 minute, and incubated at 37C for time indicated. Supernatant was transferred to 4 volumes ice-cold PBS and centrifuged at 3000 rpm for 1 minute. The cells were lysed in lysis buffer containing 2% Triton X-100, 50 mM Tris-HCl (pH 7.5), 150 mM NaCl, 50 mM β-glycerophosphate, 10 mM sodium pyrophosphate, 30 mM NaF, 1 mM benzamidine, 2 mM EGTA, 100 μM NaVO4, 1 mM dithiothreitol, 1 mM phenylmethylsulfonyl fluoride, 10 μg/ml aprotinin, 10 μg/ml leupeptin, 1 μg/ml pepstatin, 1 μg/ml microcystin-LR on ice for 20 minutes. After centrifuging at 14,000 rpm for 10 minutes at 4°C, the soluble fraction of lysate was collected (cytosolic extract) and protein concentration determined using a Micro-BCA protein assay kit (Pierce).

Western botting

For SDS-page gel electrophoresis, lysates were generated as described above and diluted to either 2 mg/ml or 4 mg/ml. Alternatively, lysates were generated by stimulation with anti-CD3 (BD Biosciences; mouse 2C11, human UCHT1) and anti-CD28 (BD Biosciences; mouse 37.51) in serum free media. Reducing Laemmli-SDS sample buffer (Boston Scientific) was added, and samples were boiled for 10 minutes. After electrophoresis, samples were transferred to polyvinylidene difluoride membrane (Bio-Rad) and blocked with 3% BSA (Sigma-Aldrich) in TBST. Blots were visualized and quantified using the Kodak Image Station 1000. Anti-phospho p44/42 (Thr202/Tyr204), anti-phospho SAPK/JNK (Thr183/Tyr185), anti-phospho p38 (Thr180/Tyr182), anti-phospho Akt (Ser473) were from Cell Signaling Technologies, and anti-rabbit HRP from Santa Cruz Biotechnology.

IL-2 ELISA

Supernatant was collected after time indicated and analyzed for IL-2 concentrations using quantitative sandwich ELISA for mouse IL-2 (BD Biosciences). 96-well plates were read and analyzed using a SpectraMax 250 (Molecular Devices) at 450 nm with wavelength correction at 570 nm.

Inhibitor Screen

The inhibitor library (Biomol, PA) was aliquoted and stored at -80 C. Inhibitor dilutions were carried out immediately prior to experiment in culture media. 150,000 H9 Cells were preincubated with inhibitor for one hour prior to CD3 or peptide stimulation.

Antibody Staining for FACS

200,000 cells were collected in 96-well round bottom plates and spun down at 1300 RPM for 5 minutes. Supernatant was removed and cells were washed two times with PBS containing 3% BSA. All wash steps in this protocol was followed by a 5 minute spin at 1300 RPM and a removal of the supernatant. Cells were then incubated in FC block (BD Biosciences, CA; clone 2.4G2) diluted in PBS containing 3% BSA for 10 minutes on ice. Primary antibody was added at 1:200 in FC block solution and incubated on ice for 30 minutes. Cells were spun down and washed twice, as before. Cells were resuspended in 300ml wash buffer and analyzed on a

FACScan (BD Biosciences, CA). Anti-CD28 (37.51), anti-CD4 and anti-TCR antibodies (H57-597) were from BD Biosciences, CA. For cell death assays Propidium Iodid was added to media immediately prior to FACS analysis.

2.3. Results and Discussion

2.3.1. Effects of soluble vs. plate-bound anti-CD3 stimulation on apoptosis and signaling dynamics in H9 cells

To test whether H9 cells respond differently to plate-bound vs. soluble anti-CD3, a time course was generated with stimulation times up to one hour. This time course was then analyzed for the phosphorylation of Erk1/2, p38, Jnk, and Akt (Fig 2.1A). Phospho-Western blots indicate soluble anti-CD3 induces a stronger Erk and p38 response at early time points; Akt is phosphorylated only in response to soluble anti-CD3; and Jnk appears to be phosphorylated more strongly in response to plate-bound anti-CD3.

To determine whether differences in the activation state of the signaling molecules correlated with a difference in cellular response, apoptosis was measured after 24 hours by propidium iodide incorporation in response to plate-bound and soluble anti-CD3 (Fig 2.1B). No clear trends were observed for differences in apoptosis to either plate-bound or soluble anti-CD3. Since no clear differences in cellular response could be observed in response to changing stimulation conditions, this cell line was not chosen for further analysis.

2.3.2. Effects of soluble vs. plate-bound anti-CD3 stimulation on apoptosis, cytokine production and signaling dynamics in 1B6 cells

To determine whether the stimulation conditions of plate-bound vs. soluble anti-CD3 were capable of inducing different cellular outcomes in 1B6 cells, 1B6 cells were stimulated with either plate bound or soluble anti-CD3. Apoptosis was determined 24 hours after anti-CD3 stimulation by measuring propidium iodide incorporation (Fig. 2.2A). Cytokine production was measured by ELISA (Fig. 2.3D). Plate-bound anti-CD3 was able to induce both apoptosis and cytokine production. Apoptotic levels varied with anti-CD3 concentration leveling off at 0.1 μg/ml. This leveling off could potentially be the result of all available receptor sites being occupied at that concentration. Soluble anti-CD3 did not induce either cell phenotype change.

To determine whether differences in Erk signaling for plate-bound and soluble anti-CD3 could be detected, cells were stimulated and a time course from 0 minute through 60 minutes was generated. Western blots for phospho-Erk indicated that soluble anti-CD3 induced strong, transient Erk activation with a peak at 20 minutes and levels reduced from peak at 60 minutes (Figure 2.2B). Plate-bound anti-CD3 induced lower levels of Erk activation. Once Erk levels could be detected in plate-bound anti-CD3 stimulation, they appeared constant through out the 60 minute time course.

Although the 1B6 system when stimulated with either plate-bound or soluble anti-CD3 exhibited two different phenotypic responses, which correlated with differences in signaling dynamics, we chose not to use this system in future studies for two reasons. First, a more physiologically relevant TCR ligand was available for the 1B6 TCR system. The 1B6 TCR is know to be specific for the myelin proteolipid protein peptide 139-151 (Nicholson et al., 1998); Second, we

were not able to quantifying the number of antibodies bound to the surface of the well and consequently the number of TCRs being stimulated per cell. This is because a plate-bound concentration refers to the concentration of antibody diluted in PBS that is used during the plate binding. The relationship between the concentration of antibody in solution vs. on the surface of the well is not known. Therefore, we could not make a direct comparison between stimulation levels of plate-bound vs. soluble antibody at different concentrations.

2.3.3. Co-stimulation does not appear to affect the phenotypic response of 1B6 cells to TCR stimulation

Co-stimulatory molecules, such as CD28, provide an important second signal to naïve T cells resulting in T cell activation in the periphery (Liu and Janeway, 1992). To determine whether 1B6 cells expressed the co-stimulatory ligand CD28, its surface expression was measured using FACS. CD28 expression could be detected at low levels in a control cell line, mouse DO11 (Fig. 2.3A). CD28 could not be detected on the surface of 1B6 cells using FACS (Fig. 2.3A). Both DO11 and mouse 1B6 cells appear to express TCR molecules on the cell surface at similar levels (Fig. 2.3B).

To exclude the possibility that CD28 levels presented at the cell surface of 1B6 cells are below the detection limit of FACS analysis, functional CD28 stimulation assays were preformed. CD28 co-stimulation is known to enhance the effects of TCR stimulation, therefore, 1B6 cells were stimulated with either plate-bound or soluble anti-CD3 with or without a stimulating form of anti-CD28. Cell death was measured by propidium iodide incorporation. IL-2 was measured using ELISA. Co-stimulation through the CD28 receptor did not appear to affect either apoptosis

(Fig. 2.3C) or IL-2 production (Fig. 2.3D) in 1B6 cells. From these studies we concluded that CD28 does not appear to be present on the surface of 1B6 cells.

2.3.4. Signaling dynamics of the PLP peptide system in the 1B6 and DAS cell lines

To determine the effects of individual peptides on signaling dynamics, 1B6 T cell hybridomas were stimulated with Q144, Y144 or L144 peptide and the activation state of Erk, Jnk, p-38, and Akt, was measured by western blotting at multiple time points after peptide stimulation (Fig. 2.4A). L144 induced the strongest Erk and Jnk signal, at 30 minutes, with a graded response for Y144 and Q144. p38 activation appeared to increase with time for all conditions measured while Akt phosphorylation was highest in the Y peptide stimulation condition.

In the above experiment, 1B6 cells were stimulated with DAS cells, fibroblasts transfected with I-A^s and B7.1 (Munder et al., 2002). One potential confounding variable of generating lysates from suspension T cells stimulated by adherent APCs is the contamination of the T cell lysate with APCs. To determine whether DAS cells respond to the addition of peptide and 1B6 T cells by upregulating the activation state of their signaling molecules, DAS cell lysates were generated and probed by western blotting for Erk, Jnk, p-38, and Akt (Fig 2.4B). Western blots indicate that the activation state of the MAPKs and Akt does not change in response to peptide addition and T cell stimulation. Since DAS cells do not change their activation state in response to peptide addition and T cell stimulation, the effect of DAS cell contamination would result in a dilution of the signal. However, we make the assumption that DAS cell contamination is low and relatively constant across samples.

Since 1B6 cells show a graded response to altered peptide ligand (APL) stimulation, data in later chapters will be generated using the 1B6 PLP system.

2.3.5. Inhibitor screen identifies key signaling components of IL-2 production in response to TCR stimulation

To identify key signaling components downstream of the T cell receptor required for IL-2 production, an inhibitor library, containing 67 kinases and 14 phosphatase inhibitors (see Appendix A, Supplementary Fig. 1) was screened. The library contained multiple inhibitors targeting the same compounds and its specificities reflected a broad range of molecules identified in the literature to be downstream of TCR signaling.

To identify molecules relevant for IL-2 production in T cells, H9 cells were pre-incubated with the compounds in the inhibitor library at two different concentrations, 10 μM and 10 nM for 60 minutes, then stimulated with anti-CD3 for 6 hours. IL-2 production was measured via ELISA (Fig 2.5A). Several inhibitors for the same target were consistently identified as capable of reducing IL-2 levels. These include inhibitors to the Akt signaling pathways (Wortmanin and LY0294002), Erk signaling pathways (PD98059 and UO126)

Multiple proteins previously described as being important in TCR signaling emerged as regulators of IL-2 production in these experiments. However, experimental variability was significant between these experiments. In addition, the concentration of inhibitor used was constant and did not reflect the potency of any individual inhibitor. To address these limitation, 21 inhibitors were selected (Appendix A, Supplementary Fig. 2) based on their IL-2 inhibition

profile and an additional screen was performed at greater than or equal to five times the IC_{50} for each inhibitor (experimental inhibitor concentrations are indicated in Appendix A, Supplementary Fig. 2). This screen was performed on 1B6 cells stimulated with L144 peptide for 6 hrs. IL-2 was measured by ELISA (Fig 2.5B). Most notably, some inhibitors targeting Src family kinases, MAPKs (with the exception of p38), NFkappaB, PI3K, and PKC potently reduced IL-2 production in 1B6 cells stimulated with L144 peptide. These molecular targets are expected to inhibit IL-2 production since they result in the activation of known IL-2 transcription factors (Jain et al., 1995). The PI3K pathway, which among other pathways activates Akt, has not been directly implicated in activating an IL-2 transcription factor in the absence of co-stimulation. However, 1B6 cells treated with the PI3K inhibitor exhibited reduced IL-2 levels. Interestingly, different inhibitors targeting the same molecule or different molecules in the same pathway did not affect IL-2 production equally (Fig 2.5B). One example of this are the two Src kinase inhibitors, PP1 and PP2 which appeared to have very different effects on IL-2 production. Also, of the three inhibitors targeting calcineurin, molecules upstream of NFAT activation, none of them reduced IL-2 production by greater than 25%. This finding is unexpected due to NFATs well defined role in IL-2 production (Ullman et al., 1990).

Taking into account the results of the inhibitor screen, further analysis of the network state downstream of T cell activation will determine the activation state of multiple signaling pathways including the MAPKs, Erk. P38, and JNK; Akt; NFAT; and NFκB.

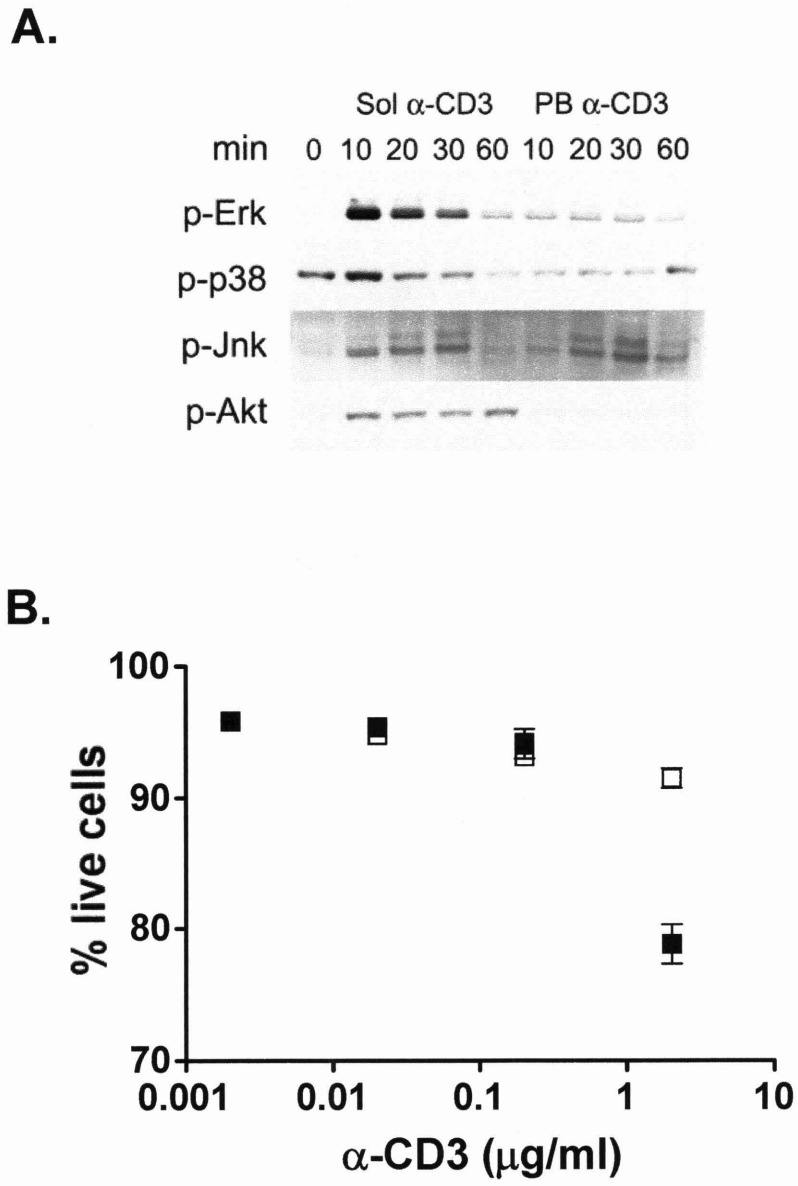

Figure 2.1. H9 cells stimulated with plate-bound vs. soluble anti-CD3

A) H9 lysates probed for indicated phosph-species. B) Percent live cells after 24 hrs. stimulation with plate-bound (*filled squares*) or soluble (*open squares*) anti-CD3 as quantified by propidium iodide incorporation and FACS analysis.

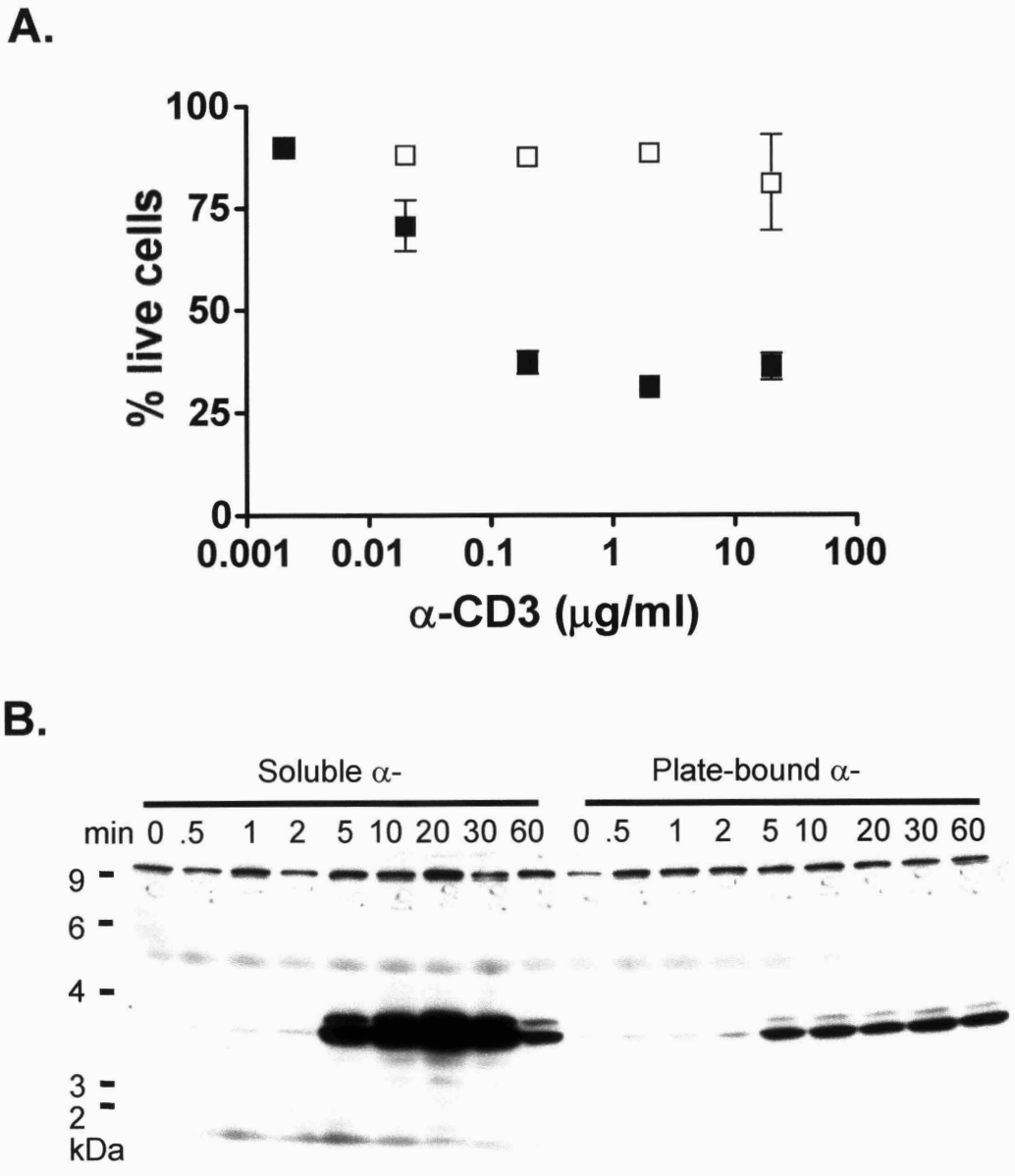

Figure 2.2. 1B6 cells stimulated with plate-bound vs. soluble anti-CD3

A) Percent live cells after 24 hrs. stimulation with plate-bound (*filled squares*) or soluble (*open squares*) anti-CD3 as quantified by propidium iodide incorporation and FACS analysis. B) Detailed time course of phospho-Erk activation following anti-CD3 stimulation.

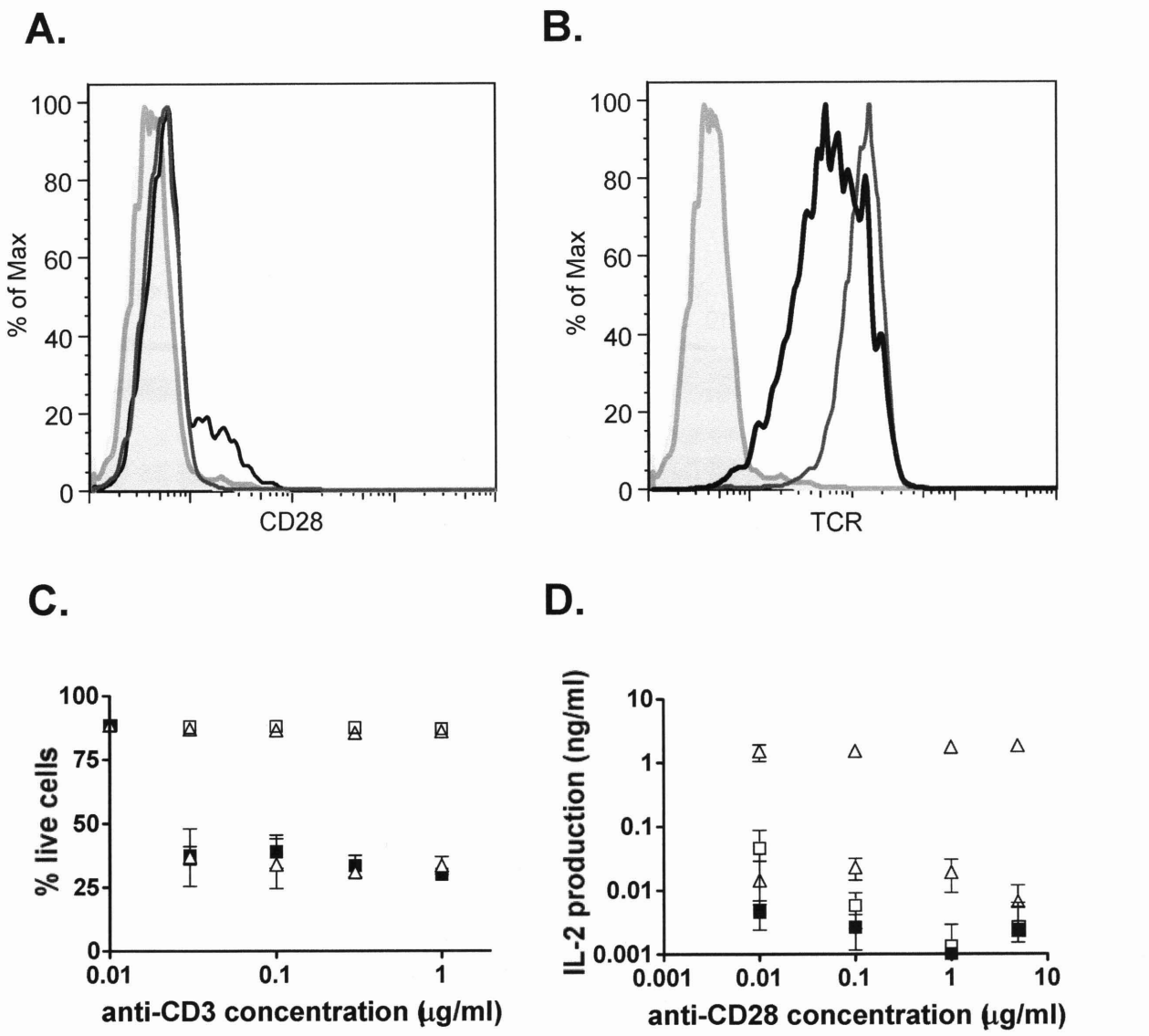

Figure 2.3. CD28 co-stimulation does not alter the 1B6 phenotypic response to TCR stimulation

A) and B) Surface expression of CD28 and TCR respectively as assessed by FACS analysis the DO11 cell line is used as a positive control for CD28 staining. Shown are negative controls for DO11 and 1B6 cells (Filled histograms) and stained DO11 (black outline) and 1B6 cells (gray outline). C) Percent live cells after 24 hrs. stimulation with plate-bound (*filled symbol*) or soluble (*open symbol*) anti-CD3 and with (*triangle*) or without anti-CD28 (*square*) as quantified by propidium iodide incorporation and FACS analysis. D) Cumulative IL-2 levels produced in the absence (*squares*) or presences (*triangles*) of plate-bound (*filled symbols*) or soluble anti-CD3 (*open symbols*).

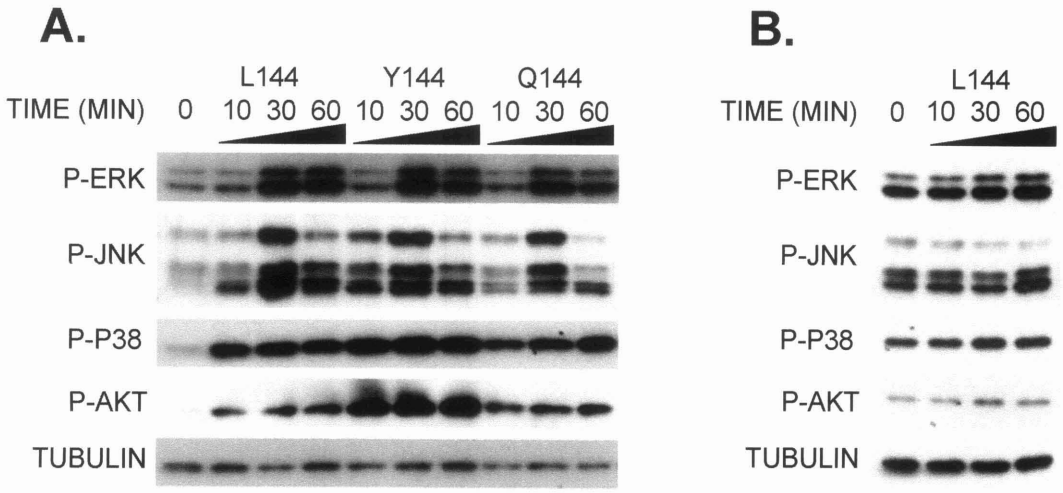

Figure 2.4. 1B6 cells respond differently to stimulation with altered peptide ligands of PLP

A) Time course of phospho-protein activation in 1B6 cells stimulated with peptide ligand. B) Time course of phospho-protein activation in DAS cells antigen-presenting cells during 1B6 peptide stimulation.

Figure 5 A.

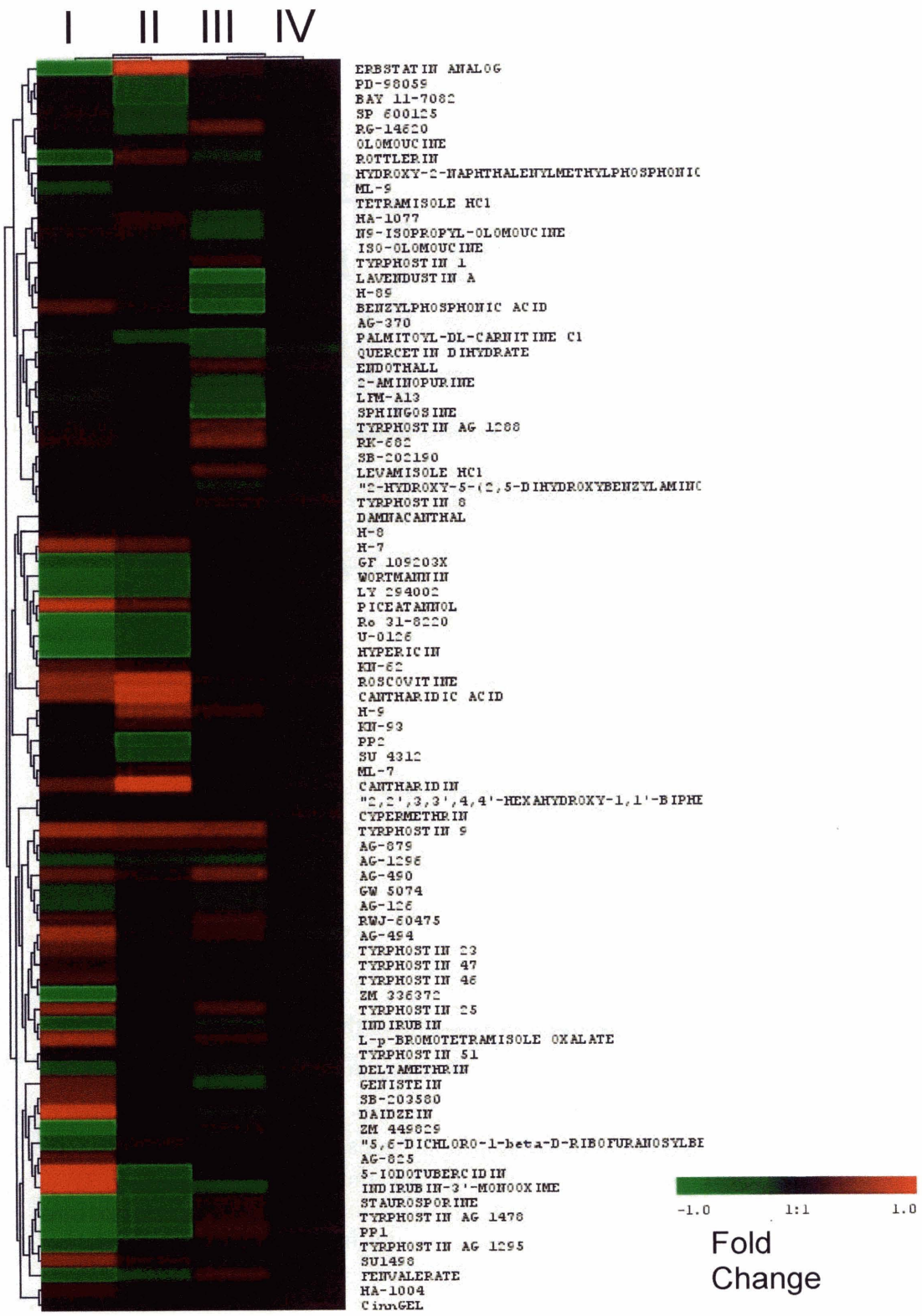
I
II
III
IV
ERBSTATIN ANALOG
PD-98059
BAY 11-7082
SP 600125
RG-14620
OLOMOUCINE
ROTTLERIN
HYDROXY-2-NAPHTHALENYLMETHYLPHOSPHONIC
ML-9
TETRAMISOLE HCl
HA-1077
N9-ISOPROPYL-OLOMOUCINE
ISO-OLOMOUCINE
TYRPHOSTIN 1
LAVENDUSTIN A
H-89
BENZYLPHOSPHONIC ACID
AG-370
PALMITOYL-DL-CARNITINE Cl
QUERCETIN DIHYDRATE
ENDOTHALL
2-AMINOPURINE
LFM-A13
SPHINGOSINE
TYRPHOSTIN AG 1288
RK-682
SB-202190
LEVAMISOLE HCl
"2-HYDROXY-5-(2,5-DIHYDROXYBENZYLAMINO
TYRPHOSTIN 8
DAMNACANTHAL
H-8
H-7
GF 109203X
WORTMANNIN
LY 294002
PICEATANNOL
Ro 31-8220
U-0126
HYPERICIN
KN-62
ROSCOVITINE
CANTHARIDIC ACID
H-9
KN-93
PP2
SU 4312
ML-7
CANTHARIDIN
"2,2',3,3',4,4'-HEXAHYDROXY-1,1'-BIPHE
CYPERMETHRIN
TYRPHOSTIN 9
AG-879
AG-1296
AG-490
GW 5074
AG-126
RWJ-60475
AG-494
TYRPHOSTIN 23
TYRPHOSTIN 47
TYRPHOSTIN 46
ZM 336372
TYRPHOSTIN 25
INDIRUBIN
L-p-BROMOTETRAMISOLE OXALATE
TYRPHOSTIN 51
DELTAMETHRIN
GENISTEIN
SB-203580
DAIDZEIN
ZM 449829
"5,6-DICHLORO-1-beta-D-RIBOFURANOSYLBE
AG-825
5-IODOTUBERCIDIN
INDIRUBIN-3'-MONOOXIME
STAUROSPORINE
TYRPHOSTIN AG 1478
PP1
TYRPHOSTIN AG 1295
SU1498
FENVALERATE
HA-1004
CinnGEL
-1.0
1:1
1.0
Fold
Change

Figure 5 B.

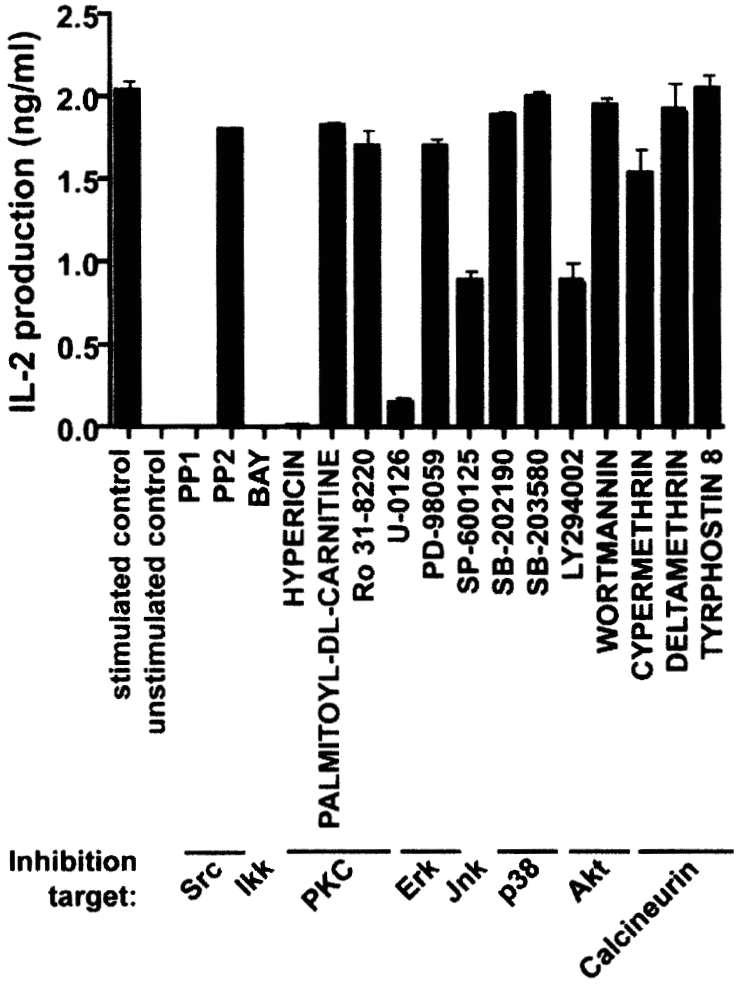

Figure 2.5. Screening for signaling pathways that control IL-2 production following TCR stimulation

A) Relative levels of IL-2 produced by H9 cells in response to the inhibitors indicated. IL-2 levels are normalized to DMSO control. H9 cells were pre-incubate with either 10 nM (I *and II* or 10 μM (*III and IV*) of inhibitor and stimulated with anti-CD3. B) Levels of IL-2 produced by 1B6 cells in response to the inhibitors indicated. Individual inhibitors were diluted to the concentrations indicated in Appendix B.

3. Network Signal Combinations Downstream of T Cell Receptor Activation Predict IL-2 Response

3.1. Introduction

Signaling through the T cell receptor (TCR) leading to cell decision processes is determined in part by the affinity of the T cell receptor for its ligand. Affinities of TCR/ligand interactions can differ by at least three orders of magnitude (Lanzavecchia et al., 1999) and can correspondingly elicit vastly different cellular responses. In mature T cells, high-affinity TCR-pMHC interactions can lead to T cell activation whereas low-affinity interactions are important for cellular homeostasis and may be involved in antigenic signal amplification. Activation of T cells by altered peptide ligands (APLs) can also induce partial activation, hyperstimulation and anergy (Gascoigne et al., 2001). Elucidating the complex molecular details underlying ligand affinity discrimination by T cells is central to our understanding of both T cell-mediated immunity to pathogens and immune dysfunctions, such as autoimmunity and aberrant immunosurveillance. A growing body of work has focused on proximal TCR signaling events in order to elucidate mechanisms of ligand affinity discrimination (Krogsgaard and Davis, 2005). However, recent work in other areas of cell biology has ascertained that quantitative combinations of signals in downstream pathways, distal to the initiating receptor activation, may better represent the receptor-mediated information governing ultimate cell phenotypic responses (Hautaniemi et al., 2005; Janes et al., 2005; Prudhomme et al., 2004). In the context of post-TCR activation, we provide evidence that multiple activation states quantitatively encoded by the signaling network define regulatory aspects for a T cell cytokine response.

Differential signals from TCR binding can result from single residue changes occurring at the ligand-receptor interface. Upon TCR engagement, changes in the ITAM phosphorylation

patterns (Madrenas et al., 1995; Sloan-Lancaster et al., 1994) activate multiple interconnected signaling pathways (Germain and Stefanova, 1999; Huang and Wange, 2004) (illustrated in Fig. 2A). Propagation of stimuli from the receptor results in eventual nuclear localization of AP-1, NFAT, NF-κB, and Oct-1 - transcription factors, all of which are known to bind to the IL-2 promoter region (Jain et al., 1995). For this reason, IL-2 production is often used as a measure for T cell activation.

In this study we employed a high level modeling approach (Ideker and Lauffenburger, 2003; Janes and Lauffenburger, 2006), partial least squares regression (PLSR) analysis, to understand the relationship between ligand avidity, downstream signaling dynamics, and IL-2 production. This type of analysis can relate a data-set of predictor variables (signaling measurements) to a response variable (IL-2 production) without prior knowledge of – or assumptions about – network structure. This method of linear multi-variate statistical modeling has been used successfully to understand signal-response relationships in cell decision processes such as apoptosis (Gaudet et al., 2005; Janes et al., 2005; Janes et al., 2004).

3.2. Methods

Generation of hybridoma

The 1B6 T cell hybridoma was generated in the laboratory of Vijay Kuchroo by fusion of the 1B6 T cell clone (Nicholson et al., 1998) with the TCR negative fusion partner BW1100. Following fusion, positive hybrids were identified by measuring growth inhibition in the presence antigen presenting cells and L144 peptide versus control peptide. Positive cells were subcloned using limiting dilution at least twice.

Lysis preparation

DAS cells (B7.1 positive fibroblasts transfected with I-A^s) (Munder et al., 2002) were grown to confluence on Nunc coated omni trays (Nunclon). Q144 (HSLGKQLGHPDKF), Y144

(HSLGKYLGHPDKF), L144 (HSLGKLLGHPDKF) peptides (Anaspec) were added at concentrations indicated to DAS media 4-12 hours prior to addition of T cells. 10^7 1B6 hybridoma cells were added to DAS plates, which were centrifuged at 1000 rpm for 1 minute, and incubated at 37C. Supernatant was transferred to 4 volumes ice-cold PBS and centrifuged at 3000 rpm for 1 minute. The cells were lysed in buffer (Janes et al., 2003) modified to 2% Triton X-100 on ice for 20 minutes. After centrifuging at 14,000 rpm for 10 minutes at 4°C, the soluble fraction of lysate was collected (cytosolic extract) and protein concentration determined using a Micro-BCA protein assay kit (Pierce). The pellet was resuspended in 420 mM NaCl, 20 mM HEPES (pH 7.9), 1mM EGTA (pH 8.0), 1 mM EDTA (pH 8.0), 1 mM sodium orthovanadate, 1 mM dithiothreitol, 1 mM phenylmethylsulfonyl fluoride, 10 μg/ml aprotinin, 10 μg/ml leupeptin, 1 μg/ml pepstatin, 1 μg/ml microcystin-LR. The pellet was sonicated for 1 min followed by 3 minutes on ice, repeated 6 times, followed by centrifugation at 14,000 rpm for 30 minutes at 4C.

Inhibition

PD098059 and LY294002 (DMSO stock), and AktX (water stock) (all Calbiochem) was diluted to working concentration in media. 1B6 cells were preincubated in PD098059 for 30 minutes; LY294002 for 30 minutes and AktX for 1 hour, prior to stimulation with peptide-loaded DAS cells.

Quantitative western blotting

For SDS-page gel electrophoresis, lysates were diluted to either 2 mg/ml or 4 mg/ml, reducing Laemmli-SDS sample buffer was added, and samples were boiled for 10 minutes. 40 μg or 80 μg lysate was loaded per well. Each sample was loaded in triplicate wells and for normalization purposes, each gel contained duplicate lanes of a positive control sample. After electrophoresis, samples were transferred to polyvinylidene difluoride (PVDF) membrane and blocked with 3% BSA in TBST. Blots were visualized and quantified using a Kodak Image Station 1000. The net intensity of individual bands was determined and normalized to the net intensity of the average of the positive control bands. Triplicates were then averaged and fold activation determined by normalization to the zero time-point. Anti-phospho p44/42 (Thr202/Tyr204), anti-phospho SAPK/JNK (Thr183/Tyr185), anti-phospho p38 (Thr180/Tyr182), anti-phospho Akt (Ser473) were from Cell Signaling Technologies, and anti-rabbit HRP from Santa Cruz Biotechnology.

Kinase activity assays

MAPKAPK2 (MK2) and IKKα/β activities were determined by a custom multi-plex kinase assay (Janes et al., 2003) with the following modifications: For the MK2 assay, Protein A microtiter strips (Pierce) were coated with anti-MK2 (Stressgen), and the reaction allowed to proceed for 1 hour. For the IKKα/βassay, 500 μg of total lysate protein was incubated in the antibody-coated wells overnight. Data were normalized by the value quantified for the zero time-point for fold-activity.

NFAT westerns

NFAT phosphorylation and localization was measured by resolving 22 μg of sample protein (boiled for 10 minutes in sample buffer) on 5% polyacrylamide gel, alternating cytosolic and nuclear fractions in the lanes. Membranes were blocked with 3% BSA in TBST followed by incubation with NFATc2 antibody (Santa Cruz Biotech) at a 1:500 dilution. Ratios of dephosphorylated bands to phosphorylated bands on the same lane were determined.

IL-2 ELISA

Supernatant was collected after 4 hours and analyzed using quantitative sandwich ELISA for mouse IL-2 (BD Biosciences).

Data processing and modelling

The compiled data matrix was transformed by the equation y = log10(x+1) where x is a measured value, to account for a skewed distribution of experimentally measured values. The column transformed data were then mean-centered and scaled by unit variance. Partial least-squares regression analysis was performed in SIMCA-P (Umetrics). The data-set was divided into two matrices: $Y \in R^{15x1}$ consisting of IL-2 measurements, and $X \in R^{15x57}$ denoting the measured protein signals. The PLSR algorithm successively finds linear combinations of the predictor variables that have maximum covariance with the response variables, so that each linear function is uncorrelated with previous ones (Wold et al., 2001). PLSR can accommodate data-set that are not fully complete (i.e., yielding matrices that are not of full rank), provided the missing values are randomly distributed across the different observations, e.g. JNK1 and JNK2 data points are missing in one of three

experimental replicates for each stimulation condition. For more detailed description on PLSR modeling we refer to a previous explication (Wold et al., 2001).

3.3. Results

3.3.1. Peptide avidity defines cellular response

In T cells containing the 1B6 TCR, the three altered peptides we use have been shown to affect proliferation, cytokine production and anergy hierarchically (Illes et al., 2005; Kuchroo et al., 2002; Nicholson et al., 1998). The altered peptide ligands (APLs) are based on the autoantigen myelin proteolipid protein peptide 139-151 but contain a single amino acid substitution at position 144 from tryptophan to glutamine, tyrosine or leucine. All three peptides bind MHC class II with equivalent affinities (Nicholson et al., 1998). We assayed apoptosis induced by different concentrations and avidities of APLs in T cell hybridomas (Ashwell et al., 1987) that express the 1B6 TCR. DAS antigen presenting cells were pulsed with proteolipid protein APLs Q144, Y144, and L144 for 4-12 hours prior to addition of 1B6 cells. After 24 hours, apoptosis of 1B6 cells was measured via propidium iodide incorporation (Fig. 3.1A). Prior experiments with Annexin V and propidium iodide double staining confirmed that cell death through peptide stimulation occurs by apoptosis (Appendix B, Fig. 1). 1B6 cells stimulated with L144 peptide showed greater than 85% cell death at both peptide concentrations measured, the Y144 peptide induced 53% cell death at 4 μg/ml, while the Q144 peptide at 4 μg/ml induced cell death at levels similar to the no peptide control (Fig. 3.1A).

The levels of IL-2 production in 1B6 cells stimulated with the various peptides correlated with the apoptotic responses (Fig. 3.1B). IL-2 production was measured after 4 hours of peptide stimulation. High levels of IL-2 were present in the media of 1B6 cells stimulated with L144 peptide and low levels of IL-2 were present in the media of 1B6 cells

stimulated with the Y144 peptide. IL-2 in the supernatant was below the detection limit in cells stimulated with Q144 peptide. Since apoptosis within a sample will affect the cumulative IL-2 produced by that sample, we avoid confounding effects between two phenotypic behaviors, IL-2 production and apoptosis, by measuring signaling dynamics and cellular responses in the first 4 hours post-activation.

3.3.2. Peptide avidity determines activation dynamics of downstream signaling molecules

To determine how the avidity of the TCR for the pMHC is encoded within these signaling pathways, we measured the activation levels of key signaling molecules known to be important for IL-2 production in T cells (highlighted molecules in Fig. 3.2A). Of the IL-2 promoter elements, we measured the nuclear translocation of one directly (NFAT), and measured activation/phosphorylation of kinases upstream of others (IKKα/β for NF-κB, JNK for Jun, ERK1/2 for Fos, and p38/MK2 as an additional surrogate of the AP-1 component ATF-2). To generate a self-consistent, multi-variate data-set (Gaudet et al., 2005; Janes et al., 2003), all protein activation measurements (Fig 3.2A) were obtained from a single lysate containing in excess of 40×10^6 cells per stimulation condition and time-point. The endpoint cellular response measurement was the level of IL-2 production acquired from media collected in the plate at 4 hours. In total, we measured for 5 peptide stimulation conditions and one no peptide control condition for the following: 11 predictor signals at 6 time-points, and one response variable (IL-2) at the final four-hour time-point. To account for biological variation within the data-set, each stimulation condition was replicated on three different days and triplicate experiments were entered into the model as separate observations (Fig. 3.2B). In a few cases, we were unable to accurately quantify signals on a lysate (Fig. 3.2B, gray squares). The final data matrix contained 1178 unique measurements. To our knowledge, this

is the first time that such a large array of signals has been analyzed systematically and concurrently for a clonal TCR line activated by peptide ligand-stimulation.

Examples of the dynamic time-courses of these signaling measurements are illustrated in Figs. 3.2C in which the replicate time-course measurements for ERK2 and Akt are each compared across the three different peptides all at a concentration of 4 μg/ml. We show that in all three peptide stimulation conditions, ERK2 and Akt are activated during the measured time course and that levels and timing of activation vary with peptide. Lysates generated from the antigen presenting cells after co-culture with the 1B6 T cells show no contribution to activation signals (Appendix B, Supplementary Figure 3A). We surmise that – within the context of this experimental system – individual altered peptides do not appear to elicit qualitatively unique signatures in network dynamics but rather mainly affect the magnitude of phosphorylation/activation of the signaling molecules sampled.

3.3.3. Information content of data-set is sufficient for IL-2 fitting within the training set data

Our objective in this work was to explore the hypothesis that IL-2 production is encoded within an appropriate set of measurements of dynamic signaling in the network downstream of TCR activation. If the levels of IL-2 production are indeed encoded within the signaling dynamics then it is feasible to construct a model capable of predicting the IL-2 production (response variable) data in Figure 2B from the signaling (predictor variables) data.

The model converged at two principal components; attempts to identify additional principal components did not yield greater information content (Appendix B, Supplementary Fig. 2A), following statistical criteria described (Wold et al., 2001). The two-component model is capable of fitting IL-2 concentrations from the input data with a line $y = 1.19x + 0.06$ and a regression coefficient (defined as R^2Y – see Methods section) of 0.97. PLSR

creates the principal components through linear combinations of the predictor variables. In highly-connected biological pathways, non-linearities may be present in the system. We examined the potential benefit of including non-linear terms to the model as described previously (Janes et al., 2004), but these further terms did not enhance the model's ability to explain data variance; in fact, they decreased the regression coefficient by amplifying noise in the data matrix (data not shown).

When individual samples are mapped onto the two principal components via their scores, IL-2 producers can be discriminated from non-IL-2 producers on the first component (Fig. 3.3A). IL-2 producers scored positive on the first component while non-IL-2 producers scored negative on the first component. A two-tailed Welch's t-test (df = 13) comparing the first principal component loadings between IL-2 producers and non-IL-2 producers demonstrates statistical significance ($p = 0.0008$). The second principal component loadings are not significantly different between the two groups. This finding suggests that the combination of signals comprised in the first component are largely responsible for binary control of IL-2 production from on to off, while the combination of signals comprised in the second component are more responsible for fine-grained tuning of IL-2 production. Therefore, it becomes of immediate interest to ascertain which signals are heavily weighted in one or the other component, for this may aid in deciphering which if any particular signal is involved in "on/off" control or "tuning" of IL-2 production. Predictor signaling variables were plotted onto the two principal components based on their weighted contributions to the component (Fig. 3.3B; Table 3.I). Signals with large values influenced the model to a greater extent than signals that were close to the origin, while signals with negative values were inversely related to the response variable (Fig. 3.3B; the complete mapping of signal weights is provided in Appendix B, Supplementary Fig. 2B). Similarly, signals that mapped close to the IL-2 response were more heavily relied upon for IL-2 fitting than signals that were close to the origin. Both ERK1 and ERK2 at multiple time-points were heavily weighted (Fig. 3.3B; Table 3.I). This is anticipated, as ERK is thought to be a major contributor to cellular outcome in response to TCR signaling. More surprisingly, Akt also emerged as a primary

contributor for both the first and the second components (Fig. 3.3B; Table 3.I). Although Akt is known to contribute to co-stimulation, a key role in transducing TCR signals has not been reported. The 1B6 cell line does not show changes in IL-2 when CD28/CTLA-4 is blocked with a CTLA-4/Fc fusion protein. In addition the 1B6 cell line does not shown changes in apoptosis levels in response to anti-CD3 in combination with anti-CD28 compared to anti-CD3 alone, suggesting that the observed influence of Akt in the model is due to primary TCR signaling (Appendix B, Supplementary Figure 3B and C). JNK scored highly on both the first and the second component and its contributions to IL-2 prediction appeared to at least roughly co-localize with NFAT (Appendix B, Supplementary Figure 2B); this may reflect an established molecular mechanism that JNK can directly activate NFAT-driven transcription (Ortega-Perez et al., 2005). In addition we found a close correlation between ERK signals and IKK signals (Appendix B, Supplementary Figure 2B). To the best of our knowledge no mechanism of cross-talk between these pathways under antigen-receptor stimulation conditions has been reported. However, this tight correlation could reflect a common origin of activation of both pathways, such as by PKCθ.

3.3.4. Information content of signals is sufficient for *a priori* IL-2 prediction of a new stimulation condition

We sought to determine whether the biological information captured in the model is capable of predicting IL-2 production for a new stimulation condition. 1B6 T cells were treated with a new condition, 0.04 μg/ml L144 peptide, and the protein signaling variables were input into the model (Fig. 3.4A). The model was then used to predict IL-2 production based upon the signal/response relationships derived from the trained model. Figure 3.4B shows the linear regression fit between experimentally measured IL-2 values and the *fitted* model IL-2 values for the trained model described by Fig. 3.2B (black, blue, green, red symbols). On the same graph, the experimentally measured IL-2 values versus the *predicted* IL-2 values (yellow

symbols) is plotted for the data in Fig. 3.4A. The model performs very successfully for two of the samples, predicting IL-2 concentrations within 2% and 18% of the experimentally measured values. For the third sample, model performance was less tight but nonetheless predicted IL-2 concentration to within a factor of 2.

To investigate whether a model trained on measurements of a single signaling protein (with full time-course; Fig. 3.5A, B) or at a single time-point (across the full set of proteins; Fig. 3.5C, D) could adequately predict IL-2 production, we constructed different models from restricted subsets of our data. We evaluated the quality of each model by three metrics: the fit to IL-2 (R^2Y; a value near 1 is desired), the fraction of variation in IL-2 measured by cross validation (Q^2Y; a value near 1 is also desired), and the sum of errors in the three *a priori* predictions (ΣDmodY; a value near zero is desired).

The optimal full model exhibited a value of 0.94 for R^2Y, 0.57 for Q^2Y, and 2.04 for ΣDmodY. By comparison, the best-performing single-protein model arose from that constructed on ERK2, with an R^2Y of 0.81 (Fig. 3.5A, B). All other single-protein models performed worse than the ERK2 model. Although Akt had been found to be a primary informer in the full model, an Akt-only model performed poorly by itself, producing an R^2Y of 0.62. We can conclude then that a satisfactory model relating signals downstream of TCR activation to IL-2 production requires a quantitative combination of measurements across multiple pathways. This conclusion is reasonable in light of the necessity for multiple transcription factors regulated by the diverse pathways to bind in combinatorial fashion to the IL-2 promoter region.

To address the inclusion of time-course data, models were also constructed across the signaling proteins at a single time-point (Fig. 3.5C, D). The large number of t=30 minutes variables identified to be heavily weighted in the full model suggested that a model using only 30-minute measurements of the 11 signaling proteins might perform well. An R^2Y=0.90 was indeed found for a model containing only 30-minute predictor variables, but the predictive ability of the model was low as evidenced by the large value of ΣDmodY=7.51.

Models built using other single time-points performed better than the t=30-minute model for ΣDmodY, but at the expense of a lower R^2Y. Clearly, inclusion of measurements at multiple time-points was required for optimal model prediction capability. These simulation results indicate that predictive information encoded in the various signaling pathways may differ temporally in kinetic rates of propagation of information relevant to IL-2 production. Therefore, we conclude that to most effectively capture the critical features of network operation, dynamic measurements are required.

3.3.5. Akt phosphorylation level is informative of IL-2 production

We have thus far demonstrated that models built upon a single signalling molecule or time-point do not contain enough information to fully capture the IL-2 response. We next asked whether a single signal (such as the top-weighted Erk and Akt) might nonetheless be capable of modulating the IL-2 response in a predictive manner as long as multi-variate relationships among pathways are maintained. Because Erk has a well established role in propagating TCR signals and is heavily weighted on the first component, we examined the predicted effect of inhibiting Erk on IL-2 production. In addition, we examined the predicted effect of inhibiting Akt on IL-2 production because the optimal model relied especially heavily on Akt in both the first and the second components. Simulated time-courses were generated by computationally reducing the levels of either Erk or Akt phosphorylation by 25%, 50%, or 75% across all time-points while keeping all other predictor variables unchanged (Fig 3.6A and C). We modified four signalling time-courses: two L144 4 μg/ml observations used in the training set and two L144 0.04 μg/ml observations used in the *a priori* prediction. The PLSR model was then used to predict IL-2 production for the new observation based upon the altered Erk or Akt signals (Fig. 3.6A and C). Reduced IL-2 production levels were predicted to be tightly correlated with both reduced Erk and reduced Akt phosphorylation, described by a slope of -0.29 for Erk and -0.84 for Akt. Reducing Erk and Akt levels by the

same degree simultaneously led to a surprising prediction in that the decrease in IL-2 was slightly less than the sum of the individual signal contributions (Fig 3.6E, slope = -1.0 vs -1.12)

To test these model predictions, we experimentally measured IL-2 levels under conditions of Erk and Akt inhibition using small molecule inhibitors and compared these values to the corresponding PLSR model predictions. An experimental dose-response curve was created for inhibition of Erk by PD98059 and Akt by LY294002 (Appendix B, Supplementary Fig 4). PD98059 is specific for the Erk pathway, and inhibits the upstream activator of Erk, Mek. LY294002 targets Akt indirectly through PI3K. 1B6 cells were pre-incubated with either PD98059, LY294002, or a combination of the two, followed by a 30-minute stimulation with 4 μg/ml L144 peptide. Cell lysates were analyzed for phosphorylation state of the inhibition target. PD98059 was found to inhibit Erk phosphorylation with an IC_{50} of 0.7 μM for ERK1 and 3.1 μM for ERK2. Akt phosphorylation was inhibited by LY294002 with an IC_{50} of 1.3 μM. To assess the effect of reduced Erk activity on IL-2 production, we inhibited Erk phosphorylation levels by concentrations 0.6, 1.7, and 5 μM based upon the above determined dose response and measured 4 hour IL-2 production under these conditions (Fig. 3.6B). As expected, we observed a tight correlation between measure IL-2 levels and Erk inhibition levels, described by a slope of -0.58 (Fig 3.6B). Similar experiments using the Akt inhibitor LY294002 at 25, 50 and 75% inhibition (0.5, 1.3, and 5.2 μM respectively) validate the model-predicted dependence of IL-2 production on Akt phosphorylation levels, with an experimental slope of -1.22 (Fig 3.6D) quite consistent with the predicted slope of –0.83.(Fig 3.6C) Most importantly, the decrease in IL-2 due to the combination of ERK and Akt inhibitors resulted in a slope experimentally measured slope of -1.36 (Fig 3.6F), less than the sum of the individual contributions as predicted by the model (Fig 3.6E).

3.4. Discussion

Through our examination of TCR ligand discrimination, we provide new insights as to how a receptor communicates information about a ligand-binding event to an interconnected signaling network and subsequently integrates these signals in the nucleus through multiple transcription factors. We chose a TCR/APL system that is optimally suited for our studies due to a multiple-ligand repertoire that can alter the magnitude of response; the cytokine output was selected because of the well-defined IL-2 promoter region and the detailed knowledge of its transcription factor recruitment. Capturing the multiple activation states generated by a signaling network through an appropriate computational model has been shown to be an especially effective approach to understanding complex biological information processing (Janes et al., 2005). Previous work on ligand discrimination has focused on molecules proximal to the TCR; by moving downstream of TCR-proximal events we have gained a better understanding of how the consequent dynamic state of the TCR signaling network integrates molecular activation dynamics to govern an important T cell phenotypic response. One obvious next step is to understand how TCR-proximal events propagate to quantitatively determine the dynamic network state. Another beckoning line of inquiry is to test whether our dynamic network state approach can help gain further understanding of related T cell phenomena, such as co-stimulation (Kroczek et al., 2004) and TCR degeneracy (Nicholson and Wraith, 2004).

Our findings emphasize the crucial requirement for combinatorial contributions of dynamic signaling pathways to ligand affinity discrimination. We were motivated to measure time-courses by previous reports indicating the importance of ERK dynamics in cell decision processes (Marshall, 1995) including T cell development and function (Altan-Bonnet and Germain, 2005; Mariathasan et al., 2001; Werlen et al., 2000). Our modelling iterations demonstrate the information gain by inclusion of multiple time-points. Furthermore, the biological significance of multiple transcription factors converging at the IL-2 promoter is reflected by the enhanced predictive power of a model consisting of multiple pathways simultaneously compared with a single molecule model. This suggests the potential

increased efficiency of multi-target modulation of IL-2 for anti-inflammatory therapeutics and graft rejection.

Akt is not known to directly activate the known IL-2 transcription factors, however, through computational modelling a novel finding emerged, that Akt phosphorylation levels could accurately predict an IL-2 response in context of the other key principal component signals in a similar manner to a known regulator of IL-2, ERK. Significantly, the model was able to predict a cancelling effect between ERK and Akt that prevented IL-2 from being reduced further with the combinatorial inhibition of both pathways.It is possible that our results in which Akt emerged as a major indicator of TCR-induced IL-2 production are due to the concerted influence of Akt on NF-κB, NFAT, and AP-1 activation (Diehn et al., 2002; Jones et al., 2000; Jones et al., 2005; Kane et al., 2001; Kane et al., 1999; Patra et al., 2004; Schade and Levine, 2004), consistent with our findings that combinatorial contributions of signaling pathways determine a cellular decision process.

Table 3.I. Largest variable influences on the projection.

VIPs for PC 1	Score	VIPs for PC 2	Score
Akt 30 min	1.77	Akt 30 min	1.68
ERK1 60 min	1.77	JNK3 60 min	1.56
ERK2 60 min	1.73	ERK1 60 min	1.48
MK2 60 min	1.67	ERK2 60 min	1.45
JNK3 60 min	1.59	MK2 60 min	1.42
JNK3 30 min	1.56	JNK3 30 min	1.39
Akt 4 hours	1.50	Akt 4 hours	1.32
Akt 10 min	1.50	Akt 10 min	1.25
ERK1 2 hours	1.41	Akt 60 min	1.23
Akt 60 min	1.41	ERK1 30 min	1.22

Values are determined by the weighted sum of squares of the loading coefficients taking into account the explained variance of IL-2 in each component dimension.

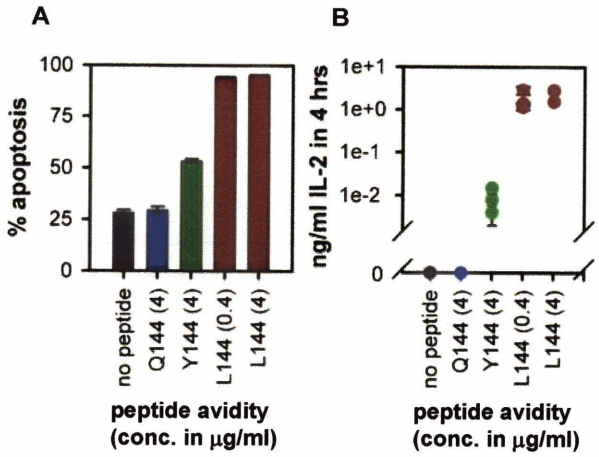

Figure 3.1. Altered peptide ligands elicit hierarchical cellular responses

(A) Percent live cells as quantified by propidium iodide exclusion 24 hours post-stimulation with control (black symbols), Q144 peptide at 4 μg/ml (blue), Y144 peptide at 4 μg/ml (green), and L144 peptide at 0.4 and 4 μg/ml (red). (B) Cumulative IL-2 levels produced 4 hours post-stimulation as detected in culture media under the same conditions as A. Error bars represent standard deviations of triplicate ELISA measurements on a single sample. Peptide stimulation conditions including the no peptide and Q144 conditions were measured by triplicate experiments.

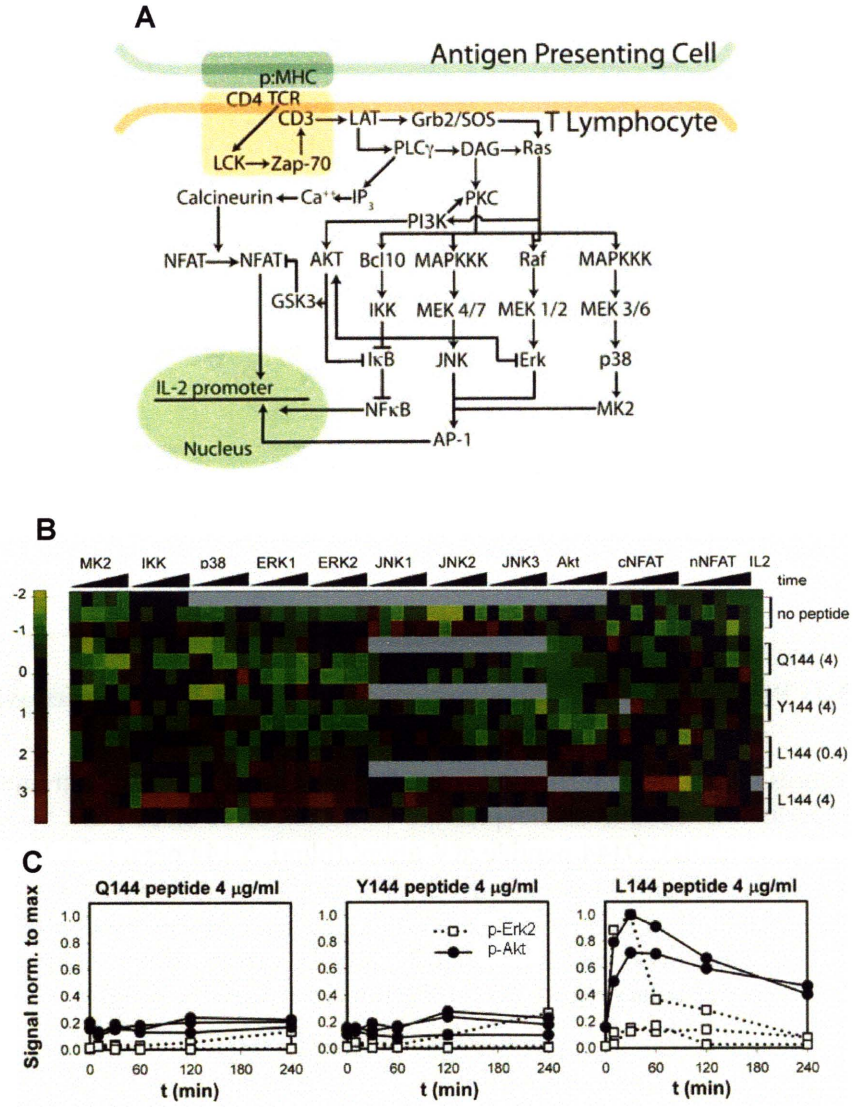

Figure 3.2. Sampling of the T cell receptor activation network

(A) Schematic of major signals involved in transduction of ligand binding events at the TCR resulting in transcription factor activation. Proteins measured in the dataset by phospho-specific western blotting are colored in blue (Akt, JNK, p38, ERK), proteins measured by kinase activity assays in green (MK2, IKKα/β), and NFAT dephosphorylation and nuclear translocation as measured by pan-NFATc2 western blotting in orange/red. (B) Heat map of the processed dataset used in the training model. Data range represents values after unit-variance/mean-centered scaling and log transformation (see supplemental information for more details). Gray coloring represents individual protein measurements that could not be accurately quantified for inclusion in the dataset. (C) Comparison of time-courses for ERK2 and Akt across the three peptides at 4 μg/ml.

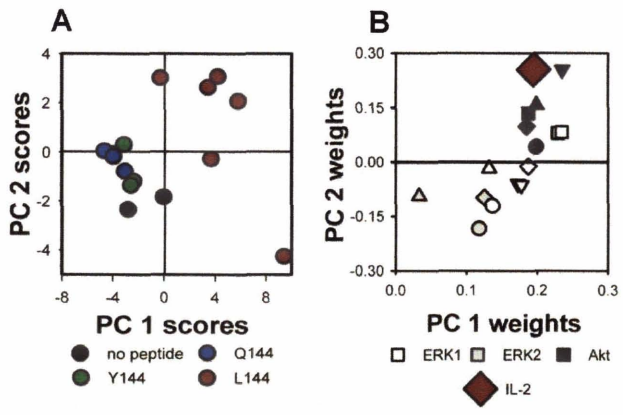

Figure 3.3. PLSR modeling can distinguish cues and signals associated with IL-2 production through a reduction in dimensionality

(A) The scores plot of the contributions of individual experiments to the trained model separates experimental conditions that produce IL-2 from those that do not. Symbol colors are control (black symbols), Q144 peptide at 4 μg/ml (blue), Y144 peptide at 4 μg/ml (green), and L144 peptide at 0.4 and 4 μg/ml (red). (B) The loading scatter plot of weights projects the response variable, IL-2 (large red diamond), on the same plot as the contributions of a subset of predictor variables, ERK1, ERK2, and Akt signals. Refer to Appendix B, supplementary figure 3B for the full set of variable weights.

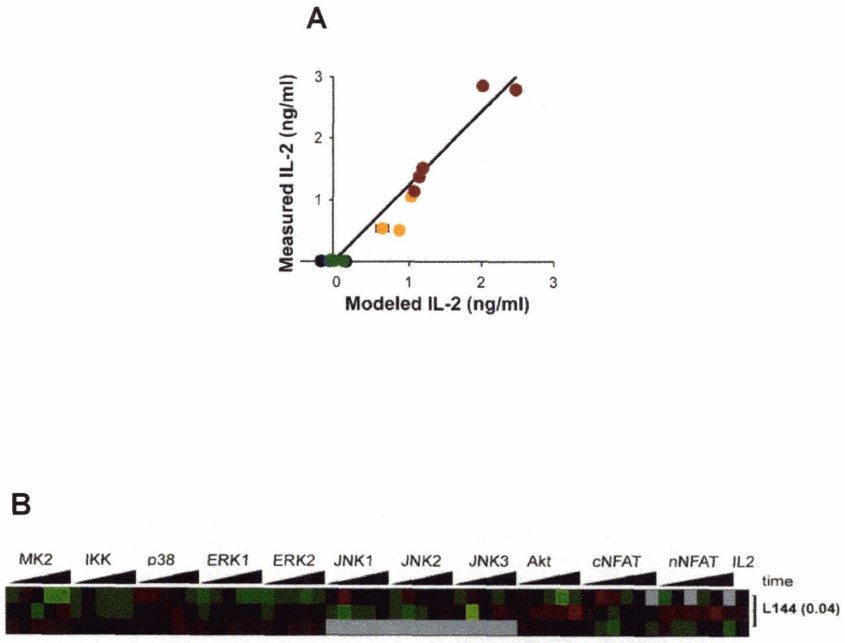

Figure 3.4. Prediction of a new stimulation condition with the trained model

(A) Heat map of the signals from new observations used for prediction. Color scale and data processing is identical to Fig 2B. (B) Fitted versus measured IL-2 production for the trained data (black, blue, green, and red symbols representing control, Q144, Y144, and L144 peptide respectively) and predicted data (yellow symbols). Error bars represent standard error of the predicted values as calculated by the sum of squares of the residuals of the training data divided by the number of observations - 1.

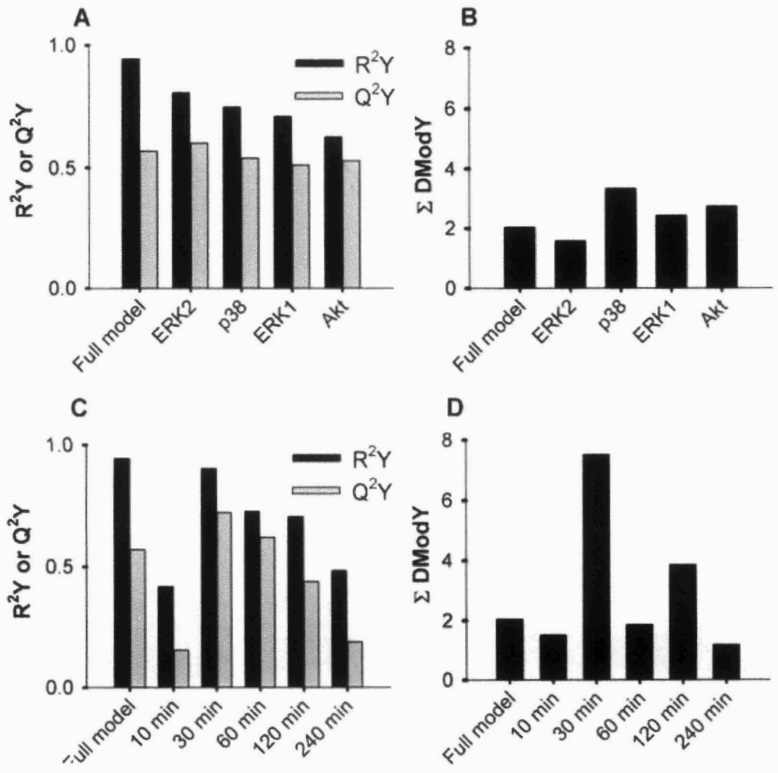

Figure 3.5. Iterations of modeling using subsets of X variables indicate that no model outperforms others for all descriptors

(A and C) Regression coefficients (R^2Y) and cumulative fraction of the total variation in IL-2 (Q^2Y). (B and D) Deviation from regression line as calculated by the root square distance summed across the three *a priori* observations. A and B depict single protein models across all time-points. C and D depict single time-point models across all proteins measured.

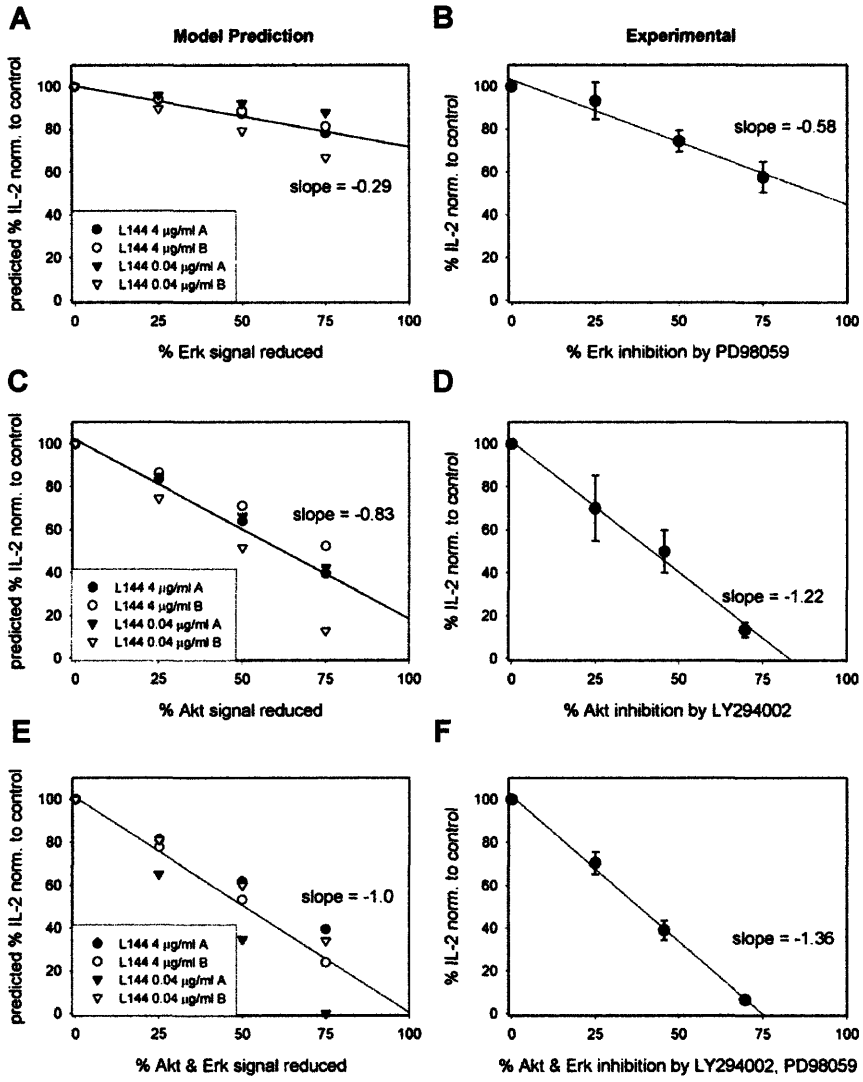

Figure 3.6. Validation of the correlative relationship between Erk or Akt phosphorylation and IL-2 production as suggested by PLSR

(A,C,E) PLSR prediction of decreasing Erk (A) Akt (C) or Erk and Akt phosphorylation levels simultaneously (E). Levels are modified to 75%, 50% and 25% of the original value, while all other signals are maintained at their original values. Predicted IL-2 values of modified data are normalized to fitted IL-2 values of unadulterated data reported in Fig. 4B. (B,D,F) Experimental measurements of IL-2 in response to L144 4µg/ml peptide in the presence of PD90859, LY 294002, or PD98059 + LY294002 inhibition on Erk and Akt phosphorylation. Error bars represent +/- standard deviation of triplicate experiments, except (F) which represents 2 experiments.

4. Generation of an epi-allelic series of Erk1 and 2 knockdowns for the quantitative analysis of Erk regulation and IL-2 production

4.1. Introduction

TCR cross-linking is known to result in the activation of Erk1/2 (MAPK1/2) through Ras (Izquierdo et al., 1992). In T cell receptor signaling, Ras can be activated by one of two guanine nucleotide exchange factors, Sos and RasGRP1. Ligand binding to the T cell receptor causes multiple proteins to localize to the membrane bound Linker for activation of T cells (LAT) including PLCγ and Grb2 and become phosphorylated. RasGRP1 is recruited to the membrane by PLCγ–dependent cleavage of PIP2 to diacylglycerol and IP3. Sos is recruited to the membrane by Grb2 binding to LAT. Ras subsequently activates the Raf-MEK-Erk cascade. Once Erk is activated, it functions to transmit the TCR-induced signal further downstream to the IL-2 promoter. Erk activation has been shown to be necessary for Jun and Fos complex to form the AP-1 transcription factor which, among other transcription factors, binds to the IL-2 promoter resulting in IL-2 production (Dumont et al., 1998; Li et al., 2004; Whitehurst and Geppert, 1996).

Erk dynamics have been implicated in determining T cell fate. Sustained versus transient Erk dynamics have been observed in naïve T lymphocytes corresponding to positive and negative selection, respectively (Werlen et al., 2000). Furthermore, the duration of Erk signaling appears to influence CD4+CD8+ lineage commitment (Nishida et al., 2004). Multiple mechanisms have been postulated to generate these differences in Erk dynamics. Recently, a positive feedback

loop in which Erk phosphorylates Lck in a regulatory manner to prevent SHP-1 deactivation of Lck was shown to sustain TCR signaling (Stefanova et al., 2003). Mathematical modeling efforts have demonstrated how the balance between this novel Erk positive feedback and negative feedback via phosphotase-mediated deactivation of molecules proximal to the TCR allows for sensitivity in ligand discrimination (Altan-Bonnet and Germain, 2005). A downstream positive feedback loop between Erk-mediated immediate early gene (IEG) expression and Erk has also been described (Murphy et al., 2002). The combination of the multiple feedbacks both upstream and downstream of Erk could account for cellular sensitivity to these MAPK molecules.

With the intense focus on MAPK activation mechanisms and its kinetic parameters (Murphy and Blenis, 2006), the independent roles of Erk1 and Erk2 in T cell activation are still not well understood. Pharmacological inhibitors employed to study Erk influences in cellular signaling cannot distinguish between the two isoforms because they act upon their common upstream kinase MEK. Embryonic lethality of Erk2 (Saba-El-Leil et al., 2003) has prevented studying this molecule in isolation, but also suggest independent roles for Erk1 and Erk2 because Erk1 cannot fully compensate for the loss of Erk2. Conversely, Erk1 knockout mice are viable, but display a phenotype of decreased thymocyte maturation beyond the double-positive stage and a weak proliferative response to TCR stimulation (Pages et al., 1999). Individual conditional deletions of Erk1 and Erk2 demonstrated that neither protein is needed for the transition from double negative to double positive T cells, however Erk2 is necessary for positive selection for mature CD4+ or CD8+ cells (Fischer et al., 2005).

Prior work demonstrated a correlation between Erk dynamics and the IL-2 cellular response (CH 3, this thesis). A statistical model based upon multiple kinase signals distal to the TCR and upstream of IL-2 promoter elements was heavily dependent on Erk -- in the context of other TCR-activated molecules -- in its ability to predict IL-2 production for peptides of varying TCR avidity. In addition, despite the above cited evidence of differences in functional roles of the Erk1/2 isoforms for development, the model attributed similar correlations of Erk1 and Erk2 in IL-2 production, suggesting functional redundancy.

Taken together, these observations regarding Erk activation and function lead us to the hypothesis that IL-2 production in response to TCR stimulation by T cells may be very sensitive to cellular Erk levels. To test this hypothesis, we generated an epi-allelic series (Hemann et al., 2003) of Erk1 and Erk2 stable shRNA knockdowns. These knockdown cell lines enable the detailed examination of the relationship between total Erk, phospho-Erk, Erk activity and IL-2 secretion resulting in a quantitative understanding of the individual contributions of different Erk parameters to IL-2 production. By analyzing eight Erk knockdown cell lines, we have determined that there is a strong relationship between Erk, phospho-Erk and IL-2 levels. This graded relationship between Erk levels and IL-2 production provides promise as a means for modulating inflammatory response through therapeutic design on a single molecular target.

The epi-allelic series also allowed for examination of how individual Erk isoforms contribute to a cell decision process. Through analysis of the range of Erk1 and 2 knockdown levels, we conclude that in the context of a T cell hybridoma cell line, Erk1 and Erk2 contribute similarly to both Erk activity and IL-2 production.

4.2. Methods

Generation of stable knockdown cell lines

Replication-deficient lentivirus was produced in 293FT packaging cells (Invitrogen) as described previously (Rubinson et al., 2003). The pLKO.1 vector and shRNA sequences were obtained from the RNAi Consortium (Moffat et al., 2006). 48 hrs after transfection viral supernatants were collected, filtered through a 0.45 micrometer filter and used for infection immediately or stored at 4C for several days. 10^5 1B6 hybridoma cells were spin-infected with viral supernatant in 24 well-plates for 1.5 hrs at 2500 rpm at 30C in the presence of 8 microgram/ml polybrene. 4 hrs after infection fresh media was added and cells were grown at 37C for 48 hrs. To eliminate uninfected cells, puromycin (2.5 microgram/ml) was added to the cells for additional 5 days. Cells were maintained in puromycin-containing media.

Semi-quantitative western blotting

$2x10^6$ cells were resuspended in 200 µl media without FBS. For stimulated samples, 2 µg/ml anti-CD3 (2C11, BD Biosciences) was added for 10 minutes at 37C. Cells were then lysed and boiled for 5 minutes in Lammeli reducing sample buffer. 10 µl of each sample was load per well. After electrophoresis, samples were transferred to polyvinylidene difluoride (PVDF) membrane and blocked with 3% BSA in TBST. Blots were visualized and quantified using a Kodak Image Station 1000. The net intensity of individual bands was determined and normalized to the net intensity of the average of the positive control bands. Triplicates were then averaged and fold activation determined by normalization to the zero time-point. Anti-total and anti-phospho p44/42 (Thr202/Tyr204) antibody was from Cell Signaling Technologies, and anti-rabbit HRP from Santa Cruz Biotechnology.

To determine the level of protein knockdown for each cell line was determined intensity of each Erk band was first normalized to its tubulin control. This normalization accounts for differences in protein loading from one sample to another. To account for differences in intensity across multiple membranes, both Erk bands across a single membrane were then individually normalized to the corresponding Luciferase control band. The standard deviations reported are representative of both biological and experimental replicates.

Kinase activity assay

Erk activity was determined in simulated (2 μg/ml anti-CD3 was added for 10 minutes at 37C) and un-stimulated samples by a custom multi-plex kinase assay as described in (Asthagiri et al., 1999; Janes et al., 2003). Myelin basic protein (Sigma) was used as the substrate in the in vitro reaction. CPM was background corrected and normalized by μg lysate protein per well as determined by micro-BCA assay (Pierce). To account for cell line variation in basal activities, the stimulated lysate value for each cell line was normalized by its respective unstimulated value prior to dividing by the luciferase value.

IL-2 ELISA

Supernatant from 100,000 1B6 cells stimulated for 4 hours on DAS cell (Munder et al., 2002)seeded- L144 peptide coated- 24-well plates was collected and analyzed using quantitative sandwich ELISA for mouse IL-2 (BD Biosciences).

4.3. Results and Discussion

4.3.1. Generating a range of stable Erk1 and Erk2 knockdown cell lines

To determine whether total Erk levels could be modulated using established shRNA techniques, four unique sequences in both Erk1 and Erk2 mRNA transcripts were targeted for knockdown in mouse 1B6 T cells, generating an epi-allelic series for both Erk1 and Erk2. Stable cell lines were generated for each shRNA using lenti-viral infections and puromycin selection. As a non-specific control, stable cell lines were generated by infection with shRNAs targeting Luciferase. The level of total protein knockdown for each sequence was determined by western blotting (Fig. 1A). Normalized Erk levels are reported (refer to Methods).

For Erk1, a range of knockdowns from 12% (Erk1-A11) to 96% (Erk1-B12) was generated (Fig. 4.1A); for Erk2, a range of knockdowns from 49% (Erk2-G5) to 85% (Erk2-G7) was generated (Fig. 4.1A). These results deomstrate the ability to generate a range of stable knockdowns using shRNA constructs of differing target sequences.

To determine whether one Erk isoform was being up-regulated in the presence of an shRNA to the other Erk isoform, the level of the knockdown isoform was plotted against the total cumulative level of both Erk1 and Erk2 (Fig. 4.1C). Given the linear relationship of Erk2 knockdowns to total Erk levels, no compensation was seen in Erk2 knockdown cell lines. On the other hand, Erk1 knockdown cell lines did appear to partially compensate for the loss of Erk1 by increasing Erk2 levels in strong Erk1 knockdowns. This compensatory effect is surprising given the larger absolute abundance of Erk2 versus Erk1 in wild-type cells.

4.3.2. Total Erk levels correlate with IL-2 production

To determine whether there is a direct correlation between total Erk levels and IL-2 production in response to TCR stimulation, 1B6 Erk1/Erk2 knockdown cell lines were stimulated with 4μg/ml of L144, an altered peptide ligand of PLP, presented on surrogate antigen presenting cells (Munder et al., 2002). IL-2 production was measured four hours after peptide stimulation by ELISA. Both Erk1 and Erk2 levels were positively correlated with IL-2 production (Fig. 4.2). This result is not unexpected, given the role Erk has been shown to play in TCR lignad discrimination (Altan-Bonnet and Germain, 2005).

4.3.3. Phospho-Erk levels correlate with total Erk levels and approximate IL-2 levels

To determine the relationship between an Erk knockdown and its associated phospho-Erk levels upon stimulation, stable knockdown cell lines were stimulated using anti-CD3 and phospho-Erk levels measured via immunoblotting then normalized as described above (Fig. 4.3A). By comparing total-Erk levels to phospho-Erk levels in these knockdown cell lines (Fig. 4.3B), we observe, with the exception of a single outlier, a positive correlation between the two measurements, suggesting that a constant fraction of the Erk1 and Erk2 present in these cells is activated in response to stimulation.

Since phospho-Erk levels are expected to be a more relevant predictor of IL-2 levels, the relationship between phospho-Erk levels and IL-2 was determined (Fig. 4.3C). Both phospho-Erk1 and Erk2 levels appear to closely correlate with IL-2. These results suggest that there is a dose-dependence of phospho-Erk for IL-2 production and that IL-2 levels can be modulated through Erk activation.

4.3.4. Understanding the relationship between Erk phosphorylation and its activity

Aggregate Erk1/2 activity in knockdown cell lines was determined for both stimulated and unstimulated cells via a kinase activity assay. Normalized Erk activity is reported here (refer to Methods). When comparing phospho-Erk1 and Erk2 levels in Erk1 and Erk2 knockdown cell lines respectively, both Erk1 and Erk2 phosphorylation levels correlate with Erk activity (Fig. 4.4A). Similar trends emerge when summed phospho-Erk1 and 2 are plotted for each cell line (Fig. 4.4B, $r^2 = 0.86$). This result is not unexpected, as phospho-Erk is often reported as a surrogate for Erk activity; however in light of the stable knockdown cell lines this indicates a lack of compensation by the unaltered isoform. In addition, it is interesting to note, that in this

system Erk1 and Erk2 appear to contribute similarly to total Erk activity, with attempts to account for relative cellular protein levels of the two isoforms (1:2 ratio Erk1:Erk2) resulting in a lower regression coefficient (r^2=0.73).

Erk1 and Erk2 knockout mice have different phenotypes (Saba-El-Leil et al., 2003), and conditional Erk2 knockouts have more severe T cell development defects than Erk1 knockout mice (Pages et al., 1999). However, we find that both Erk1 and Erk2 contribute similarly to Erk activity as measured by the ability of Erk to phosphorylate myelin basic protein. The finding presented here could be explained by differences in some but not all Erk1 and Erk2 phosphorylation targets. However, of the known Erk phosphorylation targets, little is known about their isoform specificity. And although there have been attempts to identify additional Erk phosphorylation targets (Eblen et al., 2003; Lewis et al., 2000), these have not been determined to be isoform specific.

By generating an epi-allelic series, which has been shown to be a useful tool for determining the effect of knocking down protein levels to various extents on phenotypic outcomes (Hemann et al., 2003), we have shown that an incomplete kinase knockdown can yield information consistent with the level to which the kinase is knocked-down. It remains to be seen whether these results are upheld for different proteins in multiple systems. However, it is of note, that the knockdown target, Erk, has been described as being ultrasensitive (Huang and Ferrell, 1996) or non-linearly related to the extracellular stimulus, and yet our results indicate that phenotypic outcome is not regulated by a steep threshold in knockdown levels. As ever increasing numbers of researchers rely on knockdown data generated from incomplete knockdowns, this work provides a framework for interpreting knockdown data in a consistent manner.

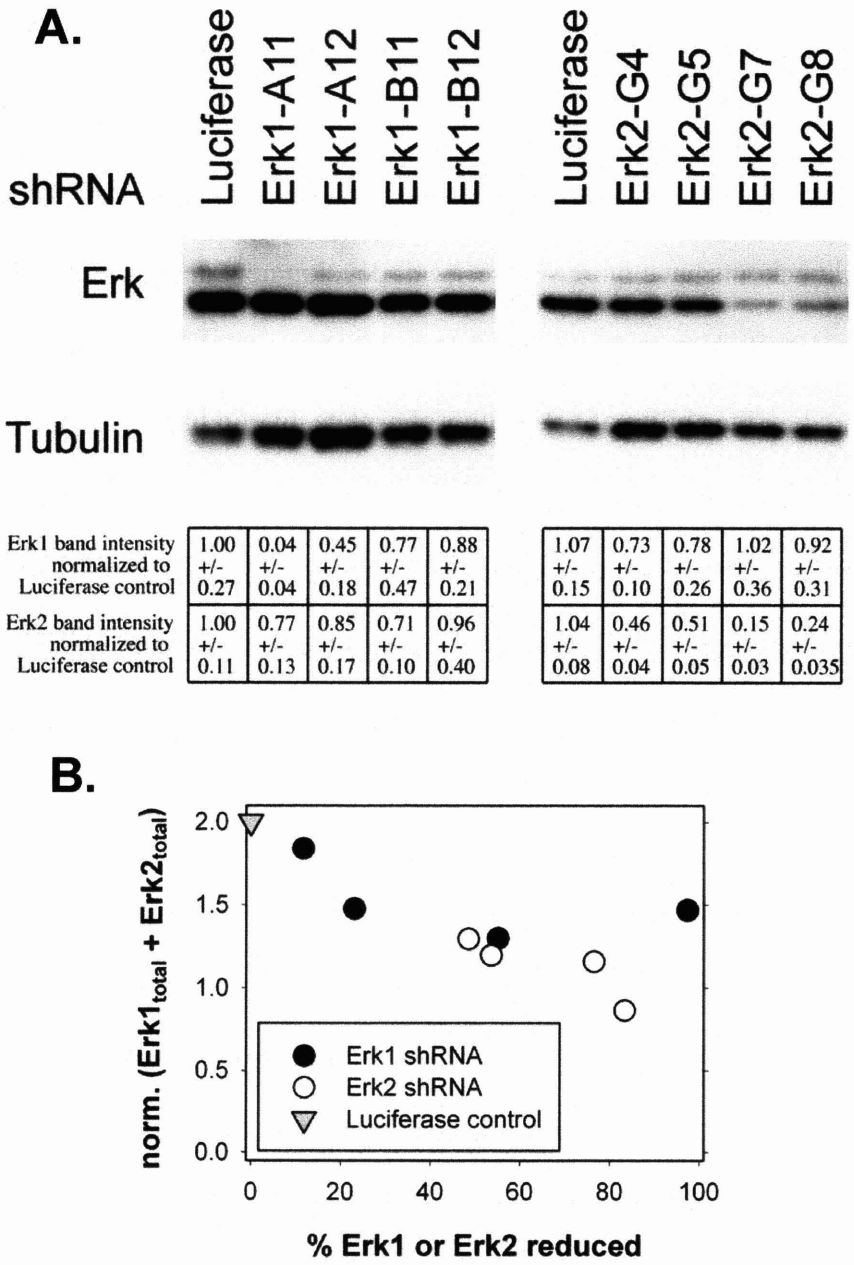

Erk1 band intensity normalized to Luciferase control	1.00 +/- 0.27	0.04 +/- 0.04	0.45 +/- 0.18	0.77 +/- 0.47	0.88 +/- 0.21	1.07 +/- 0.15	0.73 +/- 0.10	0.78 +/- 0.26	1.02 +/- 0.36	0.92 +/- 0.31
Erk2 band intensity normalized to Luciferase control	1.00 +/- 0.11	0.77 +/- 0.13	0.85 +/- 0.17	0.71 +/- 0.10	0.96 +/- 0.40	1.04 +/- 0.08	0.46 +/- 0.04	0.51 +/- 0.05	0.15 +/- 0.03	0.24 +/- 0.035

Figure 4.1. Generation of a range of stable knockdown cell lines

A) Total Erk Western blot of the knockdown cell lines. Band intensities shown are normalized as described in text. Standard deviations reported include both experimental and biological replicates. B) Sum of Erk1 and Erk2 is plotted against the fraction of either Erk1 in an Erk1 knockdown or Erk2 in an Erk2 knockdown. In the case of complete compensation by one isoform for the decreased levels of another, a horizontal line at $y = 2$ is expected.

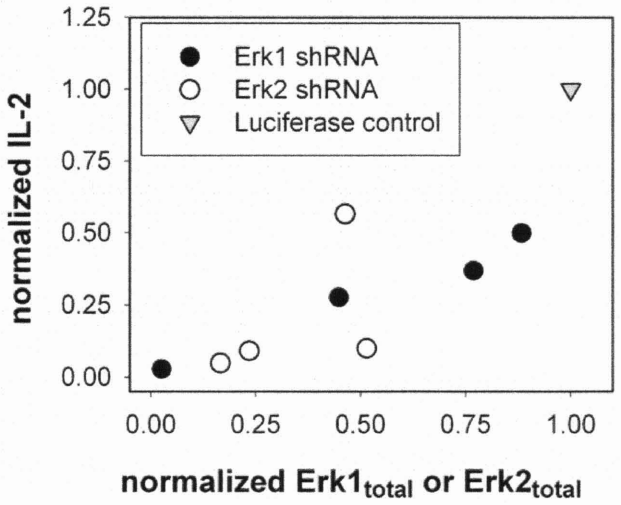

Figure 4.2. Total Erk levels are related to IL-2 levels

IL-2 levels following stimulation by 4ug/mL L144 for 4 hours normalized to Luciferase control. IL-2 levels are plotted against total Erk1 levels in an Erk1 knockdown or total Erk2 in an Erk2 knockdown.

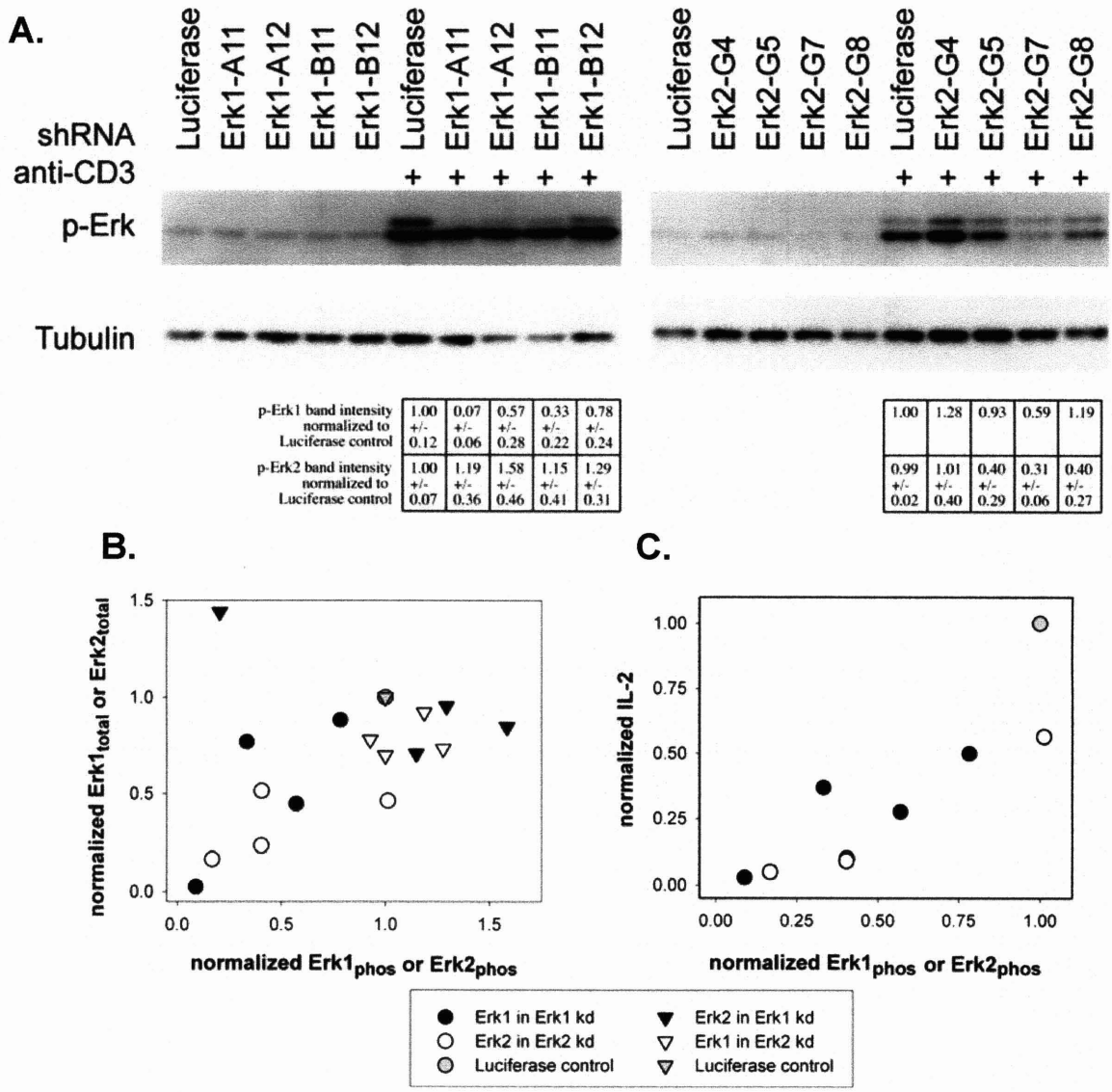

Figure 4.3. Phospho Erk levels correlated with IL-2

A) phospho-Erk levels as measured by Western blot of the knockdown cell lines following stimulation by 4ug/mL L144 for 4 hours. Band intensities shown are normalized as described in text. Standard deviations reported include both experimental and biological replicates. B) For each knockdown cell line two data points are depicted: phospho Erk1 level is plotted against total Erk1 level and phospho Erk2 level is plotted against total Erk2 level. C) IL-2 levels normalized to control Luciferase IL-2 levels are plotted against phospho Erk1 levels in an Erk1 knockdown or phospho Erk2 in an Erk2 knockdown.

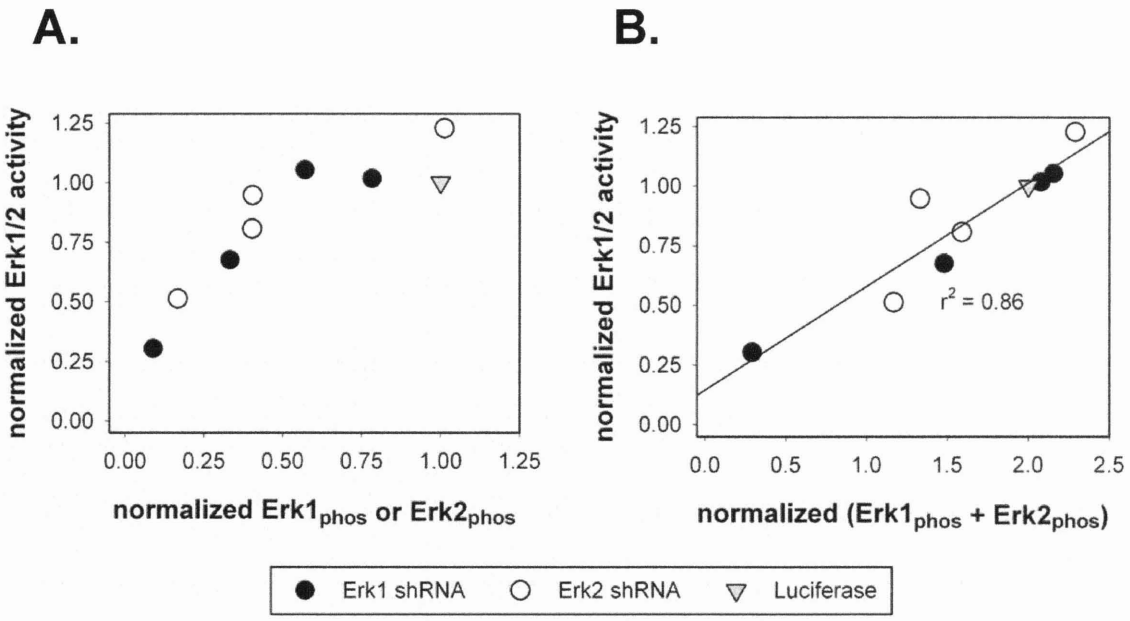

Figure 4.4. Phospho Erk vs. activity

A) Erk activity levels vs. phospho Erk1 levels in an Erk1 knockdown or phospho Erk2 in an Erk2 knockdown are shown. B) Erk activity levels vs. the sum of both phospho Erk1 and phospho Erk2 in each knockdown cell line is depicted.

5. Conclusions and Future Directions

Parallel and interconnected signaling pathways are activated downstream of T cell receptor binding to peptide MHC. Although the signaling events that occur as a result of TCR binding peptide MHC have been described, it is still unclear how the multiple pathways integrate to determine a specific cell fate. The goal of this work was to determine the predictive power on cell fate decisions of single pathways versus a combination of multiple pathways. The challenge of integrating information from multiple signaling pathways is not unique to the TCR. Many surface receptors, when bound, result in the activation of multiple signaling cascades. Therefore, this work has potential implications that are more broadly applicable to different systems.

This thesis looks at whether there are master pathways activated that alone can determine cell fate or whether multiple pathways synergize to determine cell fate. To answer this question, Melissa Kemp and I generated a data set of about 1100 measurements representing both dynamic and multivariate information of TCR signaling in response to different avidity peptides. This data set was then analyzed using a linear regression model, PLSR. Our work shows that there are indeed pathways that, when perturbed, have the ability to modulate IL-2 levels. However, we find that no pathway alone is as correlated with IL-2 production as the combination of pathways.

We tested the predictions generated by the model by using both inhibitors and shRNAs to down regulate the function of individual molecules. Akt inhibitors were used to show that Akt phosphorylation correlated linearly with IL-2 production as predicted by the model. Similarly,

we show that Erk inhibition also correlated with IL-2 production. In addition, the model predicted that the combination of Erk and Akt inhibition would reduce IL-2 production by less than the sum of either inhibition alone, which was also verified experimentally. To further analyze the relationship between Erk levels and IL-2 production, shRNAs were generated that target either Erk1 or Erk2. One surprising result of the ERK isoform knockdown experiments is that both isoforms appear to contribute equally to IL-2 production in this hybridoma cell lines.

One potential limitation of this study is the scope of the predictive power of our model. Since the PLSR model is based on the state of network activation in a hybridoma cell line in response to TCR stimulation, it remains to be seen wether it can predict cellular responses in primary T cells, both mouse and human. Another limitation is the lack of mechanistic detail inherent in the model predictions. We have shown that certain molecules are critical for predicting IL-2 production; Furthermore, we have shown that their activity correlates with IL-2 production. However, we have not been able to provide anything further than speculative mechanistic understanding of how these molecules govern IL-2 production. Further gains in our understanding of TCR ligand discrimination will be made by moving from a correlational to a more mechanistic understanding of the TCR network system.

5.1. Determining T cell Fate

Through analysis of the large signaling data set generated in the context of this study, a few key molecules were identified whose phosphorlyation states could predict IL-2 production in

response to different avidity TCR signals. Both Akt and Erk phosphorylation levels were shown to be indicative of IL-2 production levels.

It remains to be seen whether these same key molecules will be equally predictive of IL-2 production in primary mouse T cells. In addition to looking at primary mouse T cells, one could investigate whether these observations also hold true in other species, such as primary human T cells. It may even be possible to determine, at the level of signaling molecules, the predictors of certain human disease states, such as autoimmune disease. It has been shown that CD4 T cell differentiation into either Th1 or Th2 can determine the progression of multiple autoimmune diseases including EAE and diabetes (Nicholson and Kuchroo, 1996). Th1 T cells produce inflammatory cytokines and have been shown to exacerbate autoimmune diseases while Th2 cells have been shown to protect from autoimmune disease. By examining the network states that result in either the Th1 or Th2 fate, one could identify the key signaling molecules that regulate the fate of CD4 T cells. By knowing the key regulators, drugs could potentially be used to direct the course of disease by coaxing cells from one fate to another.

Co-stimulatory molecules are known to be critical for determining pathogenic versus self peptides (Liu and Janeway, 1992). In this work, we were not able to determine the significance of co-stimulation on signaling dynamics since the 1B6 cells do not respond to CD28. However, determining the contributions of co-stimulatory signals on T cell fate is possible using the methodology outlined here. In particular, one interesting question is whether co-stimulation activates additional pathways not activated by TCR signaling, or whether co-stimulation increases the magnitude of activated signals (Acuto et al., 2003). Current evidence suggests that

CD28 contributes quantitatively to TCR signaling. However, a qualitative contribution cannot yet be ruled out. A systematic data collection and analysis approach would be able to suggest which of the above is more important for T cell activation in response to non-self peptides.

Signals provided through the TCR are critical at multiple stages of T cell development in determining T cell fate. For example, signals provided by the preTCR at the DN3 stage signal a functional TCR rearrangement which results in T cell proliferation. Similarly, T cells are positively and negatively selected in the thymus based on the ability of the TCR to recognize and properly signal self-MHC peptide complexes (Starr et al., 2003). One interesting question is how the strength of the signal at different stages of T cell development – resulting in very different cell fates – is similar or different depending on the affinity of the TCR ligand. Are T cells capable of tuning their response to MHC peptide affinity through the process of selection in the thymus? There is evidence that T cells do in fact have different sensitivities as thymocytes and mature T cells (Davey et al., 1998). And if T cells are capable of tuning the response, by what mechanism do they do so? One possibility is that the number of receptors available at the cell surface is modified depending on the desired sensitivity of the T cell. Two lines of evidence could support this hypothesis: 1) it has been shown that the number of T cell receptors on the surface of T cells varies depending on the stage of T cell development (Roehm et al., 1984); 2) T cell receptors are internalized and degraded in response to a TCR stimulus (Valitutti et al., 1997). Another possible mechanism for tuning T cell sensitivity is by modifying the availability of downstream effector and signaling molecules. This kind of regulation could occur via transcriptional regulation. By using a systematic quantitative approach, one could measure, at different developmental stages, both the total number of signaling molecules, receptors, and their

activation state in responses to different avidity ligands, to determine how T cells are capable of tuning their sensitivity to antigen.

5.2. *Further understanding of signaling molecules*

Through modeling and experiments, we have shown that Akt is a good predictor of IL-2 production. The mechanism by which Akt might regulate IL-2 production is not entirely clear because Akt is not known to directly activate the known IL-2 transcription factors. However, Akt indirectly affects the signaling cascades leading to NF-κB, NFAT, and AP-1 activation. NFAT nuclear translocation is enhanced by Akt-mediated inactivation of glycogen synthase kinase-3 (GSK3) thereby leading to a prolonged dephosphorylated and activated state of NFAT (Diehn et al., 2002). A recent report observed decreased shuttling of NFAT in murine T cells with constitutively active Akt (Patra et al., 2004). However, it is conceivable that long-term compensatory effects of upregulated Akt may lead to a desensitization of this mechanism; specifically, altered calcium dynamics in these cells may impact cytosolic dephosphorylation of NFAT synchronously with the lack of nuclear phosphorylation by GSK3. This same report also observed a decrease in NF-κB nuclear shuttling due to increased Akt levels. Other evidence suggests that Akt enhances NF-κB activation (Jones et al., 2005; Kane et al., 2001; Kane et al., 1999) due to higher Iκ-B degradation rates (Jones et al., 2000). Finally, activation of the ERK/c-Fos pathway by PI3K in a stimulus-strength dependent manner has been reported, but it is unclear if the observed effects are Akt-dependent (Schade and Levine, 2004). To determine through which signaling pathway i.e. NFAT, NFκB, or Erk Akt is exerting its effects on IL-2 production, one could measure the activity of the transcription factors known to bind the IL-2

promoter using commercially available reporter constructs. The change in transcription factor activity in the presence or absence of Akt inhibition would be a good indicator of the pathways being regulated by Akt activity. This approach could potentially elucidate the signaling pathways through which Akt is exerting its effect. Then, once an Akt target pathway has been identified, a more detailed study of the activation of individual molecules in the presence of an Akt inhibitor may shed light on the molecular mechanism of Akt regulation.

Knockouts have been generated for both Erk1 and Erk2 and their T cell specific phenotypes have been determined (Pages et al., 1999; Saba-El-Leil et al., 2003). These genetic studies have shown that Erk1 and Erk2 function non-redundantly, since Erk2 knockout mice die during embryogenesis, while Erk1 knockout mice have only minor T cell defects. However, the molecular mechanism by which these two Erk isoforms uniquely contribute to cell fate has not been determined. In addition, data generated in Chapter 4 of this thesis indicates that Erk1 and Erk2 are redundant pathways for transmitting the IL-2 response in the 1B6 hybridoma cell line. Given this finding, it would be interesting to investigate two potential mechanisms that could account for both redundancy and unique functions for Erk isoforms depending on the context of the experiment. First, Erk contributions could be cell type specific; second, Erk contributions could be substrate specific. To determine whether Erk contributions are cell type specific, the pheonotype of knocking down both Erk isoform individually would be examined in different cell lines and possibly cell fates. To determine whether Erk isoforms exhibit substrate specificity, Erk kinase assays would be performed in the knockdown cell lines reported here using multiple different, known Erk substrates. If in some cases the two Erk isoforms are substrate specific,

Erk1 knockdowns would be expected to behave differently form Erk2 knockdowns for kinase assays with certain Erk substrates but not with others.

5.3. Conclusion

This work provides a framework for analyzing how cells integrate and interpret information generated by an extracellular ligand bound to a receptor. Canonical signaling pathways are activated downstream of receptors, such as the MAPKs in the case of receptor tyrosine kinases and the Jak/Stat pathway in response to cytokine signaling. A diverse set of cell fates are elicited dependent on context of activation by extracellular ligands despite utilization of a common set of signaling pathways. Here, we show that the level of activation of single molecules, in the context of the entire signaling network, can modulate cell fate. We show that the activation level of Akt and Erk have predictable effects on cell fate. This suggests that each of these molecules provides a unique piece of information that is interpreted by the cell to make critical cell fate decisions.

References

Acuto, O., and Michel, F. (2003). CD28-mediated co-stimulation: a quantitative support for TCR signalling. Nat Rev Immunol *3*, 939-951.

Acuto, O., Mise-Omata, S., Mangino, G., and Michel, F. (2003). Molecular modifiers of T cell antigen receptor triggering threshold: the mechanism of CD28 costimulatory receptor. Immunol Rev *192*, 21-31.

Alberola-Ila, J., Forbush, K. A., Seger, R., Krebs, E. G., and Perlmutter, R. M. (1995). Selective requirement for MAP kinase activation in thymocyte differentiation. Nature *373*, 620-623.

Altan-Bonnet, G., and Germain, R. N. (2005). Modeling T cell antigen discrimination based on feedback control of digital ERK responses. PLoS Biol *3*, e356.

Apolloni, A., Prior, I. A., Lindsay, M., Parton, R. G., and Hancock, J. F. (2000). H-ras but not K-ras traffics to the plasma membrane through the exocytic pathway. Mol Cell Biol *20*, 2475-2487.

Ashwell, J. D., Cunningham, R. E., Noguchi, P. D., and Hernandez, D. (1987). Cell growth cycle block of T cell hybridomas upon activation with antigen. J Exp Med *165*, 173-194.

Asthagiri, A. R., Horwitz, A. F., and Lauffenburger, D. A. (1999). A rapid and sensitive quantitative kinase activity assay using a convenient 96-well format. Anal Biochem *269*, 342-347.

Bauer, B., Jenny, M., Fresser, F., Uberall, F., and Baier, G. (2003). AKT1/PKBalpha is recruited to lipid rafts and activated downstream of PKC isotypes in CD3-induced T cell signaling. FEBS Lett *541*, 155-162.

Bivona, T. G., Perez De Castro, I., Ahearn, I. M., Grana, T. M., Chiu, V. K., Lockyer, P. J., Cullen, P. J., Pellicer, A., Cox, A. D., and Philips, M. R. (2003). Phospholipase Cgamma activates Ras on the Golgi apparatus by means of RasGRP1. Nature *424*, 694-698.

Buday, L., and Downward, J. (1993). Epidermal growth factor regulates p21ras through the formation of a complex of receptor, Grb2 adapter protein, and Sos nucleotide exchange factor. Cell *73*, 611-620.

Buday, L., Egan, S. E., Rodriguez Viciana, P., Cantrell, D. A., and Downward, J. (1994). A complex of Grb2 adaptor protein, Sos exchange factor, and a 36-kDa membrane-bound tyrosine phosphoprotein is implicated in ras activation in T cells. J Biol Chem *269*, 9019-9023.

Burack, W. R., and Shaw, A. S. (2000). Signal transduction: hanging on a scaffold. Curr Opin Cell Biol *12*, 211-216.

Chakraborty, A. K., Dustin, M. L., and Shaw, A. S. (2003). In silico models for cellular and molecular immunology: successes, promises and challenges. Nat Immunol *4*, 933-936.

Chan, C., George, A. J., and Stark, J. (2001). Cooperative enhancement of specificity in a lattice of T cell receptors. Proc Natl Acad Sci U S A *98*, 5758-5763.

Chen, T. R. (1992). Karyotypic derivation of H9 cell line expressing human immunodeficiency virus susceptibility. J Natl Cancer Inst *84*, 1922-1926.

Chen, W. S., Xu, P. Z., Gottlob, K., Chen, M. L., Sokol, K., Shiyanova, T., Roninson, I., Weng, W., Suzuki, R., Tobe, K., *et al.* (2001). Growth retardation and increased apoptosis in mice with homozygous disruption of the Akt1 gene. Genes Dev *15*, 2203-2208.

Chiu, V. K., Bivona, T., Hach, A., Sajous, J. B., Silletti, J., Wiener, H., Johnson, R. L., 2nd, Cox, A. D., and Philips, M. R. (2002). Ras signalling on the endoplasmic reticulum and the Golgi. Nat Cell Biol *4*, 343-350.

Chou, M. M., Hou, W., Johnson, J., Graham, L. K., Lee, M. H., Chen, C. S., Newton, A. C., Schaffhausen, B. S., and Toker, A. (1998). Regulation of protein kinase C zeta by PI 3-kinase and PDK-1. Curr Biol *8*, 1069-1077.

Chow, C. W., Rincon, M., and Davis, R. J. (1999). Requirement for transcription factor NFAT in interleukin-2 expression. Mol Cell Biol *19*, 2300-2307.

Choy, E., Chiu, V. K., Silletti, J., Feoktistov, M., Morimoto, T., Michaelson, D., Ivanov, I. E., and Philips, M. R. (1999). Endomembrane trafficking of ras: the CAAX motif targets proteins to the ER and Golgi. Cell *98*, 69-80.

Clarke, S. R., and Rudensky, A. Y. (2000). Survival and homeostatic proliferation of naive peripheral CD4+ T cells in the absence of self peptide:MHC complexes. J Immunol *165*, 2458-2464.

Crabtree, G. R. (2001). Calcium, calcineurin, and the control of transcription. J Biol Chem *276*, 2313-2316.

Davey, G. M., Schober, S. L., Endrizzi, B. T., Dutcher, A. K., Jameson, S. C., and Hogquist, K. A. (1998). Preselection thymocytes are more sensitive to T cell receptor stimulation than mature T cells. J Exp Med *188*, 1867-1874.

Diehl, N. L., Enslen, H., Fortner, K. A., Merritt, C., Stetson, N., Charland, C., Flavell, R. A., Davis, R. J., and Rincon, M. (2000). Activation of the p38 mitogen-activated protein kinase pathway arrests cell cycle progression and differentiation of immature thymocytes in vivo. J Exp Med *191*, 321-334.

Diehn, M., Alizadeh, A. A., Rando, O. J., Liu, C. L., Stankunas, K., Botstein, D., Crabtree, G. R., and Brown, P. O. (2002). Genomic expression programs and the integration of the CD28 costimulatory signal in T cell activation. Proc Natl Acad Sci U S A *99*, 11796-11801.

Dong, C., Yang, D. D., Tournier, C., Whitmarsh, A. J., Xu, J., Davis, R. J., and Flavell, R. A. (2000). JNK is required for effector T-cell function but not for T-cell activation. Nature *405*, 91-94.

Dong, C., Yang, D. D., Wysk, M., Whitmarsh, A. J., Davis, R. J., and Flavell, R. A. (1998). Defective T cell differentiation in the absence of Jnk1. Science *282*, 2092-2095.

Dower, N. A., Stang, S. L., Bottorff, D. A., Ebinu, J. O., Dickie, P., Ostergaard, H. L., and Stone, J. C. (2000). RasGRP is essential for mouse thymocyte differentiation and TCR signaling. Nat Immunol *1*, 317-321.

Downward, J., Graves, J. D., Warne, P. H., Rayter, S., and Cantrell, D. A. (1990). Stimulation of p21ras upon T-cell activation. Nature *346*, 719-723.

Dumont, F. J., Staruch, M. J., Fischer, P., DaSilva, C., and Camacho, R. (1998). Inhibition of T cell activation by pharmacologic disruption of the MEK1/ERK MAP kinase or calcineurin signaling pathways results in differential modulation of cytokine production. J Immunol *160*, 2579-2589.

Ebinu, J. O., Bottorff, D. A., Chan, E. Y., Stang, S. L., Dunn, R. J., and Stone, J. C. (1998). RasGRP, a Ras guanyl nucleotide- releasing protein with calcium- and diacylglycerol-binding motifs. Science *280*, 1082-1086.

Ebinu, J. O., Stang, S. L., Teixeira, C., Bottorff, D. A., Hooton, J., Blumberg, P. M., Barry, M., Bleakley, R. C., Ostergaard, H. L., and Stone, J. C. (2000). RasGRP links T-cell receptor signaling to Ras. Blood *95*, 3199-3203.

Eblen, S. T., Kumar, N. V., Shah, K., Henderson, M. J., Watts, C. K., Shokat, K. M., and Weber, M. J. (2003). Identification of novel ERK2 substrates through use of an engineered kinase and ATP analogs. J Biol Chem *278*, 14926-14935.

Evavold, B. D., and Allen, P. M. (1991). Separation of IL-4 production from Th cell proliferation by an altered T cell receptor ligand. Science *252*, 1308-1310.

Fischer, A. M., Katayama, C. D., Pages, G., Pouyssegur, J., and Hedrick, S. M. (2005). The role of erk1 and erk2 in multiple stages of T cell development. Immunity *23*, 431-443.

Fruman, D. A., Snapper, S. B., Yballe, C. M., Davidson, L., Yu, J. Y., Alt, F. W., and Cantley, L. C. (1999). Impaired B cell development and proliferation in absence of phosphoinositide 3-kinase p85alpha. Science *283*, 393-397.

Garrity, P. A., Chen, D., Rothenberg, E. V., and Wold, B. J. (1994). Interleukin-2 transcription is regulated in vivo at the level of coordinated binding of both constitutive and regulated factors. Mol Cell Biol *14*, 2159-2169.

Gascoigne, N. R., Zal, T., and Alam, S. M. (2001). T-cell receptor binding kinetics in T-cell development and activation. Expert Rev Mol Med *2001*, 1-17.

Gaudet, S., Janes, K. A., Albeck, J. G., Pace, E. A., Lauffenburger, D. A., and Sorger, P. K. (2005). A Compendium of Signals and Responses Triggered by Prodeath and Prosurvival Cytokines. Mol Cell Proteomics *4*, 1569-1590.

Genot, E., and Cantrell, D. A. (2000). Ras regulation and function in lymphocytes. Curr Opin Immunol *12*, 289-294.

Germain, R. N., and Stefanova, I. (1999). The dynamics of T cell receptor signaling: complex orchestration and the key roles of tempo and cooperation. Annu Rev Immunol *17*, 467-522.

Ghosh, S., May, M. J., and Kopp, E. B. (1998). NF-kappa B and Rel proteins: evolutionarily conserved mediators of immune responses. Annu Rev Immunol *16*, 225-260.

Giffin, M. J., Stroud, J. C., Bates, D. L., von Koenig, K. D., Hardin, J., and Chen, L. (2003). Structure of NFAT1 bound as a dimer to the HIV-1 LTR kappa B element. Nat Struct Biol *10*, 800-806.

Goldsby, R. A., Kindt, T. J., and Osborne, B. A. (2000). Kuby Immunology, 4th edn (New York, W. H. Freeman and Company).

Goldstein, B., Faeder, J. R., and Hlavacek, W. S. (2004). Mathematical and computational models of immune-receptor signalling. Nat Rev Immunol *4*, 445-456.

Gong, Q., Cheng, A. M., Akk, A. M., Alberola-Ila, J., Gong, G., Pawson, T., and Chan, A. C. (2001). Disruption of T cell signaling networks and development by Grb2 haploid insufficiency. Nat Immunol *2*, 29-36.

Grundstrom, S., Anderson, P., Scheipers, P., and Sundstedt, A. (2004). Bcl-3 and NFkappaB p50-p50 homodimers act as transcriptional repressors in tolerant CD4+ T cells. J Biol Chem *279*, 8460-8468.

Hara, T., and Fu, S. M. (1985). Human T cell activation. I. Monocyte-independent activation and proliferation induced by anti-T3 monoclonal antibodies in the presence of tumor promoter 12-o-tetradecanoyl phorbol-13 acetate. J Exp Med *161*, 641-656.

Hautaniemi, S., Kharait, S., Iwabu, A., Wells, A., and Lauffenburger, D. A. (2005). Modeling of signal-response cascades using decision tree analysis. Bioinformatics *21*, 2027-2035.

Hemann, M. T., Fridman, J. S., Zilfou, J. T., Hernando, E., Paddison, P. J., Cordon-Cardo, C., Hannon, G. J., and Lowe, S. W. (2003). An epi-allelic series of p53 hypomorphs created by stable RNAi produces distinct tumor phenotypes in vivo. Nat Genet *33*, 396-400.

Hodge, M. R., Ranger, A. M., Charles de la Brousse, F., Hoey, T., Grusby, M. J., and Glimcher, L. H. (1996). Hyperproliferation and dysregulation of IL-4 expression in NF-ATp-deficient mice. Immunity *4*, 397-405.

Holsinger, L. J., Spencer, D. M., Austin, D. J., Schreiber, S. L., and Crabtree, G. R. (1995). Signal transduction in T lymphocytes using a conditional allele of Sos. Proc Natl Acad Sci U S A *92*, 9810-9814.

Huang, C. Y., and Ferrell, J. E., Jr. (1996). Ultrasensitivity in the mitogen-activated protein kinase cascade. Proc Natl Acad Sci U S A *93*, 10078-10083.

Huang, Y., and Wange, R. L. (2004). T cell receptor signaling: beyond complex complexes. J Biol Chem *279*, 28827-28830.

Ideker, T., and Lauffenburger, D. (2003). Building with a scaffold: emerging strategies for high- to low-level cellular modeling. Trends Biotechnol *21*, 255-262.

Illes, Z., Waldner, H., Reddy, J., Bettelli, E., Nicholson, L. B., and Kuchroo, V. K. (2005). T Cell Tolerance Induced by Cross-Reactive TCR Ligands Can Be Broken by Superagonist Resulting in Anti-Inflammatory T Cell Cytokine Production. J Immunol *175*, 1491-1497.

Irvine, D. J., Purbhoo, M. A., Krogsgaard, M., and Davis, M. M. (2002). Direct observation of ligand recognition by T cells. Nature *419*, 845-849.

Izquierdo, M., Downward, J., Graves, J. D., and Cantrell, D. A. (1992). Role of protein kinase C in T-cell antigen receptor regulation of p21ras: evidence that two p21ras regulatory pathways coexist in T cells. Mol Cell Biol *12*, 3305-3312.

Jain, J., Loh, C., and Rao, A. (1995). Transcriptional regulation of the IL-2 gene. Curr Opin Immunol *7*, 333-342.

Janes, K. A., Albeck, J. G., Gaudet, S., Sorger, P. K., Lauffenburger, D. A., and Yaffe, M. B. (2005). A systems model of signaling identifies a molecular basis set for cytokine-induced apoptosis. Science *310*, 1646-1653.

Janes, K. A., Albeck, J. G., Peng, L. X., Sorger, P. K., Lauffenburger, D. A., and Yaffe, M. B. (2003). A High-throughput Quantitative Multiplex Kinase Assay for Monitoring Information Flow in Signaling Networks: Application to Sepsis-Apoptosis. Mol Cell Proteomics *2*, 463-473.

Janes, K. A., Kelly, J. R., Gaudet, S., Albeck, J. G., Sorger, P. K., and Lauffenburger, D. A. (2004). Cue-signal-response analysis of TNF-induced apoptosis by partial least squares regression of dynamic multivariate data. J Comput Biol *11*, 544-561.

Janes, K. A., and Lauffenburger, D. A. (2006). A biological approach to computational models of proteomic networks. Curr Opin Chem Biol *10*, 73-80.

Jones, R. G., Parsons, M., Bonnard, M., Chan, V. S., Yeh, W. C., Woodgett, J. R., and Ohashi, P. S. (2000). Protein kinase B regulates T lymphocyte survival, nuclear factor kappaB activation, and Bcl-X(L) levels in vivo. J Exp Med *191*, 1721-1734.

Jones, R. G., Saibil, S. D., Pun, J. M., Elford, A. R., Bonnard, M., Pellegrini, M., Arya, S., Parsons, M. E., Krawczyk, C. M., Gerondakis, S., *et al.* (2005). NF-kappaB couples protein kinase B/Akt signaling to distinct survival pathways and the regulation of lymphocyte homeostasis in vivo. J Immunol *175*, 3790-3799.

Jou, S. T., Carpino, N., Takahashi, Y., Piekorz, R., Chao, J. R., Wang, D., and Ihle, J. N. (2002). Essential, nonredundant role for the phosphoinositide 3-kinase p110delta in signaling by the B-cell receptor complex. Mol Cell Biol *22*, 8580-8591.

Kane, L. P., Andres, P. G., Howland, K. C., Abbas, A. K., and Weiss, A. (2001). Akt provides the CD28 costimulatory signal for up-regulation of IL-2 and IFN-gamma but not TH2 cytokines. Nat Immunol *2*, 37-44.

Kane, L. P., Shapiro, V. S., Stokoe, D., and Weiss, A. (1999). Induction of NF-kappaB by the Akt/PKB kinase. Curr Biol *9*, 601-604.

Kogkopoulou, O., Tzakos, E., Mavrothalassitis, G., Baldari, C. T., Paliogianni, F., Young, H. A., and Thyphronitis, G. (2006). Conditional up-regulation of IL-2 production by p38 MAPK inactivation is mediated by increased Erk1/2 activity. J Leukoc Biol.

Kontgen, F., Grumont, R. J., Strasser, A., Metcalf, D., Li, R., Tarlinton, D., and Gerondakis, S. (1995). Mice lacking the c-rel proto-oncogene exhibit defects in lymphocyte proliferation, humoral immunity, and interleukin-2 expression. Genes Dev *9*, 1965-1977.

Koprak, S., Staruch, M. J., and Dumont, F. J. (1999). A specific inhibitor of the p38 mitogen activated protein kinase affects differentially the production of various cytokines by activated human T cells: dependence on CD28 signaling and preferential inhibition of IL-10 production. Cell Immunol *192*, 87-95.

Kornfeld, K., Hom, D. B., and Horvitz, H. R. (1995). The ksr-1 gene encodes a novel protein kinase involved in Ras-mediated signaling in C. elegans. Cell *83*, 903-913.

Kroczek, R. A., Mages, H. W., and Hutloff, A. (2004). Emerging paradigms of T-cell co-stimulation. Curr Opin Immunol *16*, 321-327.

Krogsgaard, M., and Davis, M. M. (2005). How T cells 'see' antigen. Nat Immunol *6*, 239-245.

Kuchroo, V. K., Anderson, A. C., Waldner, H., Munder, M., Bettelli, E., and Nicholson, L. B. (2002). T cell response in experimental autoimmune encephalomyelitis (EAE): role of self and cross-reactive antigens in shaping, tuning, and regulating the autopathogenic T cell repertoire. Annu Rev Immunol *20*, 101-123.

Lanzavecchia, A., Lezzi, G., and Viola, A. (1999). From TCR engagement to T cell activation: a kinetic view of T cell behavior. Cell *96*, 1-4.

Layer, K., Lin, G., Nencioni, A., Hu, W., Schmucker, A., Antov, A. N., Li, X., Takamatsu, S., Chevassut, T., Dower, N. A., *et al.* (2003). Autoimmunity as the consequence of a spontaneous mutation in Rasgrp1. Immunity *19*, 243-255.

Le Good, J. A., Ziegler, W. H., Parekh, D. B., Alessi, D. R., Cohen, P., and Parker, P. J. (1998). Protein kinase C isotypes controlled by phosphoinositide 3-kinase through the protein kinase PDK1. Science *281*, 2042-2045.

Leiden, J. M., Wang, C. Y., Petryniak, B., Markovitz, D. M., Nabel, G. J., and Thompson, C. B. (1992). A novel Ets-related transcription factor, Elf-1, binds to human immunodeficiency virus type 2 regulatory elements that are required for inducible trans activation in T cells. J Virol *66*, 5890-5897.

Lewis, T. S., Hunt, J. B., Aveline, L. D., Jonscher, K. R., Louie, D. F., Yeh, J. M., Nahreini, T. S., Resing, K. A., and Ahn, N. G. (2000). Identification of novel MAP kinase pathway signaling targets by functional proteomics and mass spectrometry. Mol Cell *6*, 1343-1354.

Li, Q. J., Dinner, A. R., Qi, S., Irvine, D. J., Huppa, J. B., Davis, M. M., and Chakraborty, A. K. (2004). CD4 enhances T cell sensitivity to antigen by coordinating Lck accumulation at the immunological synapse. Nat Immunol *5*, 791-799.

Liu, J. O. (2005). The yins of T cell activation. Sci STKE *2005*, re1.

Liu, Y., and Janeway, C. A., Jr. (1992). Cells that present both specific ligand and costimulatory activity are the most efficient inducers of clonal expansion of normal CD4 T cells. Proc Natl Acad Sci U S A *89*, 3845-3849.

Lozano, J., Xing, R., Cai, Z., Jensen, H. L., Trempus, C., Mark, W., Cannon, R., and Kolesnick, R. (2003). Deficiency of kinase suppressor of Ras1 prevents oncogenic ras signaling in mice. Cancer Res *63*, 4232-4238.

Madrenas, J., Wange, R. L., Wang, J. L., Isakov, N., Samelson, L. E., and Germain, R. N. (1995). Zeta phosphorylation without ZAP-70 activation induced by TCR antagonists or partial agonists. Science *267*, 515-518.

Mann, D. L., O'Brien, S. J., Gilbert, D. A., Reid, Y., Popovic, M., Read-Connole, E., Gallo, R. C., and Gazdar, A. F. (1989). Origin of the HIV-susceptible human CD4+ cell line H9. AIDS Res Hum Retroviruses *5*, 253-255.

Mariathasan, S., Zakarian, A., Bouchard, D., Michie, A. M., Zuniga-Pflucker, J. C., and Ohashi, P. S. (2001). Duration and strength of extracellular signal-regulated kinase signals are altered during positive versus negative thymocyte selection. J Immunol *167*, 4966-4973.

Marshall, C. J. (1995). Specificity of receptor tyrosine kinase signaling: transient versus sustained extracellular signal-regulated kinase activation. Cell *80*, 179-185.

Matsuda, S., Moriguchi, T., Koyasu, S., and Nishida, E. (1998). T lymphocyte activation signals for interleukin-2 production involve activation of MKK6-p38 and MKK7-SAPK/JNK signaling pathways sensitive to cyclosporin A. J Biol Chem *273*, 12378-12382.

Matsumoto, R., Wang, D., Blonska, M., Li, H., Kobayashi, M., Pappu, B., Chen, Y., Wang, D., and Lin, X. (2005). Phosphorylation of CARMA1 plays a critical role in T Cell receptor-mediated NF-kappaB activation. Immunity *23*, 575-585.

May, M. J., and Ghosh, S. (1998). Signal transduction through NF-kappa B. Immunol Today *19*, 80-88.

McKeithan, T. W. (1995). Kinetic proofreading in T-cell receptor signal transduction. Proc Natl Acad Sci U S A *92*, 5042-5046.

Meuer, S. C., Hodgdon, J. C., Hussey, R. E., Protentis, J. P., Schlossman, S. F., and Reinherz, E. L. (1983). Antigen-like effects of monoclonal antibodies directed at receptors on human T cell clones. J Exp Med *158*, 988-993.

Moffat, J., Grueneberg, D. A., Yang, X., Kim, S. Y., Kloepfer, A. M., Hinkle, G., Piqani, B., Eisenhaure, T. M., Luo, B., Grenier, J. K., *et al.* (2006). A lentiviral RNAi library for human and mouse genes applied to an arrayed viral high-content screen. Cell *124*, 1283-1298.

Mori, A., Kaminuma, O., Miyazawa, K., Ogawa, K., Okudaira, H., and Akiyama, K. (1999). p38 mitogen-activated protein kinase regulates human T cell IL-5 synthesis. J Immunol *163*, 4763-4771.

Munder, M., Bettelli, E., Monney, L., Slavik, J. M., Nicholson, L. B., and Kuchroo, V. K. (2002). Reduced self-reactivity of an autoreactive T cell after activation with cross-reactive non-self-ligand. J Exp Med *196*, 1151-1162.

Murphy, L. O., and Blenis, J. (2006). MAPK signal specificity: the right place at the right time. Trends Biochem Sci.

Murphy, L. O., Smith, S., Chen, R. H., Fingar, D. C., and Blenis, J. (2002). Molecular interpretation of ERK signal duration by immediate early gene products. Nat Cell Biol *4*, 556-564.

Neilson, J., Stankunas, K., and Crabtree, G. R. (2001). Monitoring the duration of antigen-receptor occupancy by calcineurin/glycogen-synthase-kinase-3 control of NF-AT nuclear shuttling. Curr Opin Immunol *13*, 346-350.

Nguyen, A., Burack, W. R., Stock, J. L., Kortum, R., Chaika, O. V., Afkarian, M., Muller, W. J., Murphy, K. M., Morrison, D. K., Lewis, R. E., *et al.* (2002). Kinase suppressor of Ras (KSR) is a scaffold which facilitates mitogen-activated protein kinase activation in vivo. Mol Cell Biol *22*, 3035-3045.

Nicholson, L. B., and Kuchroo, V. K. (1996). Manipulation of the Th1/Th2 balance in autoimmune disease. Curr Opin Immunol *8*, 837-842.

Nicholson, L. B., Waldner, H., Carrizosa, A. M., Sette, A., Collins, M., and Kuchroo, V. K. (1998). Heteroclitic proliferative responses and changes in cytokine profile induced by altered peptides: implications for autoimmunity. Proc Natl Acad Sci U S A *95*, 264-269.

Nicholson, L. B., and Wraith, D. C. (2004). T-cell receptor degeneracy: the dog that did not bark. Adaptation of the self-reactive T-cell response to limit autoimmune disease. Mol Immunol *40*, 997-1002.

Nishida, T., Matsuki, Y., Ono, T., Oguma, T., Tsujimoto, K., Sato, M., and Tadakuma, T. (2004). The novel murine CD4+CD8+ thymocyte cell line exhibits lineage commitment into both CD4+ and CD8+ T cells by altering the intensity and the duration of anti-CD3 stimulation in vitro. J Immunol *172*, 6634-6641.

Oettgen, H. C., Terhorst, C., Cantley, L. C., and Rosoff, P. M. (1985). Stimulation of the T3-T cell receptor complex induces a membrane-potential-sensitive calcium influx. Cell *40*, 583-590.

Ohashi, P. S. (2002). T-cell signalling and autoimmunity: molecular mechanisms of disease. Nat Rev Immunol *2*, 427-438.

Okkenhaug, K., Bilancio, A., Farjot, G., Priddle, H., Sancho, S., Peskett, E., Pearce, W., Meek, S. E., Salpekar, A., Waterfield, M. D., *et al.* (2002). Impaired B and T cell antigen receptor signaling in p110delta PI 3-kinase mutant mice. Science *297*, 1031-1034.

Ortega-Perez, I., Cano, E., Were, F., Villar, M., Vazquez, J., and Redondo, J. M. (2005). c-Jun N-terminal kinase (JNK) positively regulates NFATc2 transactivation through phosphorylation within the N-terminal regulatory domain. J Biol Chem *280*, 20867-20878.

Oukka, M., Ho, I. C., de la Brousse, F. C., Hoey, T., Grusby, M. J., and Glimcher, L. H. (1998). The transcription factor NFAT4 is involved in the generation and survival of T cells. Immunity *9*, 295-304.

Pages, G., Guerin, S., Grall, D., Bonino, F., Smith, A., Anjuere, F., Auberger, P., and Pouyssegur, J. (1999). Defective thymocyte maturation in p44 MAP kinase (Erk 1) knockout mice. Science *286*, 1374-1377.

Park, S. H., Zarrinpar, A., and Lim, W. A. (2003). Rewiring MAP kinase pathways using alternative scaffold assembly mechanisms. Science *299*, 1061-1064.

Patra, A. K., Na, S. Y., and Bommhardt, U. (2004). Active protein kinase B regulates TCR responsiveness by modulating cytoplasmic-nuclear localization of NFAT and NF-kappa B proteins. J Immunol *172*, 4812-4820.

Peng, S. L., Gerth, A. J., Ranger, A. M., and Glimcher, L. H. (2001). NFATc1 and NFATc2 together control both T and B cell activation and differentiation. Immunity *14*, 13-20.

Popovic, M., Sarngadharan, M. G., Read, E., and Gallo, R. C. (1984). Detection, isolation, and continuous production of cytopathic retroviruses (HTLV-III) from patients with AIDS and pre-AIDS. Science *224*, 497-500.

Priatel, J. J., Teh, S. J., Dower, N. A., Stone, J. C., and Teh, H. S. (2002). RasGRP1 transduces low-grade TCR signals which are critical for T cell development, homeostasis, and differentiation. Immunity *17*, 617-627.

Prudhomme, W., Daley, G. Q., Zandstra, P., and Lauffenburger, D. A. (2004). Multivariate proteomic analysis of murine embryonic stem cell self-renewal versus differentiation signaling. Proc Natl Acad Sci U S A *101*, 2900-2905.

Ranger, A. M., Hodge, M. R., Gravallese, E. M., Oukka, M., Davidson, L., Alt, F. W., de la Brousse, F. C., Hoey, T., Grusby, M., and Glimcher, L. H. (1998). Delayed lymphoid repopulation with defects in IL-4-driven responses produced by inactivation of NF-ATc. Immunity *8*, 125-134.

Rao, A. (1994). NF-ATp: a transcription factor required for the co-ordinate induction of several cytokine genes. Immunol Today *15*, 274-281.

Reif, K., Burgering, B. M., and Cantrell, D. A. (1997). Phosphatidylinositol 3-kinase links the interleukin-2 receptor to protein kinase B and p70 S6 kinase. J Biol Chem *272*, 14426-14433.

Rincon, M., Enslen, H., Raingeaud, J., Recht, M., Zapton, T., Su, M. S., Penix, L. A., Davis, R. J., and Flavell, R. A. (1998a). Interferon-gamma expression by Th1 effector T cells mediated by the p38 MAP kinase signaling pathway. Embo J *17*, 2817-2829.

Rincon, M., Whitmarsh, A., Yang, D. D., Weiss, L., Derijard, B., Jayaraj, P., Davis, R. J., and Flavell, R. A. (1998b). The JNK pathway regulates the In vivo deletion of immature CD4(+)CD8(+) thymocytes. J Exp Med *188*, 1817-1830.

Roehm, N., Herron, L., Cambier, J., DiGuisto, D., Haskins, K., Kappler, J., and Marrack, P. (1984). The major histocompatibility complex-restricted antigen receptor on T cells: distribution on thymus and peripheral T cells. Cell *38*, 577-584.

Roy, F., Laberge, G., Douziech, M., Ferland-McCollough, D., and Therrien, M. (2002). KSR is a scaffold required for activation of the ERK/MAPK module. Genes Dev *16*, 427-438.

Rubinson, D. A., Dillon, C. P., Kwiatkowski, A. V., Sievers, C., Yang, L., Kopinja, J., Rooney, D. L., Ihrig, M. M., McManus, M. T., Gertler, F. B., *et al.* (2003). A lentivirus-based system to functionally silence genes in primary mammalian cells, stem cells and transgenic mice by RNA interference. Nat Genet *33*, 401-406.

Saba-El-Leil, M. K., Vella, F. D., Vernay, B., Voisin, L., Chen, L., Labrecque, N., Ang, S. L., and Meloche, S. (2003). An essential function of the mitogen-activated protein kinase Erk2 in mouse trophoblast development. EMBO Rep *4*, 964-968.

Sasaki, T., Irie-Sasaki, J., Jones, R. G., Oliveira-dos-Santos, A. J., Stanford, W. L., Bolon, B., Wakeham, A., Itie, A., Bouchard, D., Kozieradzki, I., *et al.* (2000). Function of PI3Kgamma in thymocyte development, T cell activation, and neutrophil migration. Science *287*, 1040-1046.

Schade, A. E., and Levine, A. D. (2004). Cutting edge: extracellular signal-regulated kinases 1/2 function as integrators of TCR Signal Strength. J Immunol *172*, 5828-5832.

Schafer, P. H., Wadsworth, S. A., Wang, L., and Siekierka, J. J. (1999). p38 alpha mitogen-activated protein kinase is activated by CD28-mediated signaling and is required for IL-4 production by human CD4+CD45RO+ T cells and Th2 effector cells. J Immunol *162*, 7110-7119.

Sha, W. C., Liou, H. C., Tuomanen, E. I., and Baltimore, D. (1995). Targeted disruption of the p50 subunit of NF-kappa B leads to multifocal defects in immune responses. Cell *80*, 321-330.

Shaw, J. P., Utz, P. J., Durand, D. B., Toole, J. J., Emmel, E. A., and Crabtree, G. R. (1988). Identification of a putative regulator of early T cell activation genes. Science *241*, 202-205.

Sloan-Lancaster, J., Shaw, A. S., Rothbard, J. B., and Allen, P. M. (1994). Partial T cell signaling: altered phospho-zeta and lack of zap70 recruitment in APL-induced T cell anergy. Cell *79*, 913-922.

Song, G. Y., Chung, C. S., Chaudry, I. H., and Ayala, A. (2000). Immune suppression in polymicrobial sepsis: differential regulation of Th1 and Th2 responses by p38 MAPK. J Surg Res *91*, 141-146.

Starr, T. K., Jameson, S. C., and Hogquist, K. A. (2003). Positive and negative selection of T cells. Annu Rev Immunol *21*, 139-176.

Stefanova, I., Hemmer, B., Vergelli, M., Martin, R., Biddison, W. E., and Germain, R. N. (2003). TCR ligand discrimination is enforced by competing ERK positive and SHP-1 negative feedback pathways. Nat Immunol *4*, 248-254.

Sugawara, T., Moriguchi, T., Nishida, E., and Takahama, Y. (1998). Differential roles of ERK and p38 MAP kinase pathways in positive and negative selection of T lymphocytes. Immunity *9*, 565-574.

Sundaram, M., and Han, M. (1995). The C. elegans ksr-1 gene encodes a novel Raf-related kinase involved in Ras-mediated signal transduction. Cell *83*, 889-901.

Suzuki, H., Terauchi, Y., Fujiwara, M., Aizawa, S., Yazaki, Y., Kadowaki, T., and Koyasu, S. (1999). Xid-like immunodeficiency in mice with disruption of the p85alpha subunit of phosphoinositide 3-kinase. Science *283*, 390-392.

Therrien, M., Chang, H. C., Solomon, N. M., Karim, F. D., Wassarman, D. A., and Rubin, G. M. (1995). KSR, a novel protein kinase required for RAS signal transduction. Cell *83*, 879-888.

Thome, M., and Tschopp, J. (2003). TCR-induced NF-kappaB activation: a crucial role for Carma1, Bcl10 and MALT1. Trends Immunol *24*, 419-424.

Tognon, C. E., Kirk, H. E., Passmore, L. A., Whitehead, I. P., Der, C. J., and Kay, R. J. (1998). Regulation of RasGRP via a phorbol ester-responsive C1 domain. Mol Cell Biol *18*, 6995-7008.

Ullman, K. S., Northrop, J. P., Verweij, C. L., and Crabtree, G. R. (1990). Transmission of signals from the T lymphocyte antigen receptor to the genes responsible for cell proliferation and immune function: the missing link. Annu Rev Immunol *8*, 421-452.

Valitutti, S., Muller, S., Salio, M., and Lanzavecchia, A. (1997). Degradation of T cell receptor (TCR)-CD3-zeta complexes after antigenic stimulation. J Exp Med *185*, 1859-1864.

Vanhaesebroeck, B., and Alessi, D. R. (2000). The PI3K-PDK1 connection: more than just a road to PKB. Biochem J *346 Pt 3*, 561-576.

Veiopoulou, C., Kogopoulou, O., Tzakos, E., Mavrothalassitis, G., Mitsias, D., Karafoulidou, A., Paliogianni, F., Moutsopoulos, H. M., and Thyphronitis, G. (2004). IL-2 and IL-10 production by human CD4+T cells is differentially regulated by p38: mode of stimulation-dependent regulation of IL-2. Neuroimmunomodulation *11*, 199-208.

Ward, S. G., June, C. H., and Olive, D. (1996). PI 3-kinase: a pivotal pathway in T-cell activation? Immunol Today *17*, 187-197.

Webb, L. M., Vigorito, E., Wymann, M. P., Hirsch, E., and Turner, M. (2005). Cutting edge: T cell development requires the combined activities of the p110gamma and p110delta catalytic isoforms of phosphatidylinositol 3-kinase. J Immunol *175*, 2783-2787.

Weber, J. R., Orstavik, S., Torgersen, K. M., Danbolt, N. C., Berg, S. F., Ryan, J. C., Tasken, K., Imboden, J. B., and Vaage, J. T. (1998). Molecular cloning of the cDNA encoding pp36, a tyrosine-phosphorylated adaptor protein selectively expressed by T cells and natural killer cells. J Exp Med *187*, 1157-1161.

Weih, F., Carrasco, D., Durham, S. K., Barton, D. S., Rizzo, C. A., Ryseck, R. P., Lira, S. A., and Bravo, R. (1995). Multiorgan inflammation and hematopoietic abnormalities in mice with a targeted disruption of RelB, a member of the NF-kappa B/Rel family. Cell *80*, 331-340.

Weiss, A., Imboden, J., Shoback, D., and Stobo, J. (1984). Role of T3 surface molecules in human T-cell activation: T3-dependent activation results in an increase in cytoplasmic free calcium. Proc Natl Acad Sci U S A *81*, 4169-4173.

Werlen, G., Hausmann, B., Naeher, D., and Palmer, E. (2003). Signaling life and death in the thymus: timing is everything. Science *299*, 1859-1863.

Werlen, G., Hausmann, B., and Palmer, E. (2000). A motif in the alphabeta T-cell receptor controls positive selection by modulating ERK activity. Nature *406*, 422-426.

Whitehurst, C. E., and Geppert, T. D. (1996). MEK1 and the extracellular signal-regulated kinases are required for the stimulation of IL-2 gene transcription in T cells. J Immunol *156*, 1020-1029.

Wold, S., Sjostrom, M., and Eriksson, L. (2001). PLS-regression: a basic tool of chemometrics. Chemometrics and Intelligent Laboratory Systems *58*, 109–130.

Xanthoudakis, S., Viola, J. P., Shaw, K. T., Luo, C., Wallace, J. D., Bozza, P. T., Luk, D. C., Curran, T., and Rao, A. (1996). An enhanced immune response in mice lacking the transcription factor NFAT1. Science *272*, 892-895.

Yang, D. D., Conze, D., Whitmarsh, A. J., Barrett, T., Davis, R. J., Rincon, M., and Flavell, R. A. (1998). Differentiation of CD4+ T cells to Th1 cells requires MAP kinase JNK2. Immunity *9*, 575-585.

Yates, A., Chan, C. C., Callard, R. E., George, A. J., and Stark, J. (2001). An approach to modelling in immunology. Brief Bioinform *2*, 245-257.

Yoshida, H., Nishina, H., Takimoto, H., Marengere, L. E., Wakeham, A. C., Bouchard, D., Kong, Y. Y., Ohteki, T., Shahinian, A., Bachmann, M., *et al.* (1998). The transcription factor NF-ATc1 regulates lymphocyte proliferation and Th2 cytokine production. Immunity *8*, 115-124.

Yu, W., Fantl, W. J., Harrowe, G., and Williams, L. T. (1998). Regulation of the MAP kinase pathway by mammalian Ksr through direct interaction with MEK and ERK. Curr Biol *8*, 56-64.

Yun, T. J., and Bevan, M. J. (2001). The Goldilocks conditions applied to T cell development. Nat Immunol *2*, 13-14.

Zhang, J., Salojin, K. V., Gao, J. X., Cameron, M. J., Bergerot, I., and Delovitch, T. L. (1999a). p38 mitogen-activated protein kinase mediates signal integration of TCR/CD28 costimulation in primary murine T cells. J Immunol *162*, 3819-3829.

Zhang, W., Sloan-Lancaster, J., Kitchen, J., Trible, R. P., and Samelson, L. E. (1998). LAT: the ZAP-70 tyrosine kinase substrate that links T cell receptor to cellular activation. Cell *92*, 83-92.

Zhang, W., Sommers, C. L., Burshtyn, D. N., Stebbins, C. C., DeJarnette, J. B., Trible, R. P., Grinberg, A., Tsay, H. C., Jacobs, H. M., Kessler, C. M., *et al.* (1999b). Essential role of LAT in T cell development. Immunity *10*, 323-332.

Zhong, H., May, M. J., Jimi, E., and Ghosh, S. (2002). The phosphorylation status of nuclear NF-kappa B determines its association with CBP/p300 or HDAC-1. Mol Cell *9*, 625-636.

Appendix A

FENVALERATE, CYPERMETHRIN, DELTAMETHRIN, TYRPHOSTIN 8 - **Calcineurin (PP2B) inhibitors.**
KN-62, KN-93 - **CaM kinase II inhibitors.**
2-HYDROXY-5-(2,5-DIHYDROXY BENZYLAMINO)BENZOIC ACID - **CAM Kinase II, EGF receptor tyrosine kinase, and pp60 kinase inhibitors.**
5,6-DICHLORO-1-beta-D-RIBOFURANOSYLBENZIMIDAZOLE - **Casein kinase II inhibitor.**
RWJ-60475 - **CD45 tyrosine phosphatase inhibitor.**
N9-ISOPROPYL-OLOMOUCINE - **cdc2 kinase inhibitor.**
GW 5074 - **cRAF1 kinase inhibitor.**
INDIRUBIN-3'-MONOOXIME - **Cyclin dependent kinase inhibitor.**
TYRPHOSTIN 23, TYRPHOSTIN 25, TYRPHOSTIN 47, TYRPHOSTIN 51, LAVENDUSTIN A, ERBSTATIN ANALOG, TYRPHOSTIN AG 1478 - **EGF receptor kinase inhibitors.**
TYRPHOSTIN 46 - **EGF receptor kinase, p56, and PDGF receptor kinase inhibitor.**
RG-14620 - **EGF-stimulated HER14 cell proliferation inhibitor.**
5-IODOTUBERCIDIN - **ERK2, adenosine kinase, CK1, CK2, and insulin receptor kinase inhibitor.**
SU1498 - **Flk-1 kinase inhibitor.**
INDIRUBIN - **GSK-3beta and CDK5 inhibitor.**
AG-825 - **HER1-2 tyrosine kinase inhibitor.**
BAY 11-7082 - **I-kappa B-alpha kinase inhibitor.**
HYDROXY-2-NAPHTHALENYL METHYLPHOSPHONIC ACID - **Insulin receptor tyrosine kinase inhibitor.**
AG-490 - **JAK-2 tyrosine kinase inhibitor.**
ZM 449829 - **JAK-3 tyrosine kinase inhibitor.**
SP 600125 - **Jun-N-terminal kinase inhibitor.**
LEVAMISOLE HCl, TETRAMISOLE HCl - **Mammalian alkaline phosphatase inhibitors.**
PD-98059, U-0126 - **MEK inhibitors.**
ML-7, ML-9 - **MLC kinase inhibitors.**
OLOMOUCINE - **p33 cdk2/cyclin A, p33 cdk2/cyclin E, p34 cdc2/cyclin B, p33 cdk5/p35 inhibitor.**
ROSCOVITINE - **p34 cdc2/cyclin B kinase inhibitor.**
ZM 336372, SB-202190, SB-203580 - **p38 MAP kinase inhibitors.**
DAMNACANTHAL - **p56 tyrosine kinase inhibitor.**
2-AMINOPURINE - **p58 PITSLRE beta1 inhibitor.**
AG-370, TYRPHOSTIN 9, AG-1296 - **PDGF receptor tyrosine kinase inhibitors.**
LY 294002, WORTMANNIN, QUERCETIN DIHYDRATE - PI 3-kinase inhibitor.
H-8, HA-1004, HA-1077 - **PKA and PKG inhibitors.**
H-89 - **PKA inhibitor.**
STAUROSPORINE - **PKA, PKG, CaMK, tyrosine kinases, and phosphorylase kinase inhibitors.**
H-7 - **PKA, PKG, MLCK, and PKC inhibitor.**
ROTTLERIN - **PKC delta inhibitor.**
SPHINGOSINE, Ro 31-8220, PALMITOYL-DL-CARNITINE Cl - **PKC inhibitors.**
2,2',3,3',4,4'-HEXAHYDROXY-1,1'-BIPHENYL-6,6'-DIMETHANOL DIMETHYL ETHER - **PKCalpha and PKCgamma Inhibitor.**
CANTHARIDIC ACID, CANTHARIDIN - **PP1 and PP2A inhibitors.**
ENDOTHALL - **PP2A inhibitor.**
GF 109203X, HYPERICIN, H-9 - **Protein kinase inhibitors.**
CinnGEL - **PTP1B inhibitor.**
PP1, PP2 - **Src tyrosine kinase inhibitors.**
PICEATANNOL - **Syk inhibitor.**
AG-494, TYRPHOSTIN AG 1288, TYRPHOSTIN AG 1295, AG-126, AG-879, GENISTEIN, LFM-A13 - **Tyrosine kinase inhibitors.**
BENZYLPHOSPHONIC ACID, L-p-BROMOTETRAMISOLE OXALATE, RK-682 - **Tyrosine phosphatase inhibitors.**
SU 4312 - **VEGF receptor tyrosine kinase inhibitor.**
DAIDZEIN - **Negative control for Genistein.**
ISO-OLOMOUCINE - **Negative control for olomoucine.**
TYRPHOSTIN 1 - **Negative control for tyrosine kinase inhibitors.**

Supplementary Fig. 1

List of kinase and phosphatase inhibitors screened for their ability to inhibit IL-2 production in human H9 T cells.

CONC. (μM)	INHIBITOR	INHIBITION TARGET	IL-2 Conc. (ng/ml)	% of Control IL-2
	stimulated Control	stimulated Control	2.042 ± 0.07	100.00
	unstimulated Control	unstimulated Control	0.00	0.00
10	**PP1**	Src family tyrosine kinase inhibitor.	0.00	0.00
20	**BAY 11-7082**	I-kappa B-alpha kinase inhibitor.	0.00	0.00
2.8	**HYPERICIN**	Protein kinase C inhibitor.	0.015 ± 0.00	0.73
10	**U-0126**	MEK inhibitor.	0.151 ± 0.04	7.39
10	**LY 294002**	Phosphatidylinositol 3-kinase inhibitor.	0.891 ± 0.12	43.63
8	**SP 600125**	Jun-N-terminal kinase inhibitor.	0.894 ± 0.07	43.78
10	**AG-879**	Tyrosine kinase inhibitor.	1.246 ± 0.31	61.02
0.02	**CYPERMETHRIN**	Calcineurin (PP2B) inhibitor.	1.539 ± 0.16	75.37
50	**PD-98059**	MAP kinase inhibitor.	1.704 ± 0.05	83.45
0.01	**Ro 31-8220**	Protein kinase C inhibitor.	1.71 ± 0.10	83.74
2.4	**TYRPHOSTIN AG 1295**	Tyrosine kinase inhibitor.	1.745 ± 0.09	85.46
50	**2,2',3,3',4,4'-HEXAHYDROXY-1,1'-BIPHENYL-6,6'-DIMETHANOL DIMETHYL ETHER**	PKCalpha and PKCgamma Inhibitor.	1.747 ± 0.10	85.55
0.01	**PP2**	Src tyrosine kinase inhibitor.	1.807 ± 0.03	88.49
0.01	**PALMITOYL-DL-CARNITINE Cl**	PKC inhibitor.	1.833 ± 0.02	89.76
0.03	**SB-202190**	p38 MAP kinase inhibitor.	1.889 ± 0.03	92.51
0.02	**DELTAMETHRIN**	Calcineurin (PP2B) inhibitor.	1.931 ± 0.16	94.56
0.05	**WORTMANNIN**	Phosphatidylinositol 3-kinase inhibitor.	1.946 ± 0.06	95.30
0.05	**H-89**	PKA inhibitor.	1.983 ± 0.09	97.11
0.05	**SB-203580**	p38 mitogen-activated protein kinase inhibitor.	2.015 ± 0.04	98.68
20	**TYRPHOSTIN 8**	Calcineurin inhibitor.	2.058 ± 0.09	100.78
54	**RK-682**	Tyrosine phosphatase inhibitor.	2.131 ± 0.14	104.36
0.4	**KN-93**	CaM kinase II inhibitor.	2.268 ± 0.11	111.07
1	**KN-62**	CAM Kinase II inhibitor.	2.531 ± 0.03	123.95

Supplementary Fig. 2

List of kinase and phosphatase inhibitors screened for their ability to inhibit IL-2 production in 1B6 cells. Inhibitors used at concentrations indicated.

Appendix B

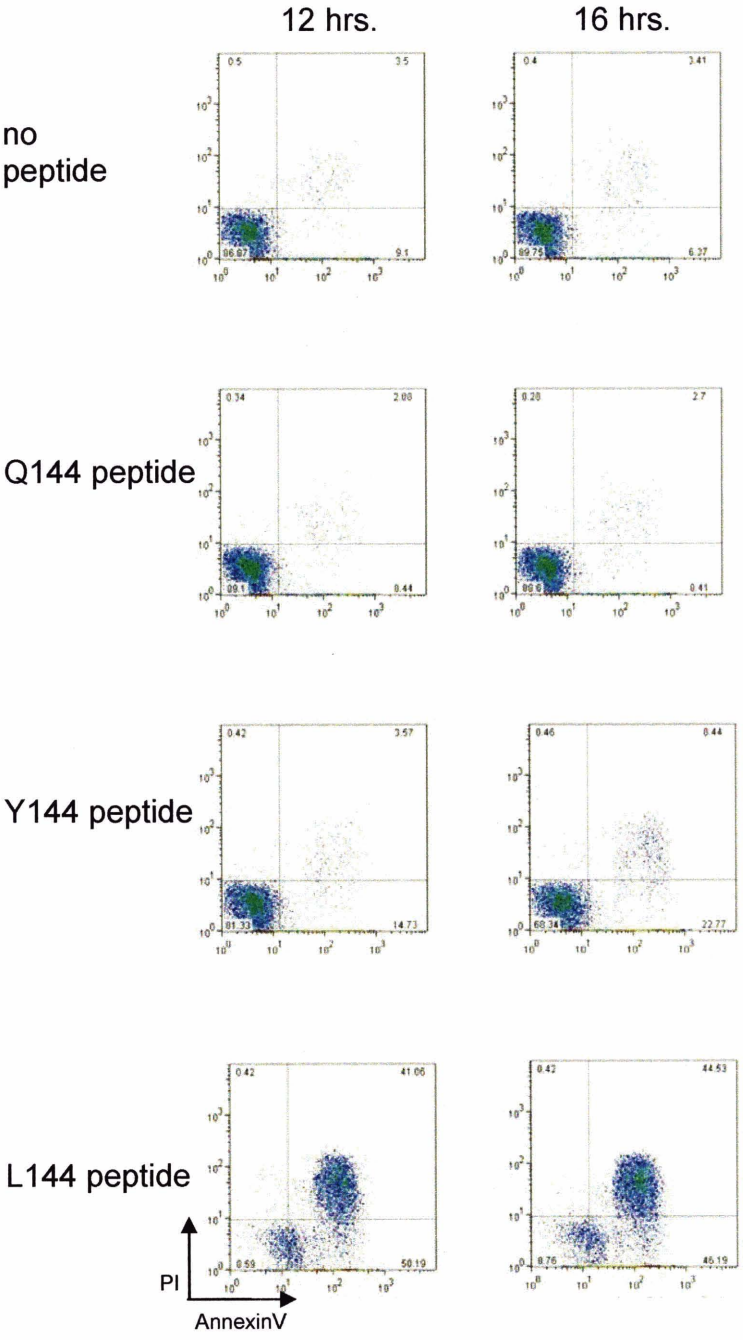

Supplementary Fig. 1

FACS analysis of AnnexinV-PI stained 1B6 cells stimulated with PLP altered peptide ligands.

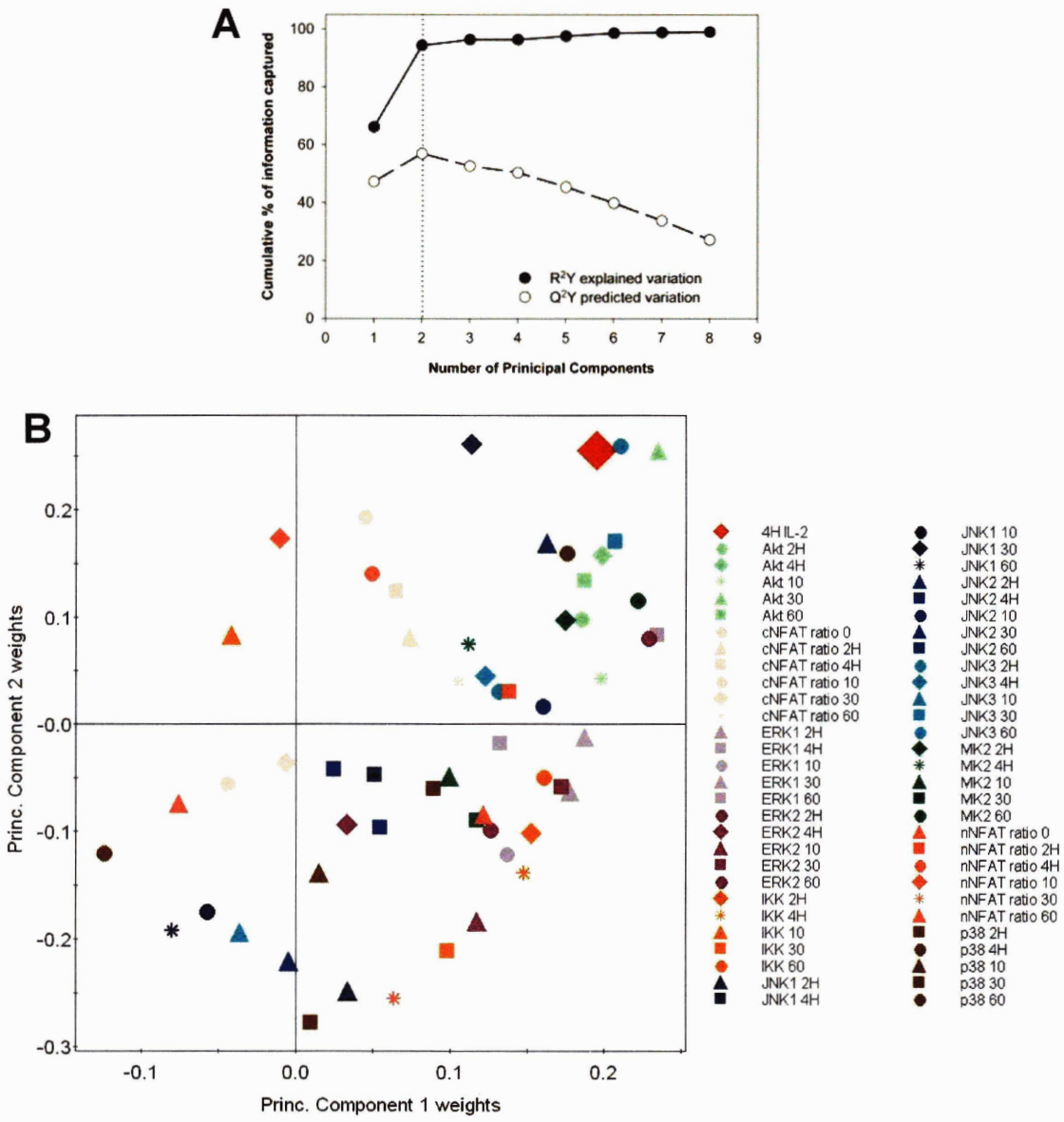

Supplementary Fig. 2

(A) The PLSR algorithm converges at 2 principal components, resulting in a regression coefficient of 0.94 for the IL-2 data. Illustrated is the cumulative regression coefficient and cumulative fraction of the total variation in IL-2 that can be predicted by each component. The components beyond the second are not significant and shown only for illustrative purposes. (B) Complete loading plot of all X variables used in the model, projected with IL-2. Coloring is as follows: IL-2, red diamond; Akt, light green; Erk1, lavender; ERK2, dark purple; IKK, orange; JNK1, navy; JNK2, blue; JNK3, cyan; cytosolic NFAT, light pink; nuclear NFAT, dark pink; MK2, dark green; p38, brown.

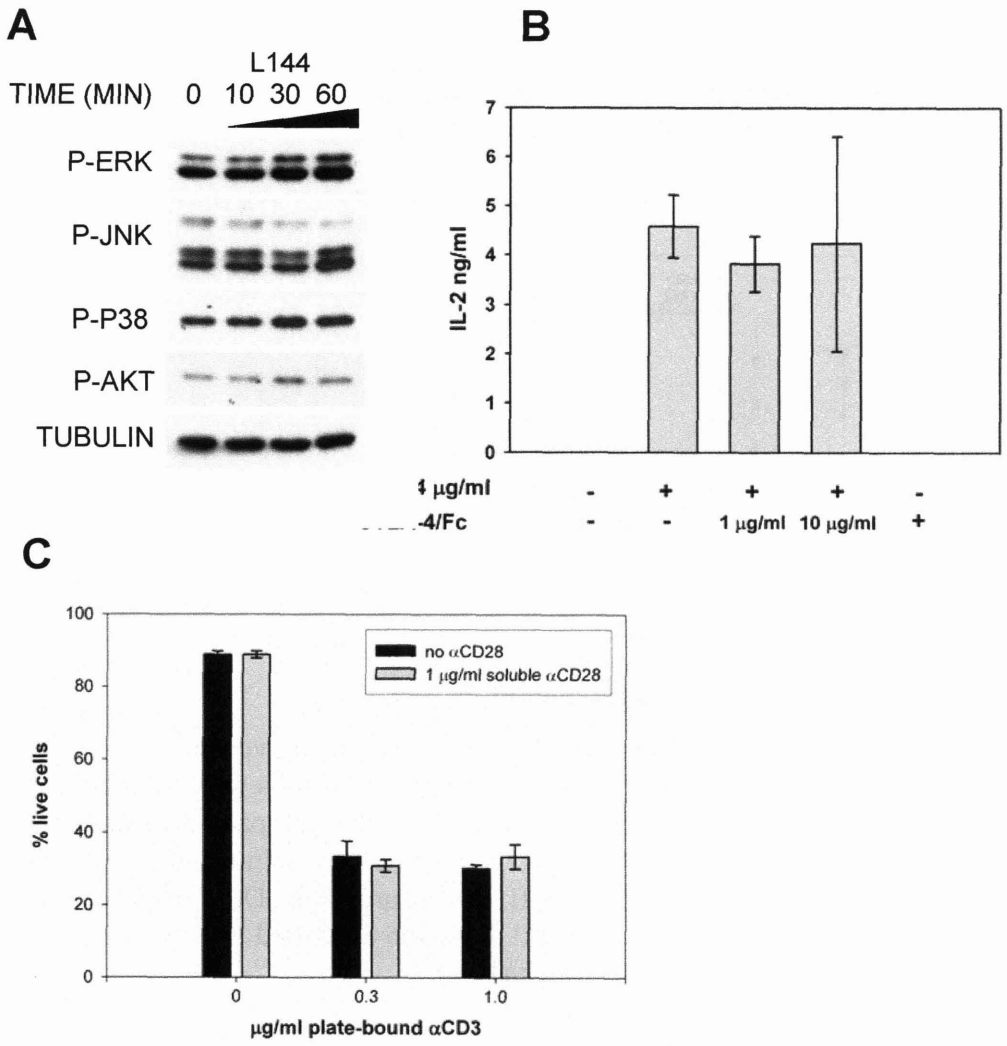

Supplementary Fig. 3

(A) Western blot of ERK, JNK, p38 and Akt phosphorylation in DAS cell lysates during co-culture with 1B6 cells (B) IL-2 production in 1B6 cells from 4 µg/ml L144 peptide stimulus with and without CTLA-4/Fc chimera fusion protein (R & D Systems). (C) activation-induced apoptosis due to plate-bound antiCD3 stimulation with and without soluble antiCD28. Error bars represent +/- standard deviation.

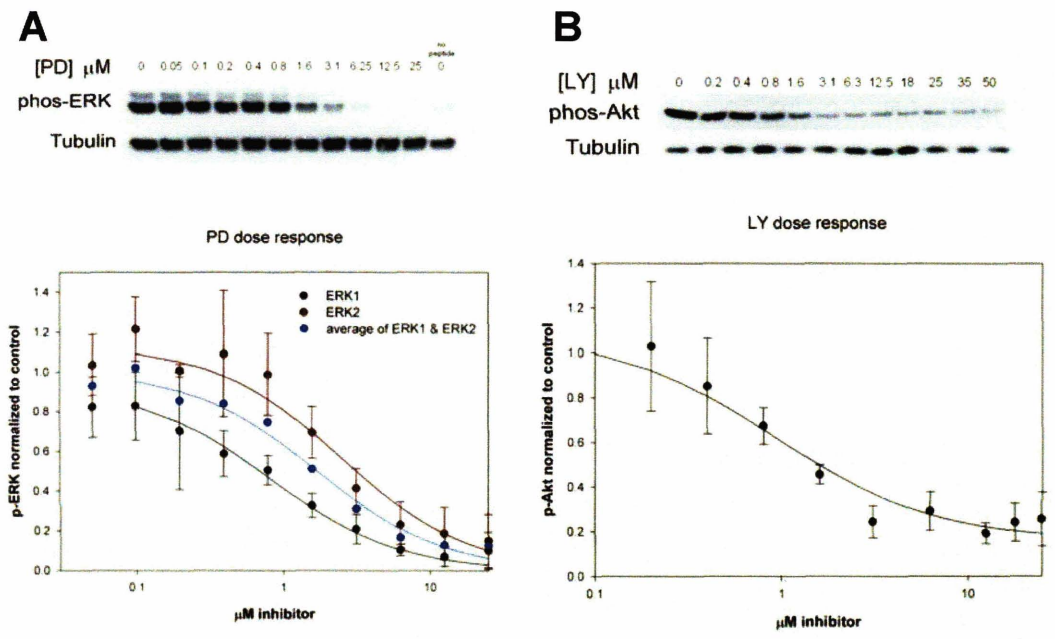

Supplementary Fig. 4

Generation of dose resonse curves for inhibitors. Representative western blot and dose response curves based upon triplicate measurements. 1B6 cells were preincubated with inhibitor for 30 minutes with PD98059 (A) or LY294002 (B) prior to stimulation with DAS cells loaded with 4 μg/ml L144. Cells were lysed at 30 minutes for western blotting or supernatant collected at 4 hours for IL-2 measurements. Dose response curves represent triplicate experiments +/- standard deviation and fitted to a function of the form y=ab/(b+x).

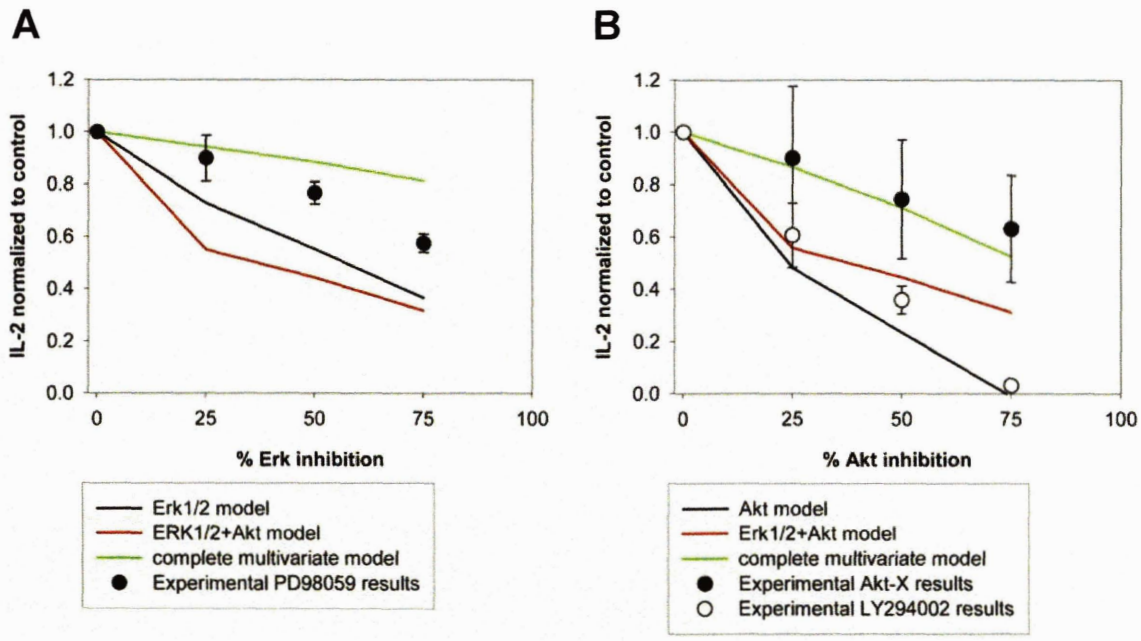

Supplementary Fig. 5

Reduced models as described in Fig. 5 are compared in their ability to predict IL-2 as in Fig. 6. (A) ERK1/2 only or ERK1,2 + Akt only models superimposed with the data from Fig. 6B. (B) Akt only or Akt + ERK1/2 only models superimposed with the data from Fig. 6D.